Resource efficient process chain development of a modular CubeSat spaceframe

By

Johannes Francois Oberholzer

Thesis presented in fulfilment of the requirements for the degree of Masters in Engineering in the faculty of Industrial Engineering at Stellenbosch University

UNIVERSITEIT
iYUNIVESITHI
STELLENBOSCH
UNIVERSITY

100
1918 · 2018

Supervisor: Prof. Gert Adriaan Oosthuizen

March 2018

Declaration

By submitting this thesis electronically, I declare that the entirety of the work contained therein is my own, original work, that I am the sole author thereof (save to the extent explicitly otherwise stated), that reproduction and publication thereof by Stellenbosch University will not infringe any third party rights and that I have not previously in its entirety or in part submitted it for obtaining any qualification.

November 2017

Abstract

The Southern African Amateur Radio Satellite Association (SA AMSAT) is designing and manufacturing an amateur satellite based on the CubeSat design. The mission of SA AMSAT is to provide Radio Amateurs in Southern Africa with access to a Low Earth Orbit (LEO) Satellite on as many of the available passes as possible. Rather than acquiring a CubeSat from an established company, they have decided to manufacture the entire satellite themselves and have reached out to the Stellenbosch University to help improve on their current spaceframe prototype. A CubeSat is a 10×10×10 cm cube that can weigh up to 1.33 kg. This design offers a less expensive alternative for space enthusiasts to explore the cosmos, even though the total weight is very limited.

For a CubeSat to be allowed to launch, it must adhere to certain specifications outlined in the CubeSat Design Specifications document. This places several restrictions on the satellite in terms of weight, size and centre of gravity, and innovative solutions needs to be explored during integration to meet these specifications. Having a spaceframe that can easily be assembled and disassembled will help smooth out the integration stage and save a lot of time that can now be allocated elsewhere in the development stages.

The increasing relevance of resource efficient manufacturing is prevalent through the continually rising costs of resources and energy. In order to stay competitive, one must develop resource efficient process chains to gain an advantage in the market. This study focused on developing a resource efficient process chain to manufacture a modular CubeSat spaceframe. This spaceframe must adhere to the CubeSat Design Specifications, as well as meet all of the customer's needs. A unique assembly process was designed that eliminated the need for screws structure together. Instead the spaceframe relies on interference fits, and utilizes the unique deployment method of the P-POD to ensure that the assembly does not fail.

A material selection procedure was utilized, along with resource efficient manufacturing process chains to develop a CubeSat structure that was very cost effective to produce, was easily assembled and disassembled and weighed less than most of the market leading CubeSat structures.

Opsomming

Die Suid-Afrikaanse Amateur Radio Satelliet Vereniging (SA AMSAT) is in die proses om ‘n amateur satellite, wat gebaseer is op die CubeSat ontwerp, te vervaardig. Die missie van SA AMSAT is om Radio-amateurs in Suider-Afrika te voorsien met toegang tot 'n Lae Omwnteling (LEO) Satelliet. In plaas daarvan om 'n CubeSat by 'n gevestigde maatskappy te verkry, het hulle besluit om die hele satelliet self te vervaardig en het die Universiteit Stellenbosch genader om te help met die vervaardiging van die vlugraam. 'n CubeSat is 'n 10 × 10 × 10 cm kubus wat tot en met 1.33 kg kan weeg. Hierdie ontwerp bied 'n goedkoper alternatief vir toegang tot die ruimte, alhoewel die totale gewig baie beperk is.

Voordat 'n CubeSat toegelaat moet word om deel te neem aan ‘n ruimtevlug, moet dit voldoen aan sekere spesifikasies soos uiteengesit in die CubeSat-ontwerpspesifikasiedokument. Dit plaas verskeie beperkings op die satelliet in terme van gewig, grootte en swaartepuntposisie, en innoverende oplossings moet tydens die integrasie proses ondersoek word om aan hierdie spesifikasies te voldoen. As jy 'n vlugraam het wat maklik ann mekaar gesit en uitmekaar gehaal kan word, sal die integrasie proses glad verloop en baie tyd bespaar wat nou elders in die ontwikkelingsfases toegewy kan word.

Die toenemende relevansie van hulpbron-doeltreffende vervaardiging kom voor deur die koste van hulpbronne en energie wat voortdurend styg. Om mededingend te bly moet 'n mens hulpbron-effektiewe proseskettings ontwikkel om 'n voordeel in die mark te verkry. Hierdie studie het gefokus op die ontwikkeling van 'n hulpbron-doeltreffende prosesketting om 'n modulêre CubeSat-vlugraam te vervaardig. Hierdie raam moet voldoen aan al die CubeSat-ontwerpspesifikasies, asook aan al die behoeftes van die kliënt. 'n Unieke metode is ontwerp wat die behoefte aan skroewe vir die aan mekaar sit van die struktuur uitskakel. In plaas daarvan berus die vlugraam op interferensie-pas tegnieke, en gebruik die unieke ontplooiingsmetode van die P-POD om te verseker dat die raam nie uitmekaar val tydens die ruimtevaart nie.

'n Keuringsprosedure om die optimale material vir vervaardiging te bepaal is aangewend, tesame met verskeie hulpbron-doeltreffende vervaardigingsproseskettings om 'n CubeSat-struktuur te ontwikkel, wat baie koste-effektief is om te produseer. Dit was maklik aan mekaar gesit en uit mekaar gehaal en weeg minder as meeste van die markleidende CubeSat-strukture.

Acknowledgements

I would like to express my deepest gratitude towards the following people who each contributed in their own way to help make my study a success:

- To my supervisor, Prof GA Oosthizen: Thank you for all the support during my studies. The knowledge I have received from you, with regards to my thesis and to life will stay with me till the end of time.

- To my friends and co-workers, Mr. MD Burger and Mr. P de Wet, for making this an unforgettable experience. I now no longer see you as only my colleagues, but as two of my closest friends.

- To the STC-LAM research group for providing me with an endless amount of knowledge and outside perspective when I needed it most.

- To Mr. D Hagedorn-Hansen for his contributions towards helping me reach my goal.

- To my family, whose prayers kept me strong in my time of need.

- To my lovely fiancé, who kept me sane during the most trying of times and always reminded me that there is an end in sight.

- Finally, to my Heavenly Father, who provided me with the opportunities and mental capacity to complete this thesis. I pray that His hand will be seen in the work that I do, now and forever.

Table of Contents

List of Figures

List of Tables

Nomenclature

BCC	body-centred cubic
CDS	CubeSat Design Specification
CSIR	Council for Scientific and Industrial Research
CSLI	CubeSat Launch Initiative
DE	design efficiency
DFM	Design for Manufacture
DST	Department of Science and Technology
EDM	Electrical Discharge Machining
FM	Frequency Modulation
HCP	hexagonal close packed
HF	high frequency
ISIS	Innovative Solutions In Space
ISS	International Space Station
LBC	Laser Beam Cutting
LEO	Low Earth Orbit
LV	launch vehicle
LV	launch vehicle
MarCO	Mars Cube One
NASA	National Aeronautics and Space Administration
NRCSD	NanoRacks CubeSat Deployer
OPAL	Orbital Picosatellite Automated Launcher
PCB	Printed Circuit Board
P-POD	Poly-Picosatellite Orbital Deployer
SA AMSAT	Southern African Amateur Radio Satellite Association
SANSA	South African National Space Agency
SSB	Single Sideband Modulation
SSDL	Space Systems Development Laboratory
STC-LAM	Stellenbosch Technology Centre Laboratory fon Advanced Manufacturing
STEM	Science, Technology, Engineering and Mathematics
SUNSAT	Stellenbosch UNiversity SATellite
SuperDARN	Super Dual Auroral Radar Network
TiCoC	Titanium Centre of Competence
TML	Total Mass Loss
WEDM	Wire Electrical Discharge Machining

Chapter 1: Introduction

1.1 Project Background and Origin

1.1.1 History of the CubeSat Project

Stanford University's Department of Aeronautics and Astronautics established the Space Systems Development Laboratory (SSDL) in 1994 with the purpose of providing project based learning programs for engineering students [1]. The goal of this program is for students to gain experience in systems engineering and was designed to take the students through the life cycle of a project. In this case, the project was the design, development, fabrication, testing, launch integration and space operations of a microsatellite [1]. The Orbital Picosatellite Automated Launcher (OPAL), Stanford University's first student built satellite was launched on January 26, 2000 [2]. Opal had three primary payloads: the mothership/daughtership mission, the magnetometer testbed and the accelerometer testbed, the first of which would inevitably pave the way for CubeSats, as we know today.

The CubeSat program was initially conceptualised as a tool to not only help teach students about the process involved in the development of a spacecraft, but the launching and operational processes as well [3]. The driving force behind the idea was to create a small and inexpensive standardized satellite design to support a wide variety of demonstration applications while having a much shorter development cycle [4]. The ideal program would allow graduate students to see the development of a spacecraft through its entire lifecycle by providing a hands-on experience, and inevitably producing competent graduates who are able to become productive members of the industry right after graduating [3]. The accelerated schedule of the CubeSat program allows students to be involved in the complete life cycle of a satellite, including mission requirements and planning; design, analysis and testing; fabrication, assembly and quality control; system level testing; integration and launch and ground based satellite operations [5].

A key enabler to the CubeSat approach is the development and use of a standardised deployment system, which from the perspective of a launch provider, will appear identical from mission to mission, in terms of interface and functionality [3]. The development of the Poly-Picosatellite Orbital Deployer (P-POD) was driven by the need for consistency in the design and launching of the picosatellite class CubeSat systems [6]. The P-POD was developed to meet these primary goals [3], [6]:

- Protect the launch vehicle (LV) and the primary payload
- Provide a safe and reliable deployment system for the CubeSats
- To maintain flexibility in launch vehicle options

The flexibility of the P-POD for LV options, in conjunction with its ability to hold multiple satellites and combine them as a single payload, greatly decreases the launch costs. Since its conception, the P-POD has undergone multiple design changes. Figure 1 is a depiction of the P-POD Mk. III, which is the current version being used. The P-POD MK. III offers a larger access port on two sides of the deployment vehicle, larger spring plungers for easier CubeSat integration, and door bracket modifications to account for shear relief of the release mechanisms [6].

Figure 1: Poly-Picosatellite Orbital Deployer (P-POD) MK. III (Adapted from [6])

From this standardised launch vehicle design, a CubeSat standard was born. A CubeSat is a 10 cm cube with a mass of up to 1.33 kg [7]. This is known as a 1U design, and designs of up to 3U is available to launch via the P-POD. Table 1 below illustrates some of the most common CubeSat units in use today.

Table 1: Most commonly used CubeSat units (Adapted from [7])

CubeSat Unit	Dimensions (l×h×b)	Maximum Weight
1U: 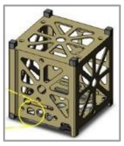	100×100×113.5 mm	1.33kg
1.5U: 	100×100×170.25 mm	2.00kg
2U: 	100×100×227 mm	2.66kg
3U: 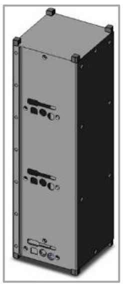	100×100×340.5 mm	4.00kg

The standard deployment system allows the CubeSat Program to function with reduced mission costs and accelerates the satellite development time [5]. This framework enables universities and organizations worldwide to develop and launch Nano-satellites at a more affordable rate. Presently, the CubeSat Project is an international collaboration with more than 100 universities, high schools, and private firms developing picosatellites containing scientific, private, and government payloads [7].

In an attempt to further extend the capabilities of CubeSats beyond that of academic and technology validation, the 6U and 12U platforms have been proposed to achieve more complex science and defence goals. Mars Cube One (MarCO), as seen in Figure 2, is a 6U CubeSat being developed by NASA's Jet Propulsion Laboratory for the upcoming InSight mission to mars.

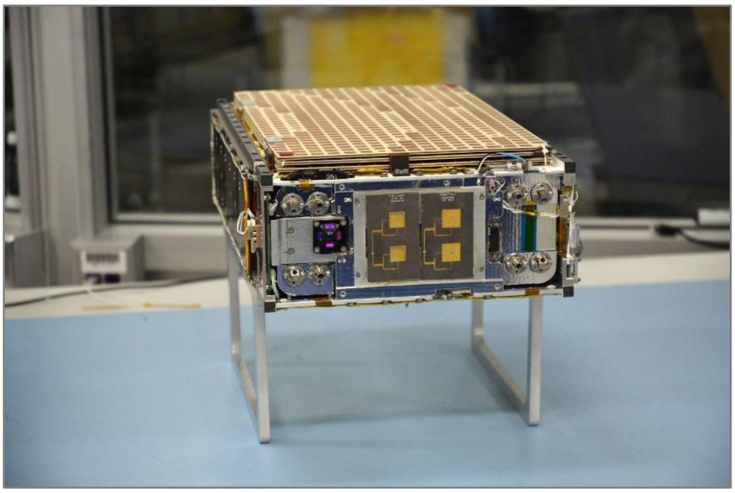

Figure 2: MarCo 6U CubeSat spacecraft

InSight will be the twelfth mission of NASA's Discovery Program, and will perform the first surface-based geophysical investigation of Mars [8]. The scientific goals of the insight mission are to understand the formation an evolution of terrestrial planets through investigation of the interior structure and processes of Mars, and to determine the planets current level of tectonic activity and impact flux.

1.1.2 The South African Amateur Radio Satellite Association

The South African Amateur Radio Satellite Association (SA AMSAT) is a specialist organization that focusses on amateur satellites and weak signal communication. They have embarked on the journey of designing and manufacturing their own communications satellite based on the CubeSat principle. The primary mission of the CubeSat will be to provide radio amateurs in Southern Africa with access to a Low Earth Orbit (LEO) satellite on as many of the available passes as possible. They hope to stimulate interest in space and amateur radio amongst young South Africans by making satellites more accessible to all. The secondary mission will be to carry a scientific payload, designed by an educational institution in South Africa, into orbit, further increasing the participation in the project and facilitating in the development of Science, Technology, Engineering and Mathematics (STEM) in young South Africans.

Due to the high costs associated with the development of a satellite, the team at SA AMSAT have decided to design and manufacture the satellite themselves. Because of the relatively low costs associated with the CubeSat platform, the decision was made to utilise this design for the project.

This design offers a unique challenge to find the optimal strength-to-weight ratio of the spaceframe in order to maximise the payload capabilities of the satellite. Previous work has been done on this subject and a Material Selection procedure was designed to help with the process of designing and manufacturing a spaceframe prototype.

Apart from the spaceframe, several other components needs to be designed, manufactured, successfully integrated and tested before the CubeSat will be considered for launch. The primary payload of the CubeSat will consist of a linear transponder with a 70cm uplink and a 2m downlink, utilizing a bandwidth of 20 kHz for both Frequency Modulation (FM) and Single Sideband Modulation (SSB), while a separate 70cm frequency will be used for command and control purposes. Frequencies in the range of 435.100 MHz to 435.140 MHz is currently under consideration for the uplink and frequencies between 145.860 MHz and 145.980 MHz are being considered for the downlink.

1.1.3 South Africa's Titanium Strategy

South Africa's Department of Science and Technology (DST) have been spearheading a research-led industrialization initiative over the past eight years, with the aim of establishing a titanium metals industry in the country [9]. South Africa does not contribute to, or benefit from any downstream beneficiation of the mineral, in spite of the fact that South Africa's reserve base is approximately 16% of that of the World.

The DST, in collaboration with other South African departments such as the Department of Public Enterprises (DPE), have developed the South African Titanium Industry strategy framework [9]. This framework, aims to deliver titanium related competencies across the entire titanium value chain, from production of titanium minerals to the manufacture of final products [9]. The production of titanium metal powder via a proprietary process will provide South Africa with a sustainable competitive advantage to initially enter the market. It is intended to build on this platform to expand the local industrial capacity and capabilities to include the production of titanium mill products such as plate, sheet and bar material [9]. From here the manufacturing industry will be able to capitalize on the rapidly growing demand for titanium by producing finished products targeted at the industrial, aerospace and biomedical markets [9].

In order for South African Titanium Strategy to be realised, the technology building blocks required for the establishment of a titanium industry in South Africa needs to be developed and commercialised. The Titanium Centre of Competence (TiCoC), based and led by the Council for Scientific and Industrial Research (CSIR), operates within a network where various research institutions, universities, and industrial partners collaborate to address the development of these technology platforms [9]. A key building block of the TiCoC model is targeted at the machining of titanium metal. Rather than solely focussing on improving the competency for machining titanium, the TiCoC is developing improved process chains for the production of finished parts in the aerospace, automotive and biomedical industries [9]. This will allow local manufacturers to develop high-end skills and build the capacity to position themselves to competitively participate in national and international supply chains.

The research of this study forms part of the Titanium Centre of Competence and is aimed at developing a resource efficient process chain for a modular titanium CubeSat spaceframe.

1.2 Problem Statement

The issue of energy and resource efficiency has increasing relevance in the manufacturing industry. The rising prices of energy and resources, coupled with an environmentally conscious society has put pressure on manufacturers to continuously improve their business processes. By adapting a more resource efficient approach, and having a refined process chain, it is possible for a company to enter a product into the market and retain a competitive edge over established competitors.

The use of the CubeSat platform to carry out missions in space have greatly increased over the last decade, when compared to other satellite classes. This surge in growth is supported by massive advancement in the technologies used by these small satellites. This environment is an excellent incubator for innovation, which in turn promotes a steady growth in the industry. The biggest limiting factor of the CubeSat platform is the weight restriction of the final satellite, which can force the designers to either compromise on certain aspects of the design, or move the satellite into a different class. Although the advancement of the technologies used by the satellites are big, the same innovation is not shared when it comes to spaceframe development. Several companies have brought a good product to market, but never improved on the design when it was successful.

The problem that SA AMSAT is facing at the moment is that the current prototype for the space frame takes up more than 35% of the total allowable weight of the satellite. This leaves a lot of room for improvement through innovative designs and manufacturing processes. Through the development of a resource efficient process chain, it would be possible to manufacture a modular CubeSat spaceframe according to customer specifications. By focusing on modularity, the spaceframe can be integrated with many systems and carry a wide variety of payloads. Taking into account the weight restrictions imposed by the CubeSat Design Specifications document, care should be taken to keep the spaceframe structurally sound, and not just focus on weight saving.

1.3 Research Questions

When taking the problem statement into account, it is evident that several knowledge gaps exist that must be filled, in order to create a resource efficient process chain to manufacture a resource efficient process chain. The following research questions arose from the introduction and problem statement:

- Does South Africa have a history when it comes to satellite design and development of satellites?
- What does the future market allocation look like, and who are the current major manufacturers of CubeSat spaceframes?
- What innovations in design and material selection can be used to gain an advantage over the current spaceframe designs?
- What is resource efficiency and how can it be incorporated into the process chain design?
- How does the final CubeSat prototype compare with current spaceframe designs?

1.4 Research Objectives

This study aims to develop a resource efficient process chain to manufacture a modular CubeSat spaceframe. In order for this to be realised, the following research objectives arose from the research questions:

1. Determine the market allocation for small satellites and identify the current major manufacturers of CubeSat spaceframes.
2. Investigate methods to gain a competitive advantage during the manufacturing process of the CubeSat spaceframe.
3. Design a modular spaceframe that is easy to assemble, affordable to manufacture and meets all of the customer needs and design specifications.
4. Develop a resource efficient process chain that will provide the CubeSat spaceframe with a competitive edge.
5. Validate the design by comparing the prototype to the other leading products on the market.

1.5 Project Scope

This study included the investigation of the current and future market allocation for small satellites. As satellites in the range of 1 – 10 kg is the most popular in this class, the assumption is made that this is a good representation for small satellites built on the CubeSat platform. The main focus of this research was the design and development of a modular CubeSat spaceframe. Various manufacturing methods and material properties had to be investigated in order to gain an in-depth understanding of the process at hand. These processes were completed with resource efficiency in mind, as it would provide a competitive edge when the final structure is compared to the current market leaders.

Developing a CubeSat platform to be fully compatible with most of the products available on the market is a challenging undertaking, as not all manufacturers of small satellite components conform to the same standard. This prototype is based on the assumption that the customer will utilize the PC-104 board for the payload of the CubeSat. PC-104 is an accepted standard in the CubeSat community and many manufacturers will be able to accommodate this assumption.

The designs for the CubeSat spaceframe were developed, along with the resource efficient process chains for the manufacturing procedures. The process chains contains the data received from the manufacturers, as they completed the manufacturing processes. The actual manufacturing processes could not be influenced, but the design and material selection played a major role towards making these process chains resource efficient. Because the spaceframe could not yet be fully integrated with the payload, the design validation focussed on the cost, and design efficiency. It is assumed that a higher design efficiency correlates with an easy-to-manufacture and easy-to-assemble spaceframe.

Chapter 2: Literature Study

2.1 The Value Stream Perspective

2.1.1 Value Stream Design

In-depth optimization of individual production processes, with specific emphasis on quality, reliability and output, are vital factors for sustainable corporate success, however it is not always enough to defy competition. Improvements of individual production processes can easily get lost in the bigger picture if not planned and implemented with reference to the entire production process. The main difference between the traditional supply chain and the value stream is that the supply chain includes the complete list of activities of all of the stakeholders involved, whereas the value stream is only concerned with the specific processes that adds value to the end consumer [10]. The value stream perspective takes into account the correlation between various individual production- and business processes, material and information flow, and the customer and supplier to provide a holistic view which will enable an improvement of the entire production procedure [11]. Figure 3 is an example of a value stream in a factory where each of the six basic elements interact with each other to form the *bigger picture* of the production process.

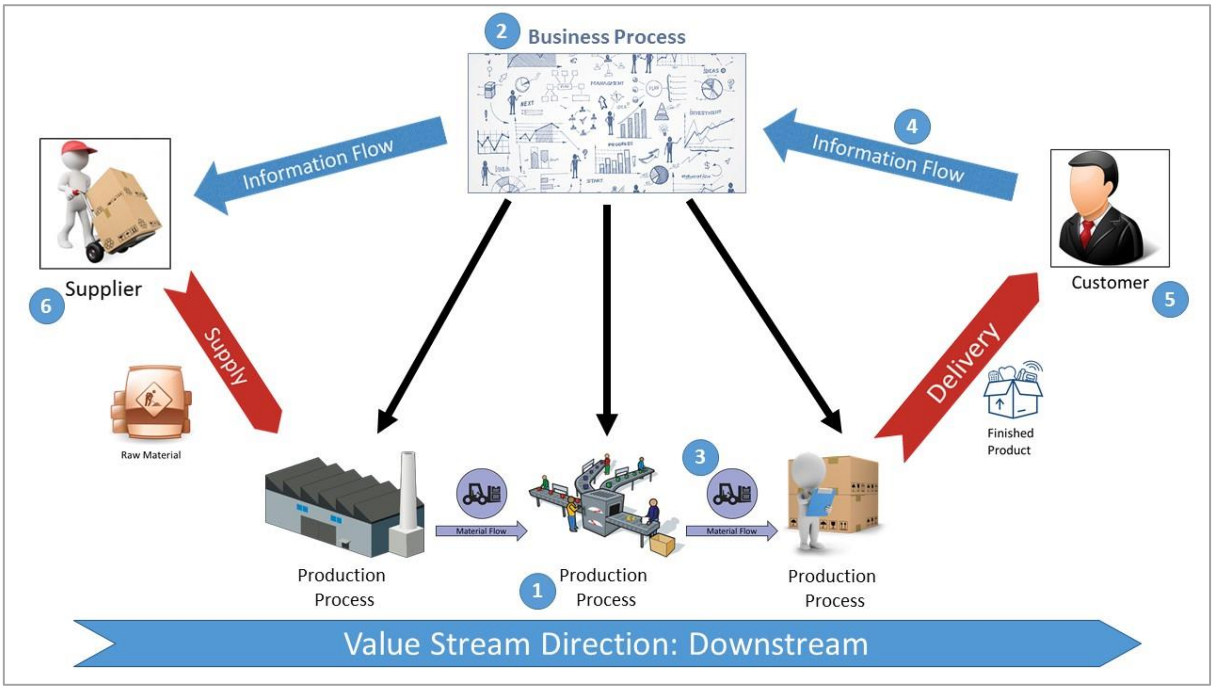

Figure 3: Value stream in a factory (Adapted from [11]*)*

The six basic elements seen in Figure 3 is described as follows:

1. The *production process* not only encompasses all of the production processes within the factory, but all of the external processing activities as well. This involves modelling each product within the entire process range as an individual production procedure, focussing only on the production process level and leaving aside the resource-related aspects, with the aim of outlining the differences between the various production procedures.

2. The *business processes* generate, process and store all the information required during production planning and control to complete a customer's order. The mapping of business processes during value stream design is not explicitly aimed towards a detailed systematic

representation of the entire work process, but rather a clear, well-arranged depiction of the overall procedure.

3. The movement of materials between production processes is defined as *material flow*. Within the value stream, material flow consist of three components: transport, handling and storage. The temporary placement of materials, products or parts is described by storage. This usually occurs within an appropriate storage facility. Transport is the moving of materials, products and/or parts to their respective retrieval areas, while handling describes the manual activities required in stockpiling and removal of stock. The production processes are logistically linked by material flow.

4. *Information flow* not only includes the transmission of data and documents between business- and production processes but also between individual business processes. The business processes are connected to by the information flow in a similar manner as the production processes are linked to each other by the material flow. In addition to this, information is also passed on from business processes to production processes, controlling everything from production scheduling to the appropriate material flows.

5. *The customer* depicts the demand that needs to be met by the production process. Value stream design aims at customer-oriented production, which means that the customer is the first element to be observed after the production process.

6. The production system's supply of raw materials is intuitively represented by *the supplier*.

2.1.2 Identification and Elimination of Waste

The fundamental underlying idea of value stream design is the identification and elimination of waste in a production process and directing the main focus towards production optimization and cost reduction [11]. Waste can be defined as every activity that adds costs to the product or process, but are non-value-added to the customer [12]. There are several ways in which waste can be classified. A traditional Japanese approach, the 3 MU, defines three types of waste [13]:

- Muda – Describes any activity that does not add value to the customer
- Muri – Describes waste associated with overloading resources beyond its capacity
- Mura – Refers to waste as a result of variation in production scheduling or uneven production workload

Ishikawa invented a cause and effect (fishbone) diagram in the 1950s to which the 4M is related [14]. This is a simple yet practical framework for examining what actions need to be taken, what are the current constraints, and how they can be overcome to improve performance. The different types of waste are Man, Material, Machine and Method. Figure 4 is a basic representation of the fishbone framework to identify and eliminate waste to increase performance. In-depth research is done on material types and machining processes to eliminate excessive waste during manufacturing. A material selection procedure was developed to help curb methodical waste and the structure was designed to be easy to assemble, thus providing the user with a product that does not waste excessive time during integration.

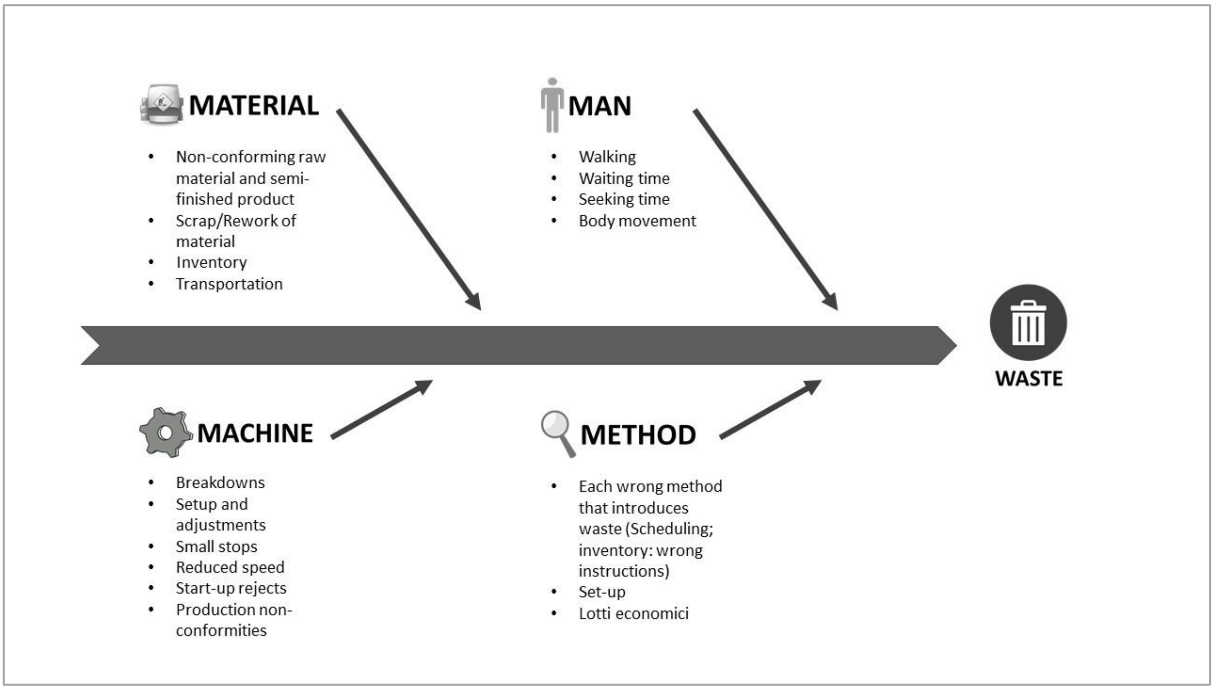

Figure 4: Ishikawa's 4M methodology for classifying waste (Adapted from [12]*)*

Hitoshi Takeda identified seven types of waste within the context of manufacturing systems [15]. These types of waste were taken into consideration during the development of the process chains for the CubeSat spaceframe. The seven relevant types of waste according to the Toyota Production System are [10]:

1. Overproduction. This is generally described by excess production of the relevant market demand and is regarded as the most serious waste because it inhibits quality and productivity by discouraging smooth production flow. Overproduction tends to lead to increased lead and storage times, and excessive WIP stocks. In value stream design, it is not only important to know when to produce, but also when not to produce. Methods for overcoming overproduction include employing the pull or Kanban system and moving away from a push production system [10].

2. Inventory. Inventory waste is materialised through stockpiling finished and semi-finished goods, raw materials and WIP [11]. All inventory requires additional handling and floor space and because of that, its presence can significantly increase extra processing. Excessive inventory tends to increase the production lead-time and prevent rapid problem identification thus discouraging communication. Unnecessary inventories not only increases the storage costs, but also the material handling and tracking costs associated with large storage areas, not including the cost of lowered productivity. This significantly lowers the competitiveness of an organization.

3. Motion. Poor ergonomics and inadequate workplace design are some of the main causes of waste through inappropriate motion sequences of operators. Any movements in production where operators have to stretch, bend or pick up something could lead to poor productivity and even quality problems [10]. Because excessive and unnecessary motion takes time and adds no value to the product or service, it is regarded as waste.

4. Defects. The finished goods or services that do not meet the necessary requirements are classified as defects and are the bottom line waste of any process [10]. In a manufacturing perspective, defects not only attributes to non-creation of value, but also destroys value that was created in previous value-adding processes. If the fault is not immediately identified, then further value-adding activities of downstream processes will be turned into waste. Defects should be seen as an opportunity to improve the production system and not a trade-off in terms of increased throughput.

5. Transportation. Any movement in a factory, where products are either moved between processes or to and from storage areas, could be viewed as waste [10]. Transport minimization should be the focus, rather than total removal, as it would be impossible to remove any and all transportation activities within a factory. There are two main reasons for transportation waste [11]. Inconvenient layout of the factory increases the length and frequency of transportation routes and are likely to cause damage and deterioration because the distance of communication between processes are directly proportional to the time it takes to feed back reports of poor quality and to take the necessary corrective actions [10]. The second reason for transportation waste is seen as an organisational issue. The transportation effort may be increased by interruptions of partially processed orders. Because storage places are not always defined, stores are overflowing or a transport order is interrupted, parts are sometimes provisionally put down wherever an open space is found. Waste due to transportation can almost be totally avoided with consistent value stream-orientated factory planning, a smooth flowing production process, a suitable special arrangement of the factory floor, and clearly marked material retrieval areas.

6. Over-processing. Over-processing can be defined as extra operations such as rework, reprocessing, handling or storage of products or parts that occur because of defects, overproduction or excess inventory [15]. The application of unsuitable technology during manufacturing is a major source of waste during processing operations. Over complex solutions need to be found for simple procedures because large inflexible machines are used instead of small flexible production operations [10]. Ownership is generally discouraged by this over-complexity and encourages employees to overproduce to recover the large investments of the complex machines.

7. Waiting. Waiting is sometimes referred to as queuing and occurs when delays in upstream activities cause periods of inactivity in downstream processes, which are then used for activities that either adds no value, or result in over-production [15]. This waste not only affects goods, but workers as well, as they also spend time waiting. The time spent by operators standing idle during machine cycles or equipment failure could be used for extra training activities. In cases where a high level of automation is applied to production, one operator can be used to monitor multiple machines, rather than one operator per machine, which will also decrease the waiting time of the worker.

2.2 Resource Efficient Manufacturing

Modern life is highly dependent on the limited supply of natural resources, with demand rapidly increasing due to emerging economies of developing countries [16]. This section explores the concept of resource efficiency during manufacturing with the end goal of reducing the dependency on natural resources through the 6R-based material flow and product and production optimization.

2.2.1 Evolution of Production Systems

The manufacturing industry has undergone many revolutionary changes over the years, yet it remains as the backbone of a modern industrialised society and has cemented itself as the cornerstone of the world's economy. These changes in the manufacturing paradigms can be attributed to changes in market and social imperatives, and the development of new and enabling technologies [17]. Figure 5 illustrates the above mentioned paradigm shifts in terms of product volume, product variety and increasing degree of complexity.

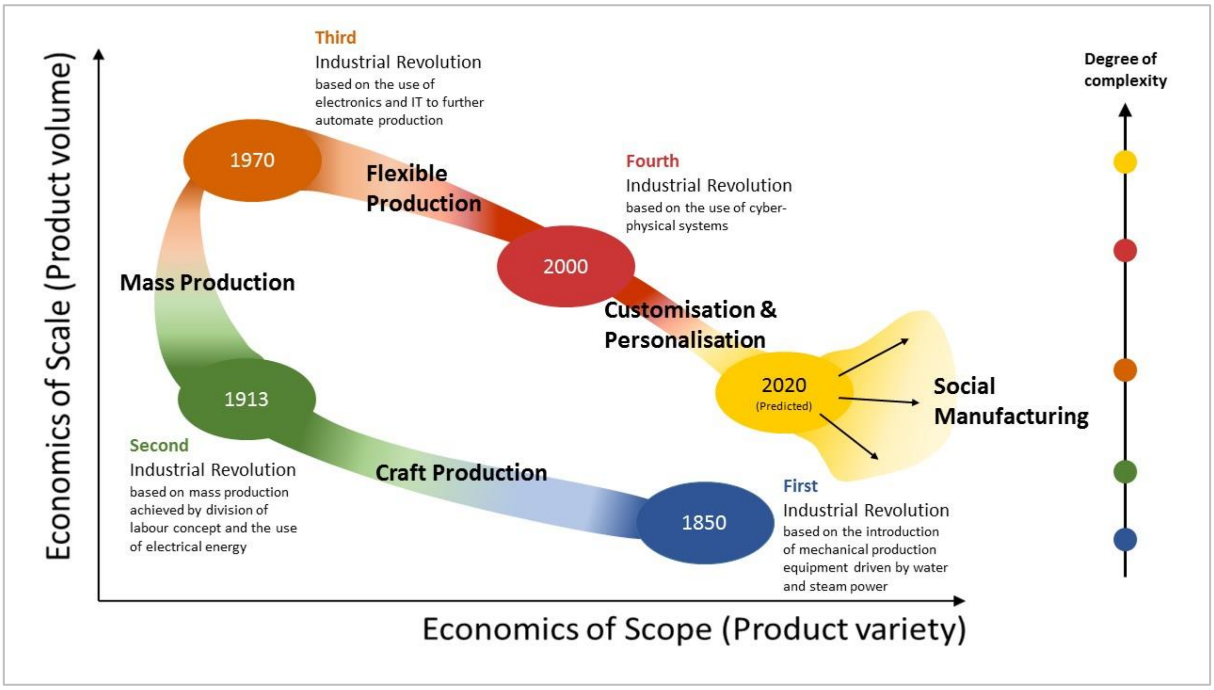

Figure 5: Production Paradigm Transformation (Adapted from [18]*)*

The first industrial revolution enabled craft production to focus more on economics of scale, and was supported by the invention of assembly lines. With specific products saturating the market in the 1970's, society demanded greater product variety, which lead the industry to move into an era of customisation and personalisation. Since the fourth industrial revolution the customers' needs has shifted from mass produced products, to high-tech, personalised, consumer driven items. These complex processes of product variability and shortened product life cycles requires an in depth knowledge of consumer preferences and open communication to the customers and suppliers.

Industry 4.0 is the fourth industrial revolution, which will enable companies to have machines, which communicate with each other to manufacture products. There is a continuous desire to improve quality of manufacturing and industry has been significantly developing to provide the high level of production. Unfortunately, the manufacturing processes implemented currently lack sustainability. Production contributes to climate change as well as the depletion of natural resources. This creates a need in industry for sustainable production solutions through the implementation of resource efficient manufacturing practices.

2.2.2 Goals of Production

The primary objectives of a production process has always been to reduce the cost, improve the quality and shorten the lead-time. If we take into account the most recent paradigm shift, as described in Figure 5, we can add variability as the fourth goal dimension of production. Figure 6 below illustrates the four goal dimensions through which the efficiency of production can be increased. Each goal dimension comprises of several partial goals, which in their reciprocal correlations define a production's system of goals and accordingly also the factory goals [11].

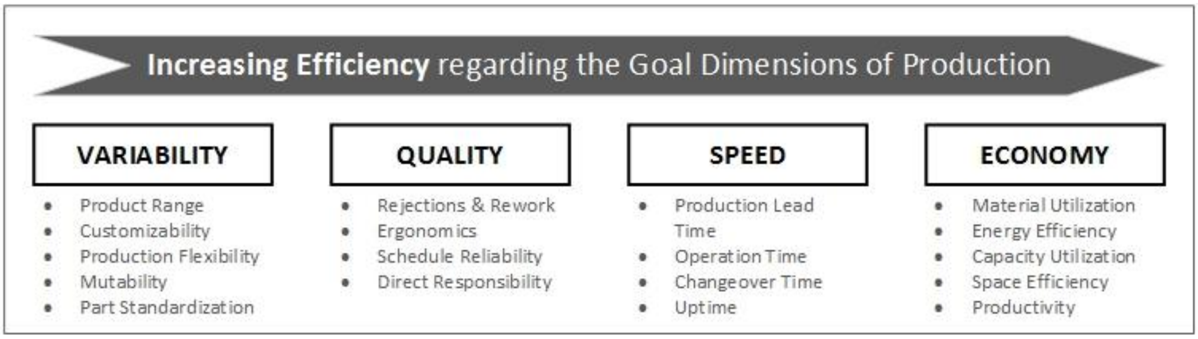

Figure 6: Goal dimensions for achieving resource efficiency in a manufacturing process (adapted from [11]*)*

The variability of production is an indication of how wide the attainable production range is. This dimension indicates how many variants of a certain product will be produced and whether or not customized products are available. Having a highly flexible production system will ensure that short term variations in market demand is met, while mutability will enable production to respond to product requirements changing in the short to medium term. The quality of production indicates the reliability of any of the production processes, and how well the tolerance levels are complied with. The speed of production is a good indication of how time-consuming the value-adding steps of production are. Finally, the productivity is indicated by the economy of production. This takes into account all the production cost factors that are influenced by the requirements of variability, quality and speed. Intuitively, if you increase the efficiency of each of the above-mentioned goals, then the overall efficiency of the entire process will be increased. This however, is not true due to the fact that the four goal dimensions conflict with each other. These goal conflicts are more or less severe, with some goals more easily achievable than others, some goals being compatible to some extent, and the attainment of certain goals are completely incompatible [11]. Figure 7 depicts the four goal dimensions arranged in a square, with the conflicting relationships between each goal dimension indicated by the four sides and the two diagonal lines of the square.

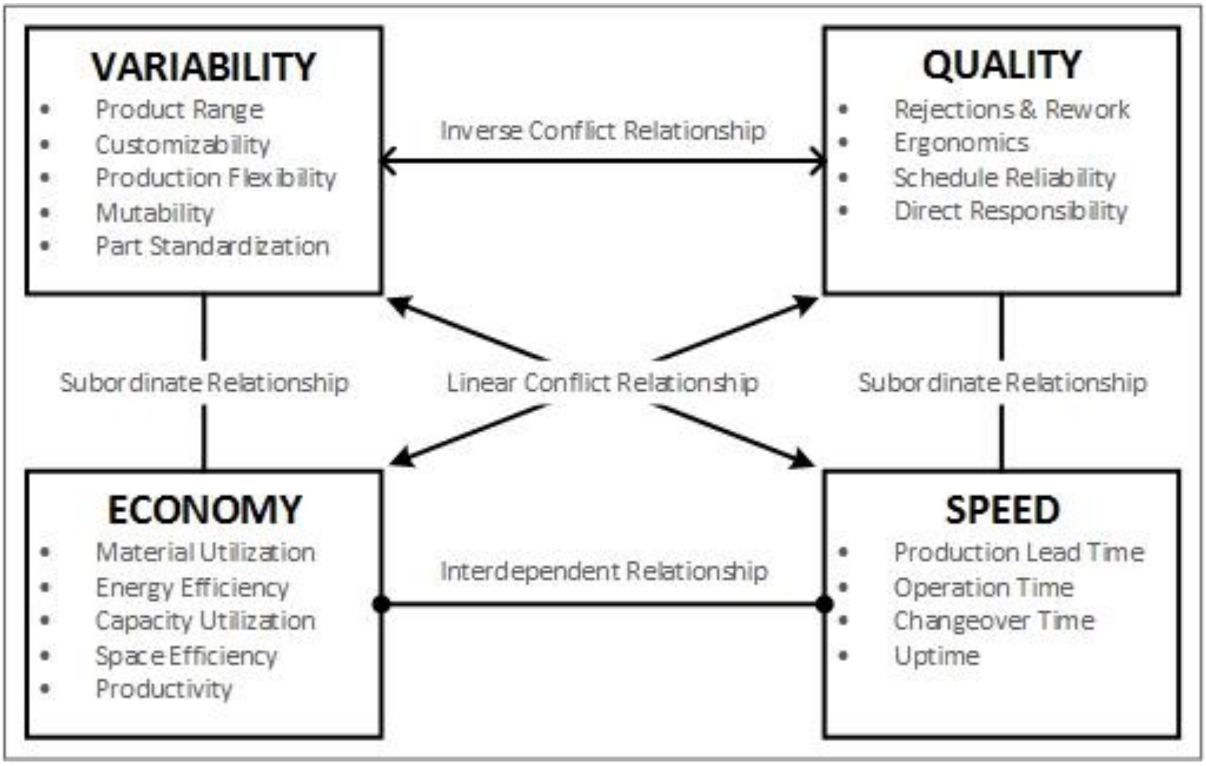

Figure 7: The four goal dimensions of production with six conflict lines (Adapted from [11]*)*

The conflict line between Quality and Economy suggest that an improvement in quality will increase the production costs. If one focusses to increase the quality of a product, then you require more precise and expensive equipment, highly skilled, therefore better payed, workers to operate the machinery and additional quality assurance processes. Refraining from these additional expenses will lead to an increase in product defects, as fewer parts will fall within the higher quality requirements. Finding a balance where adequate quality is achieved while still producing an economically competitive product is a key aspect of increasing the production efficiency.

The goals of trying to increase variability while trying to decrease speed is contradicting due to the fact that an increase in variability will lead to longer delivery times and/or higher inventory levels. The shortest possible delivery time can be achieved by holding all the products on stock, since it is faster to withdraw stock than to manufacture the product. By limiting the variability of a product, one can increase the delivery speed and decrease the manufacturing time, but this will limit the number of customers as consumers are moving towards mass customization and personalization of products [18]. A solution to this dilemma could exist in providing a consumer with a sense of customization, where they can specify certain requirements while in fact keeping the product variability to a minimum. This concept will be explored further later on in the study.

The conflict line between variability and quality is an indication that with an increased variability, it would be more difficult to meet the quality goals, and on the other hand, an increase in quality requirements would restrict variety and flexibility. A new type of risk associated with unplanned delays during production is brought about by an increase in product variety due to customer specific design adaptations. Quality problems due to slow or incorrect design adaptations can be eliminated by having a customer select a product from a catalogue, but this will in turn limit the variability or greatly increase the inventory cost if a very large product catalogue is available.

In most cases, it is easier to improve productivity and utilization, as indicated by the conflict line between variability and economy. It is generally easier to reduce the manufacturing cost of a standard product than to make an existing production system more flexible in order to manufacture a more diverse product range. Increasing the adaptability of an existing production system is a challenging undertaking since it requires changing the design of the existing manufacturing resources, even though a more flexible machine can be better utilised than an inflexible one. It is possible to fulfil both goal dimensions, even though they are located on completely different levels of production design. They still conflict with each other, as too much flexibility will decrease the overall production efficiency.

It is much easier to decrease the manufacturing- or delivery time of a production process than to increase the standards to which a product must adhere, as indicated by the conflict line between the speed and quality goal dimensions. By developing a good strategy to manage the manufacturing process, it is possible to improve production reliability by reducing the manufacturing lead-time. Similarly, the quality of some production processes will rise, if execution is accelerated.

Finally, the conflict line between economy and speed is an indication that both of these goal dimensions can be improved at the same time. By reducing the setup times in conjunction with smaller lot sizes will result in decreased inventories, reduced lead times, an increase in machine utilization and lower setup costs. Decreasing lead-time inevitably reduces the associated inventory costs, thus to some extent indicating that both economy and speed correlate positively to one another.

An optimal solution would then be to develop a process chain with emphasis on quality, rather than variability. The increased production costs that results from focussing on quality can be countered by standardising the components. This will decrease the manufacturing time, increase the delivery speed of the product, and minimize the inventory needed for a flexible production system.

2.2.3 6R's for Sustainable Manufacturing

Sustainable manufacturing can be defined as the creation of products that utilizes processes that [19]:

- Minimize negative environmental impacts
- Conserve energy and natural resources
- Are safe for employees, communities and consumers
- Are economically sound

Finding a solution to the issues of sustainable manufacturing, involves viewing it as a complex systems problem with three integral interacting levels: products, processes and systems [20]. Figure 8 below is a visual representation of this systems problem where the interaction between the levels in order to achieve sustainable manufacturing.

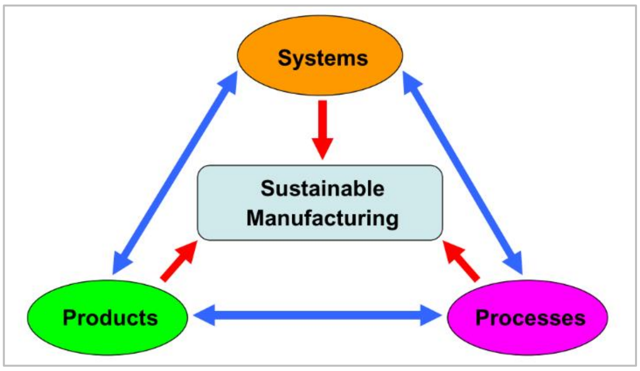

Figure 8: Integrated elements of sustainable manufacturing (Adapted from [20]*)*

The principles of 3R's: *Reduce, Reuse and Recycle,* can be seen as the foundation on which green manufacturing is based [21]. These principles were derived from lean manufacturing practices, which focussed on the elimination of waste throughout the entire process, and lean manufacturing is in turn based on 1R (Reduce) which was introduced in the 1980's [20]. The interaction between each of these manufacturing principles, as well as the approximate stakeholder value can be seen in Figure 9 below. It can be seen that the current trend for achieving sustainable value in manufacturing requires the transformation from lean manufacturing, to green manufacturing, to sustainable manufacturing.

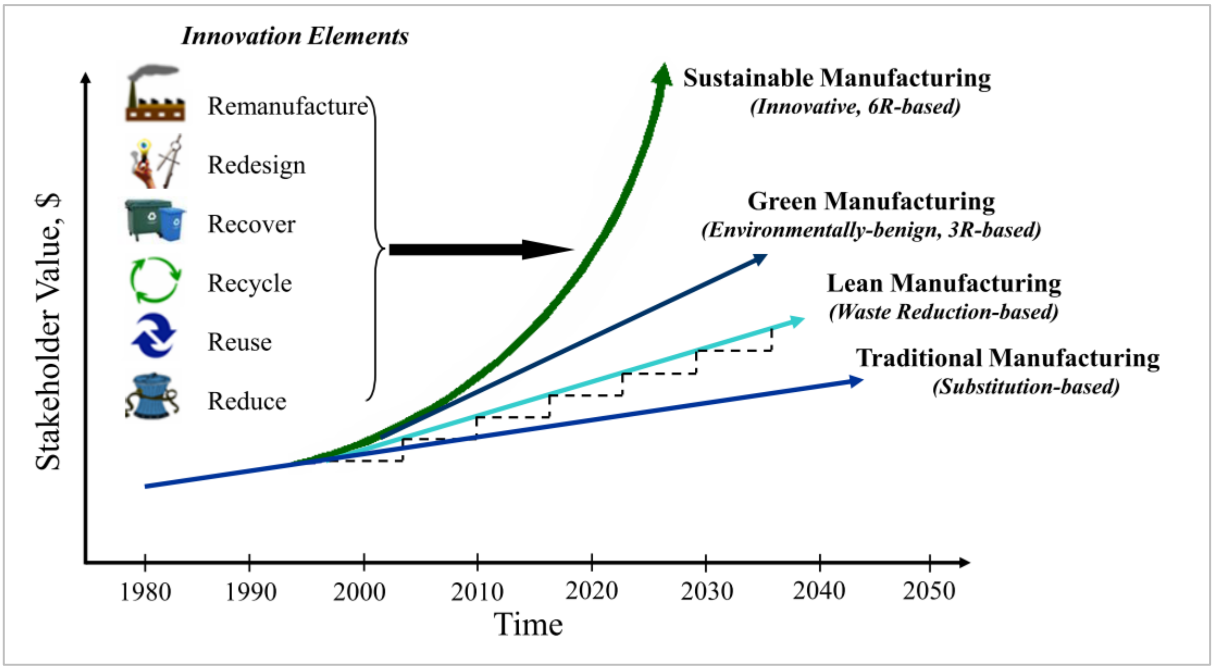

Figure 9: Evolution of sustainable manufacturing (Adapted from [20])

The interaction between the manufacturing process chain and the 6R principles have a positive influence on the environment, as it enables a near-perpetual material flow while facilitating the optimal use of energy, raw materials and other resources [22]. The six principles can be explained as follows [20]:

- ***Reduce*** focusses on the first three stages of the product lifecycle. The reduced use of resources in pre manufacturing, reduced use of energy, materials and other resources during manufacturing, and reduction of emissions and waste during the *use* stage.
- ***Reuse*** refers to the reuse of either the entire product, or its components, after its first life cycle. The end-goal of this principle is to reduce the usage of virgin materials during production of new products.
- ***Recycle*** is the process of converting material that would otherwise be considered waste into new materials or products.
- ***Recover*** involves the collection of products at the end of the *use* stage, disassembling, sorting and cleaning for utilization in subsequent life cycles.
- ***Redesign*** involves the act of redesigning the next generation of products to use components, materials and resources recovered from previous life cycles.
- ***Remanufacture*** is the process of restoring used products to their original state through the reuse of as many parts as possible.

2.3 Subtractive Manufacturing Processes

The family of shaping operations in which excess material is remove to achieve the final part geometries are known as material removal processes. Figure 10 below is a schematic illustration of the material removal family tree.

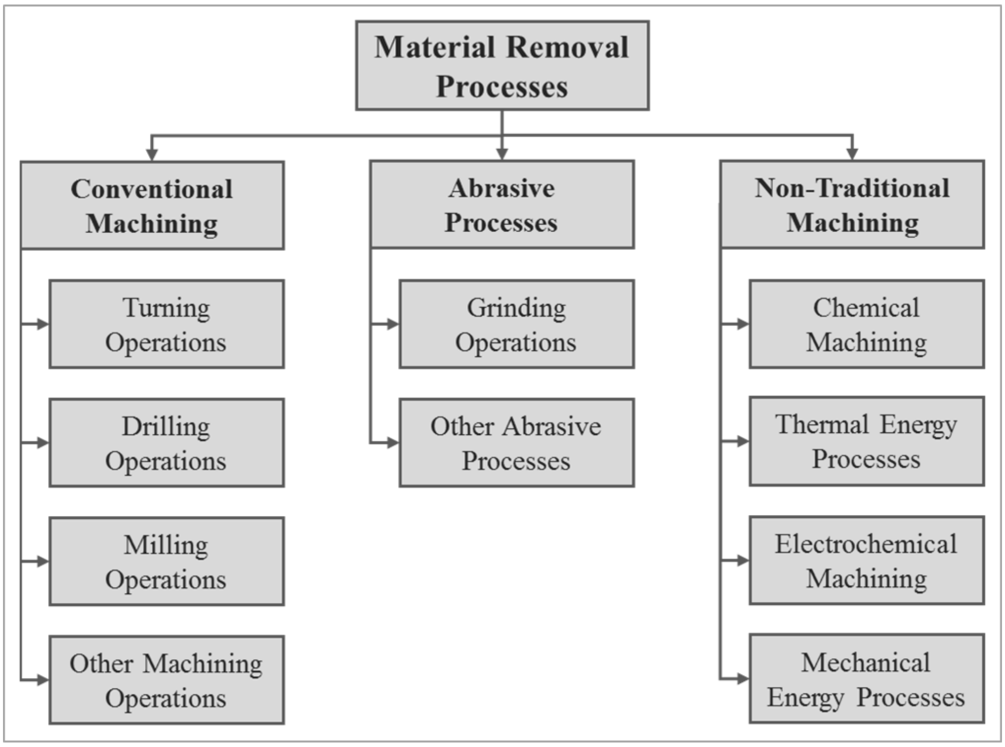

Figure 10: Schematic illustration of the material removal process family tree (Adapted from [23])

The three branches, Conventional Machining, Abrasive Processes and Non-Traditional Machining are shown with their respective sub-groups branching out below them. The material removal process is one of the most important manufacturing operations, as it allows the final part to achieve very high dimensional accuracies and extremely fine surface finishes [23].

2.3.1 Conventional Machining Processes

Conventional machining is considered to be the most important branch of the material removal family [24]. This process involves the use of sharp cutting tools to mechanically cut material to achieve the desired part geometries. Turning, drilling and milling operations are the principal machining processes, and is defined as cutting processes in which layers of material are mechanically separated from the workpiece by means of a cutting tool [25]. The separated pieces of material are known as chips, and chip formation plays a vital role in the science of machining processes. Other machining operations include shaping, planning, broaching and sawing.

2.3.1.1 Milling Operations

Milling is known as a subtractive machining process, where a rotating tool with defined cutting edges is moved relative to a workpiece to remove material with the end-goal of obtaining the desired part geometry [25]. This manufacturing technique is one of the most commonly used processes in a variety of industries ranging from tool and dye making, automotive, aerospace and biomedical to name a few. The cutting process uses a rotary tool with multiple cutting points to remove material from the work piece. The cutter moves perpendicular to the cutting surface at certain speeds called the feed rate. During the cutting process, chips form at the base of the cutter and is sheared off the work piece, thus removing the material. Figure 11 is a schematic representation of the chip formation and removal process that happens at the contact point between the tool and the workpiece.

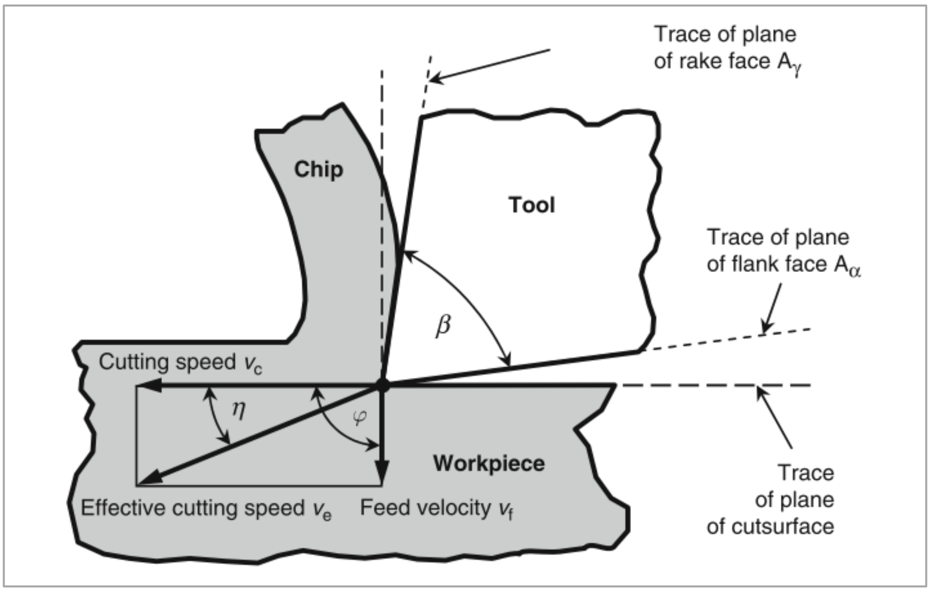

Figure 11: Mechanics of chip formation at the cutting edge of the tool (Adapted from [25]*)*

The cutting edge of the tool is known as the rake face A_γ and the face on the cutting wedge is called the flank face A_α. The workpiece is assumed to be fixed during the manufacturing process. The speed at which the cutting tool moves, relative to the workpiece, is intuitively called the cutting speed v_c, and the speed of which the tool is moved in the feed direction (into the workpiece) is called the fed velocity v_f. The resulting velocity vector of v_c and v_f is designated as the effective cutting speed v_e. The angle between the effective cutting direction and the direction of primary motion is known as the effective cutting speed angle η. The feed motion angle φ is the angle between the feed direction and the direction of primary motion. This concept forms the basis of calculating the material removal rate, which will give an estimation as to how long it will take to manufacture a certain part [26]. With the CAD/CAM software available today, these times can easily and accurately be simulated. It is however necessary to understand these concepts as it plays a vital role during process chain development.

A scaled down version of this manufacturing process is known as Micro-Milling. This manufacturing process has rapidly gained momentum because of its viability to directly produce miniature 3-D functional parts [27]. The micro-milling process is not only fast to fabricate 3-D features but also cost effective when compared to other micro-manufacturing processes. Parts with 3-D geometries are directly machined one at a time and do not require batch set-up. Micro-milling can achieve good accuracy, low surface roughness, and can provide high material removal rates (MRR), relative to the part size, with features as small as 5-10 µm [28].

2.3.2 Abrasive Machining Processes

The second branch of the material removal family is that of abrasive processes. These processes remove material from the workpiece by action of hard, abrasive particles that are usually in the form of a bonded wheel, or abrasive belts [29]. Grinding operations remove material by means of abrasive particles, usually contained in a bonded grinding wheel that is rotating at very high speeds.

In order to appropriately grind the different work materials, different abrasive materials should be used. These abrasive particles vary in grain size and play an important role in determining the surface finish and material removal rate [30]. The bonding material that holds the abrasive grains together establishes the overall shape and structural integrity of the grinding wheel. In addition to having bonding material and abrasive grains, grinding wheels also contain air gaps or pores, as illustrated in Figure 12.

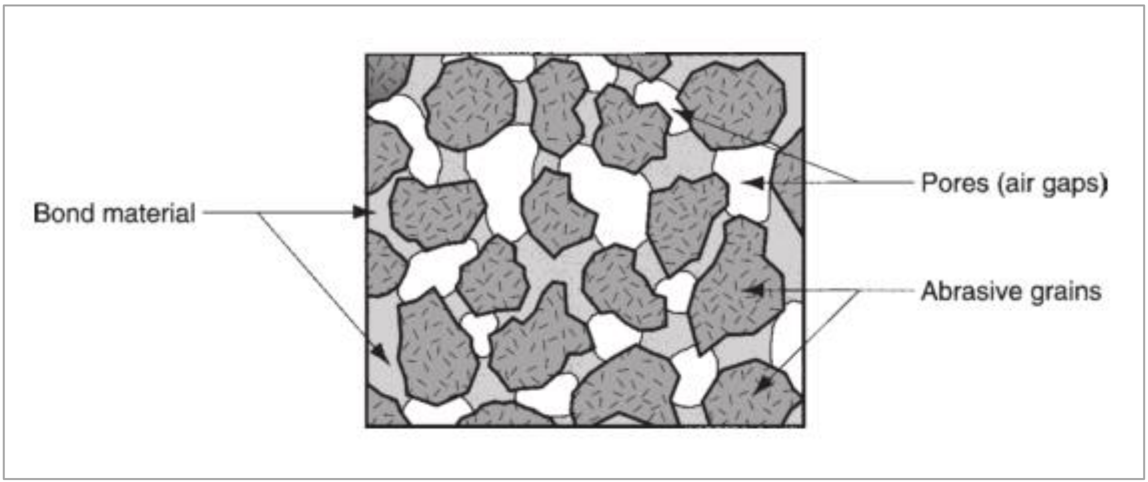

Figure 12: Typical structure of a grinding wheel illustrating the abrasive grains, bonding material and air gaps (Adapted from [25])

Grinding is not only the most important abrasive process, but also the most common of all metalworking processes, as it is generally used for finishing operations to produce extremely fine surface finishes and extremely close dimensional tolerances [29]. The other abrasive processes include honing, lapping, superfinishing, polishing and buffing

2.3.3 Non-Traditional Machining Processes

Non-Traditional Machining refers to manufacturing processes that remove excess material through various techniques involving mechanical, thermal, electrical, chemical, of a combination of these energies. They do not make use of a sharp cutting tool in the conventional sense, and was largely developed in response new and unusual machining requirements that could not be satisfied by conventional methods.

2.3.3.1 Wire Electrical Discharge Machining

Electrical Discharge Machining is a non-conventional material removal process based on thermoelectric energy between the work piece and an electrode. The electrical discharge phenomena observed in EDM occurs over a very short period of time, in a very narrow space filled with dielectric fluid, and involves the evaporation and melting of the work piece and electrodes [31]. The principle concept of EDM is shown in Figure 13. Material is removed by a pulse discharge in the small "gap" between the work piece and the electrode [32]. This gap is filled with an insulating dielectric fluid such as hydrocarbon oil or de-ionized water. The insulating effect of the dielectric medium has some importance in avoiding electrolysis effects on the electrodes during the EDM process [31].

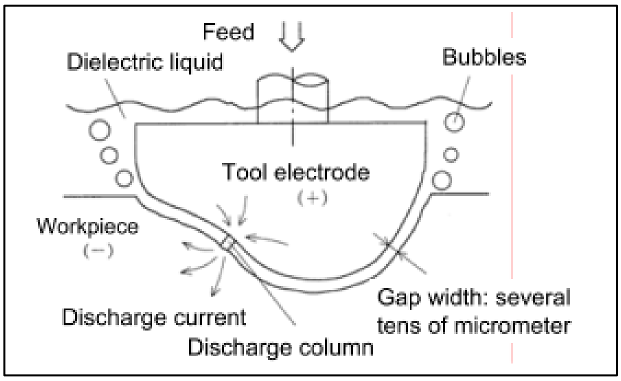

Figure 13: EDM concept. (Adapted from [35])

A unique adaptation of the EDM process is Wire Electrical Discharge Machining (WEDM). WEDM involves the utilization of continuously traveling wire electrode, made of thin copper, brass or tungsten, with a nominal diameter varying between 0.05-0.3 mm [33]. This specialized thermal machining process is capable of achieving a considerable dimensional accuracy and surface finish on parts with complex shapes and varying degrees of hardness that are difficult to produce by using traditional machining processes [34].

The WEDM process utilizes a thin wire electrode that is constantly feeding through the workpiece by a microprocessor and kept under tension using a mechanical tensioning device while submerged in a bath filled with dielectric fluid. A series of discrete sparks between the workpiece and the wire then erodes the material from the part producing exceptionally high dimensional accuracy with a good surface finish [31]. The microprocessor maintains a gap varying from 0.025 to 0.05mm between the wire and the workpiece [33]. The most important characteristics in WEDM process are cutting rate, wire wear rate and wire failure frequency, kerf size and most importantly quality of machined surface [33]. Those characteristics are influenced by the different machining parameters. Optimization of these parameters for each material or group of materials is necessary; otherwise failure of the components can occur. The WEDM process is displayed in Figure 14. Wire passes through the workpiece during machining and the precise gap, known as the sparking gap, must be maintained between the wire and the workpiece. The width of the final kerf is given by diameter of wire diameter plus two times spark length, as seen in Figure 14.

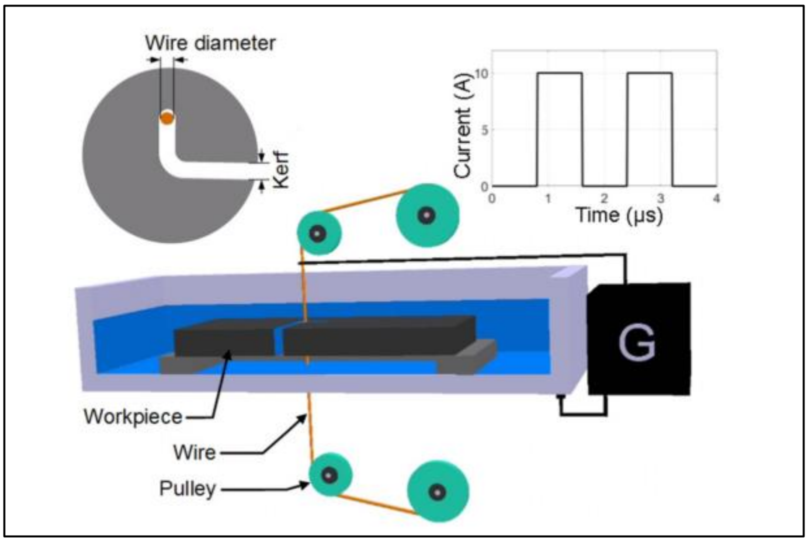

Figure 14: Diagram of the WEDM Process. (Adapted from [8])

2.3.3.2 Laser Beam Cutting

Laser Beam Cutting (LBC) is a thermal energy based non-conventional cutting method in which sheet material is cut mainly due to melting and vaporisation and the molten material is then ejected with the help of high-pressure assist gas jet [35]. The schematic of the LBC process is shown in Figure 15. LBC can successfully be used for the cutting of conductive and nonconductive difficult-to-cut advanced engineering materials such as reflective metals, plastics, rubbers, ceramics and composites. Apart from cutting difficult-to-cut materials, LBC is most widely used in industries to achieve complex shapes/profiles with close tolerances for cutting of steel sheets [36]. multi-objective optimisation. The results of multi-objective optimisation using Taguchi's quality loss function only have also been compared with the results from hybrid approach.

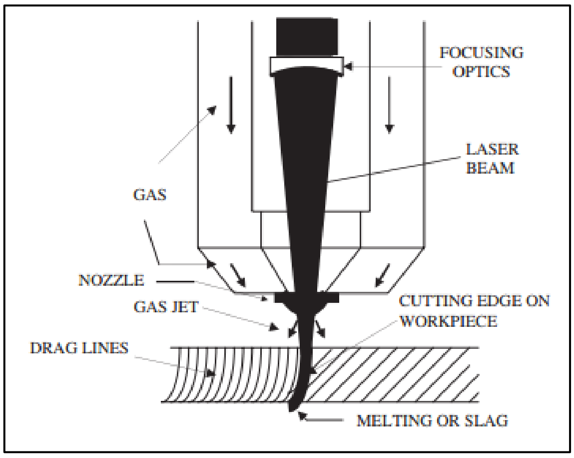

Figure 15: The Laser Beam Cutting Process. (Adapted from [35])

2.4 Material Properties and Applications

2.4.1 Titanium and Titanium Alloys

Titanium was first discovered in 1791 by a British reverend, mineralogist and chemist, named William Gregor. He examined magnetic sand, which external appearance resembled that of gunpowder, from a local river in Cornwall, England. After removing the iron with a magnet, he treated the remaining portion of the sand, which external appearance resembled that of gunpowder, with hydrochloric acid to produce the impure oxide of a new element that he named *"mechanite"*, after the Menachan Vallei where the discovery was made [37]. A German scientist named Martin Heinrich Klaproth was investigating a red ore from Hungary in 1795. He independently isolated titanium oxide, and after realizing that it was of a previously unknown element, he named it Titanium, from the Greek word titanos (Titans) [37].

More than 100 years after the discovery of titanium, Matthew Albert Hunter, a metallurgist from Rensselaer Polytechnic Institute in Troy, N.Y., was able to isolate 99.9% pure titanium by heating titanium tetrachloride (TiCl4) with sodium in a steel bomb [38]. In 1932, the father of the titanium industry, Wilhelm Justin Kroll, was finally able to produce significant quantities of titanium by combining TiCl4 with calcium [38]. After fleeing to the United States at the beginning of World War II, he was able to demonstrate that titanium could be extracted commercially by reducing TiCl4 by changing the reducing agent from calcium to magnesium. This process is known as the *"Kroll process"* and is still the most widely used method for extracting titanium.

The DuPont Company was the first to produce titanium on a commercial scale in 1948, with the worldwide production reaching just over 3 tons per annum. Scientists and engineers soon realised the desirable properties of this element and in 8 years, the worldwide production skyrocketed to 25000 tons a year [37].

The physical properties of high-purity polycrystalline α titanium can be seen in Table XX. The two properties that primarily causes titanium alloys to stand out are the high specific strength and excellent corrosion resistance of the metal [39]. With a density of 4.51 g/cc, titanium is classified as the heaviest light metal, with a specific weight of about half that of nickel and iron [40].

Table 2: Physical properties of high-purity polycrystalline α titanium

Properties	**Metric**
Density	4.51 g/cc
Brinell Hardness	120
Ultimate Tensile Strength	240 MPa
Modulus of Elasticity	105 GPa
Poisson's Ratio	0.37
Charpy Impact	310 J
Shear Modulus	45 GPa
Electrical Resistivity	4.5e-005 ohm-cm
CTE, linear 250°C	9.2 µm/m-°C
Specific Heat Capacity	0.52 J/g-°C
Thermal Conductivity	16 W/m-K
Melting Point	Max 1670 °C
Beta Transus	888 °C

2.4.1.1 Crystalline Structure of Titanium

Pure titanium, along with the majority of titanium alloys, crystallizes at low temperatures in a hexagonal close packed (HCP) structure, called α-titanium [41]. At high temperatures, the body-centred cubic (BCC) structure known as β-titanium is stable [41]. Figure XX is a schematic representation of the HCP α- and BCC β-titanium crystalline structures. The allotropic transformation of pure titanium happens at the β-transus temperature of 882 ± 2^{0}C. By dissolving certain elements into titanium, the transformation temperature can strongly be influenced [37].

Alloying elements of titanium are classified depending on their influence on the β-transus temperature ad neutral, α-stabilizers, or β-stabilizers. Alpha stabilizers produce an increase in the transformation temperature and include elements such as aluminium, oxygen, nitrogen and carbon. The lattice parameters of the HCP crystal structure in α-titanium are a = 0.295nm and c = 0.468nm. This yields a c/a ratio of 1.587 [41]. The ideal c/a ratio for a HCP lattice is 1.633, which can be achieved through the insertion of interstitially dissolved atoms in the HCP lattice, like carbon, nitrogen or oxygen [41]. Beta stabilizers produce a decrease in temperature of transformation and consist of molybdenum, vanadium, niobium, copper and silicon. Other elements have very little effect on the transformation temperature and are called neutral element. Even though more than 100 titanium alloys are known, only about 20 to 30 of them have reached commercial status. Of these commercially available titanium alloys, Ti-6Al-4V covers more than 50% of the total usage [42]. Because Ti-6Al-4V is one of the recommended materials to use for the CubeSat spaceframe, the rest of this section will focus on this alloy during further investigation.

2.4.1.2 Machinability of Titanium

The ability of titanium and titanium alloys to retain high levels of hardness at high temperatures poses a major difficulty when machining titanium-based alloys [43]. The lower thermal conductivity of titanium is seen as a positive in the various areas of application, but it hinders the quick dissipation of heat caused by machining, which leads to increased tool wear during the cutting process [44], [45]. Titanium's lower modulus of elasticity leads to significant spring back after deformation under load, causing the parts to move away from the cutting tool during manufacturing [46]. The chemical reactivity of this alloy, along with the high temperatures in the tool/chip contact area, causes galling between the tool and the part, leading to increased tool wear [46].

Milling of titanium components is more difficult when compared to turning, because of titanium's tendency to smear and gall with the tooling [47]. This process is best performed by using sharp, short length cutters with sufficient flute space to avoid chip clogging. Drilling is best done by having a high feed rate, low cutting speed and cooling with chlorinated cutting oil to prevent excessive friction [25]. The rake angle should be sufficiently large to avoid welding the tool to the work piece, and the drill should be raised frequently to remove the drilling chips. Titanium can be sawn using conventional band saws, but requires a reduced saw speed and appropriate cooling because of the poor heat dissipation. To achieve the best results during grinding operations, the wheel speed should be half to one third that of conventional operating speeds, with ample coolant to prevent smearing or intense sparking [29].

Taking into account the above-mentioned material properties and machining difficulties, the following guidelines should provide a baseline for the successful machining of titanium parts:

- Only sharp cutting tools should be used, and replaced at the first sign of wear, to prevent total tool failure
- The work piece should be mounted to be vibration free in the machine to prevent chatter phenomena. Keeping the work piece as short as possible and having a stiff tool-part-machine system will help in this regard
- Low cutting speeds should be used in conjunction with a high feed rate. Maintaining a continuous feed rate while the cutting tool and work piece are in contact, will limit the occurrence of galling and smearing at the cutting edge
- By effectively cooling the titanium work piece and promoting rapid heat dissipation through the use of copious amounts of cutting fluid, the tool life can be extended
- Before machining commences, the hard surface scales should be removed, either by grit blasting, or by submerging the part in a pickling solution of 2% hydrofluoric acid and 20% nitric acid

2.4.1.3 Applications of Titanium

In the 1940s, the United States developed titanium and its alloys specifically for aerospace applications, and accounts for 50% of the worldwide titanium consumption today [48]. This is not surprising, as the higher tensile strength and lower density of titanium and titanium alloys allows for increased strength-to-weight properties when compared to steel and aluminium, making the material well suited for the aerospace industry. The aerospace market however, is categorized by vigorous boom-to-bust demand and price cycles, and efforts are being made to substantially increase titanium consumption in less cyclic, non-aerospace markets [48], [49]. This section will look at both the aerospace and non-aerospace applications of titanium to provide more background into this material and its various uses.

2.4.1.3.1 Titanium Alloys for Aerospace Applications

The biggest reason for choosing titanium in aircraft airframe applications is attributed to the higher payoff for weight reduction. A standard Boeing 747 carries about 100 tons of fuel, which is equal to approximately one third of the take-off weight, substantially limiting the remaining payload of the jumbo jet. By lowering the fuel consumption by only 10%, the total payload could be increased by an estimated 10 tons. Less fuel means less weight, which will allow for the use of smaller, lighter engines. Similarly, the landing gears, wings, support structures and various other components could be downsized to cause a *"snowball effect"* which will lead to further weight savings, and effectively cost savings as well. This simple example is the economic driving force for using titanium alloys for weight saving purposes in aerospace applications [50].

The main application for titanium alloys in the aerospace industry is in the gas turbine engine. The first component to be manufactured from titanium was the compressor blades, with the compressor disks being introduced next, and the large front fan blades of modern jet engines are now often made from titanium alloys too [51]. This increased use of titanium is fuelled by the need for further weight reduction of fan blades and disks in the jet engines, while extending component life or inspection intervals. Since the fan blades and disks are used at low temperatures, they are normally manufactured from Ti-6Al-4V [51].

For fuselage applications, thin, narrow titanium alloy rings are placed around the aluminium aircraft airframe to prevent fatigue cracks from growing and propagating catastrophically in the outer skin of the aircraft. Weight savings of up to 40% are possible when using titanium alloys for the hydraulic tubing of modern aircraft [52]. The α+β alloy, Ti-3Al-2.5V, is primarily used for this application as it is easily deformed and demonstrates sufficient strength, when compared to steel tubes. The floors surrounding the aircraft's on-board kitchens and toilets require a high corrosion resistant material with moderate strength, and commercially pure titanium is used for this application [46]. Unalloyed titanium is used to manufacture the piping system for the de-icing equipment, as thermal stability and excellent corrosion resistance is required to transport aggressive media at temperatures exceeding 200^0C.

Although aircraft landing gear components manufactured from forged titanium alloys have a higher initial cost than its high-strength steel counterparts, the investment pays off over the long term, as TIMETAL 10-2-3 components do not need to be replaced during an aircraft's lifetime [53]. Forged titanium alloys are also used for the manufacturing of the cockpit window frames, because of the potentially high loads from bird strikes and other airborne debris. Finally, the larger thermal and mechanical loads associated with greater manoeuvrability and supersonic cruise speed of military fighter aircraft, accounts for the proportionate use of titanium alloys in these aircraft fuselages to exceed 50% [53].

Forged Ti-6Al-4V rotor heads are used in helicopters, as this is the most highly stressed component.

The comparatively small payload of space vehicles, the structural weight saving is even more important when compared to aircrafts. The standard application for titanium alloys in spacecraft are in the fuel and satellite tanks [51]. Because of titanium's low weight, high strength and long-term compatibility with fuel, titanium alloys provides more advantages than high-strength steels.

2.4.1.3.2 Titanium Alloys for Non-Aerospace Applications

The high strength, low weight and excellent corrosion resistance of titanium and its alloys has caused an increasing trend to use this material outside the aerospace market. Several uses in the chemical, medical, energy and transportation industries, as well as applications in architecture, sports, and leisure have all played a pioneering role in developing high quality industrial and consumer products.

The extreme corrosion resistant properties of titanium alloys means that the material usually requires no corrosion allowance when used in the chemical, process and power generation industries. Even though the initial costs are higher, it is compensated for with less down time and reduced maintenance costs. As the main requirements for these applications are corrosion resistance, unalloyed and low-alloy titanium grades are used [54]. Commercially pure titanium have demonstrated their superior corrosion resistance and good thermal conductivity in applications for heat exchangers where the cooling medium is seawater, brackish water or even polluted water. This application is prevent in land based oil refineries and offshore oilrigs where both tubular and plate-type heat exchangers are applications [54]. Grade 2 commercially pure titanium is used for containment and tank construction in the chemical, electrochemical and petrochemical industries.

The high cost of the raw material is the limiting factor for widespread use of titanium alloys in the mass market of the automotive industry [55]. Although titanium sees uses in the racing and high performance sectors, it is not yet economically viable for widespread use in low-end markets.

Titanium is mostly used for parts that are exposed to aggressive atmospheric conditions, and does not degrade during service. This makes the material the most competitive of all architectural metals on a life-cycle basis, as it is 100% recyclable. Grade 1 titanium is the most widely used alloy and allows for wall thicknesses ranging from as thin as 0.4mm in architectural components.

Various types of sports make use of titanium alloys when manufacturing the equipment. Golf clubs, tennis racquets, baseball bats, pool cues and even bicycles make use of the various desirable properties of titanium alloys to provide their users with a competitive edge. Certain kitchen knives, scuba diving equipment and high strength climbing gear is manufactured from titanium, utilizing the low weight, high strength properties of the metal.

Titanium's excellent compatibility with the human body is regarded as the key property of choice for use in the biomedical industry. Furthermore, the material's inherent resistance to corrosion ensures its longevity when exposed to bodily fluids, it is elastically deformable as a thin foil to match the necessary contours for joint replacements, and its compatibility with bone and living tissue drastically reduces the chances of the human body rejecting the implant [56]. Titanium can withstand repeated sterilization cycles, which makes it an ideal material to use for surgical equipment. Titanium also sees widespread use in the dental industry, where the pure elemental form avoids chemiophysical reactions in the mouth, thus excluding the danger of the patient having a metal allergy [57].

2.4.2 Aluminium and Aluminium Alloys

The ancient Greeks and Romans first used a form of aluminium, called alum, as an astringent in medicine, as well as in dyeing processes. In 1807, an English chemist with the name of Sir Humphrey Davy underlined the existence of the element, which according to him, should be named *"alumium"*. He argued that alum was the salt of an unknown metal, but was unsuccessful in his efforts to produce aluminium, as it was later renamed by scientists. Following Davy's work, H.C. Oersted, a Danish physicist, managed to produce the first nodules of aluminium in 1825, by heating potassium amalgam with aluminium. It was only in 1845, when German chemist Friedrich Wöhler discovered the metals remarkable lightness while characterising many of the metals properties, that researchers truly got excited about this material [58]. The smelting process that is still used today was simultaneously, but independently discovered in 1886 by Charles Martin Hall in the United States, and Paul Lois Toussaint in France. Both men dissolved aluminium oxide in molten cryolite, then extracted aluminium by means of electrolysis. This process was further advanced in 1888 when and Austrian chemist named Carl Josef Bayer invented a process for extracting aluminium oxide from bauxite, which made the metal a commercially available commodity [59].

Aluminium is characterised by its low density, high strength of some alloys, and its ability to resist the kind of progressive oxidization that causes steel to rust away [60]. This unique combination of properties makes this metal one of the most versatile, economical and attractive materials for a broad range of uses. With a density of only 2.7g/cm^3, aluminium alloys are second only to steels for use as structural metals.

Aluminium's surface, when exposed to oxygen, forma a very thin aluminium oxide film, which prevents further oxidization. This aluminium oxide film does not flake off to expose a fresh surface to further oxidise, and when scratched, it instantly reseals itself [61]. This this colourless, layer is what gives aluminium its inherent ability to resist corrosion. Even though aluminium typically displays excellent electrical and thermal conductivity, specific alloys have been developed with high degrees of electrical resistivity to be used in high-torque electric motors. With a thermal conductivity of about 50% to 60% that of copper, aluminium alloys displays many advantages to use in heat exchangers, evaporators, electrically heated appliances and automotive cylinder heads [62]. Another important asset of aluminium is the ease of which it can be fabricated into any form. The metal can be cast by any of the known methods or rolled down to any desired thickness, including foil, that is thinner than paper. Aluminium sheets can be stamped, drawn, spun or roll formed, and the metal can also be hammer forged to the desired shape, and there is almost no limit to which profiles the metal can be extruded to [63].

2.4.2.1 Classification of Aluminium Alloys and Their Uses

Aluminium is divided into two categories: wrought compositions, and cast compositions. The alloys are then further categorised based on the primary mechanism of property development, such as solution heat treatment, quenching and precipitation hardening [64]. A large number of wrought compositions however, rely on work hardening through mechanical reduction, and is usually used in combination with various annealing procedures for property development. Some cast alloys are not heat treatable and are used only as-cast [64]. This section will define the nomenclature for describing the different categories within wrought and cast aluminium alloys.

2.4.2.1.1 Wrought Aluminium Alloys

Wrought alloys use a four-digit system to describe the list of composition families. The general characteristics and uses of each wrought aluminium alloy is described as follows [62]–[65]:

- ***1xxx:*** This series contains aluminium of 99.00% purity or higher. It is characterised by high electrical and thermal conductivity, low mechanical properties, excellent workability and high corrosion resistance. These grades of aluminium has many applications, but are especially favoured in the electrical and chemical industries.
- ***2xxx:*** The principal alloying element in the *2xxx* series is copper, with magnesium often used as a secondary addition. Through solution heat treatment, these alloys obtain mechanical properties that are similar to, and sometimes exceed that of low-carbon steel. These mechanical properties can further be increased through precipitation heat treatment. Even though they do not have as good corrosion resistance as most other aluminium alloys, the *2xxx* series is particularly well suited for parts and structures that require high strength-to-weight ratios, like truck wheels and suspension parts, and aircraft fuselage, wing skins and integral structural parts.
- ***3xxx:*** Manganese is the major alloying element of the *3xxx* series of alloys, which are generally non-heat-treatable, but have about 20% more strength than the *1xxx* series. These alloys are intended as a general-purpose material and are used for architectural applications and various other products that require moderate strength and good workability.
- ***4xxx:*** In this alloy series, silicon is the principal alloying element, which can be added in quantities up to 12% to substantially lower the melting range, without producing brittleness. They are thus used as welding wire and braising alloys for joining aluminium.
- ***5xxx:*** Magnesium is used as the major alloying element in the *%xxx* series to obtain a moderate-to-high-strength workhardenable alloy with good welding characteristics, as well as good corrosion resistance in marine atmospheres. These alloys are used in boat hulls, gangplanks, and other products that are exposed to the marine environments.
- ***6xxx:*** The good formability, weldability, machinability and corrosion resistance of the *6xxx* series of alloys is attributed to silicon and magnesium being the principle alloying elements. Although the *6xxx* series is not as strong as most *2xxx* and *7xxx*, it can be strength hardened to full T6 properties through precipitation heat treatment, and is commonly used for architectural extrusions and automotive components.

- ***7xxx:*** Zinc is the major alloying element in the *7xxx* series, and is used in amounts of 1% to 8%. When zinc is coupled with a smaller percentage of magnesium, the result yields a heat treatable alloy of moderate to very high strength. The *7xxx* series is the strongest of all the aluminium alloys, and are used in aircraft structural components and other high-strength applications.
- ***8xxx:*** This alloy series constitutes a wide range of chemical compositions and may contain appreciable amounts of tin, lithium, and/or iron.
- ***9xxx:*** This series is reserved for future use.

2.4.2.1.2 Cast Aluminium Alloys

Many similarities exist between cast- and wrought aluminium alloys. The same alloy systems are used to describe both, they are strengthened by the same mechanisms, with the general exception of strain hardening, and are similarly classified into heat treatable and non-heat treatable types [64]. The biggest difference between the two alloys is that casting alloys contain alloying additions of silicon far in excess to that of most wrought alloys. This addition of silicon is what makes the casting of high-volume aluminium economically viable. A three digit system, followed by a decimal value is used to describe the casting compositions of this class of aluminium alloys. The *.0* decimal pertains, in all cases, to casting alloy limits, and the *.1* and *.2* decimals are concerned with ingot compositions, which should result in chemistries conforming to casting specification requirements after the melting and processing procedures are completed [64]. The alloy families and their uses for casting compositions are described as follows [62]–[64], [66]:

- ***1xx.x:*** This series contains unalloyed compositions of aluminium and are usually used to manufacture rotors.
- ***2xx.x:*** The *2xx.x* aluminium-copper group are used when high-strength is the predominant requirement. In order to realise the full mechanical-property capabilities of these alloys, good casting design and foundry techniques must be employed. Even though the *2xx.x* alloys have the highest strengths and hardness of all cast aluminium alloys, their general corrosion resistance is lower than that of the other classes.
- ***3xx.x:*** Nearly 90% of all shaped aluminium castings are produced from the *3xx.x* series. Both copper and magnesium is used to increase the strength and hardness and with an increase addition of silicon, wear resistance can be increased, making it beneficial to use in engine applications such as pistons and cylinder blocks.
- ***4xx.x:*** Alloys from the *2xx.x* alloy group are based on the binary aluminium-silicon system and contains silicon from 5% up to 12%. These cast alloys find use where combinations of moderate strength, high ductility and impact resistance is required, such as bridge railing support systems.
- ***5xx.x:*** the primary advantage of aluminium-magnesium castings in the *5xx.x* group are the moderate-to-high strength and toughness, and high corrosion resistance, especially in marine atmospheres. These single phase binary alloys have good machinability and an attractive appearance when anodized, making it well suited for welded assemblies to fulfil architectural and other decorative building needs.
- ***6xx.x:*** This series is unused.
- ***7xx.x:*** This series contain aluminium-zinc-magnesium alloys and are most notable for their combinations of good finishing characteristics, good general corrosion resistance and the capability of developing high strength through natural aging.

- ***8xx.x:*** Tin is used as the principle alloying element in the *8xx.x* group and also contain small amounts of copper and nickel for strengthening. These alloys were mainly developed for bearing applications for connecting rods and crankcase bearings for diesel engines.

2.4.2.2 Machinability of Aluminium

Aluminium and aluminium alloys are considered to be relatively easy to shape metals, especially in material removal processes and offer the offer the highest levels of machinability when compared to other families of lightweight metals such as titanium and magnesium alloys [67]. Pure, unalloyed aluminium is a relatively soft and ductile material and tends to cause a build-up of material on the cutting tool, thereby reducing the tool-life without causing considerable wear on the tool [58]. Machining characteristics of aluminium can considerably be improved by adding alloying elements to the solution [68]. The built-up edge on the cutting tool is reduced by alloying elements that makes the aluminium alloy work-hardenable or heat-treatable, which is why most wrought aluminium alloys have excellent machinability characteristics [69]. Cast aluminium alloys that contain very hard constituents such as silicon, chromium or manganese noticeably decreases the tool life. The use of small rake angles can however improve machinability for these cases [26].

In summary, the poorest machining characteristics are attributed to the alloys that are in the softest condition and have the lowest alloy content. The low cutting forces involved when machining aluminium alloys renders the process relatively easy and the expected tool life is relatively high if there is no built-up edge or material adhesion to the cutting tool. The surface finish is a product of chip formation and can be regulated through the addition of elements out of solution to act as chip breakers.

2.5 CubeSat

This chapter will look at the current market trends for CubeSats, and the future predictions for their uses in space. Several companies that manufacture CubeSat spaceframes will be investigated. The different spaceframe designs are analysed and used as a benchmark for the KletsKOUS prototype to determine the viability of the new design. The CubeSat Design Specification document (CDS), is thoroughly studied and provides the basis for understanding the specifications to which the satellite must adhere.

2.5.1 Satellites in South Africa

In 1992, the Stellenbosch UNiversity SATellite (SUNSAT) microsatellite project was started. The University of Stellenbosch initiated the project in 1992 with the aim of producing South African satellite engineers for a future satellite industry and fostering international university space cooperation [70]. This program was very successful and led to the launch of SUNSAT-1, Africa's first indigenous orbiting satellite [71]. The Department of Electrical and Electronic Engineering at Stellenbosch University decided in 1991 to add a micro-satellite project to the list of curricular activities [71]. This programme would satisfy the following goals:

- Adding a multi-disciplinary engineering research opportunity to the graduate portfolio
- Stimulating significant international interaction through a challenging research initiative
- Helping to stimulate the interest of youth in science and technology

The plan was to send three satellites into orbit, but funding and launch delays extended SUNSAT's development until 1999. During this time, over 96 students were involved in the project, over 45 graduate degrees were completed and over 25000 children were involved with assembling school electronic kits through the MTN-SUNSTEP schools programme [71].

SUNSAT-1 is seen in Figure 16a. It was launched into orbit via a United States Air Force Delta II rocket on 23 February 1999. The micro-satellite weighed in at 64 kg and was designated with the call sign OSCAR 35 (SO-35) after starting South African and international Amateur Radio activities through the on board VHF Parrot receiver and UHF transmitter. The primary payload of SUNSAT-1 could return 15 meter resolution, 3456 pixel/line, 3-band stereo images [71]. The satellite had a lifetime of almost two years and made final contact in January 2001 [70].

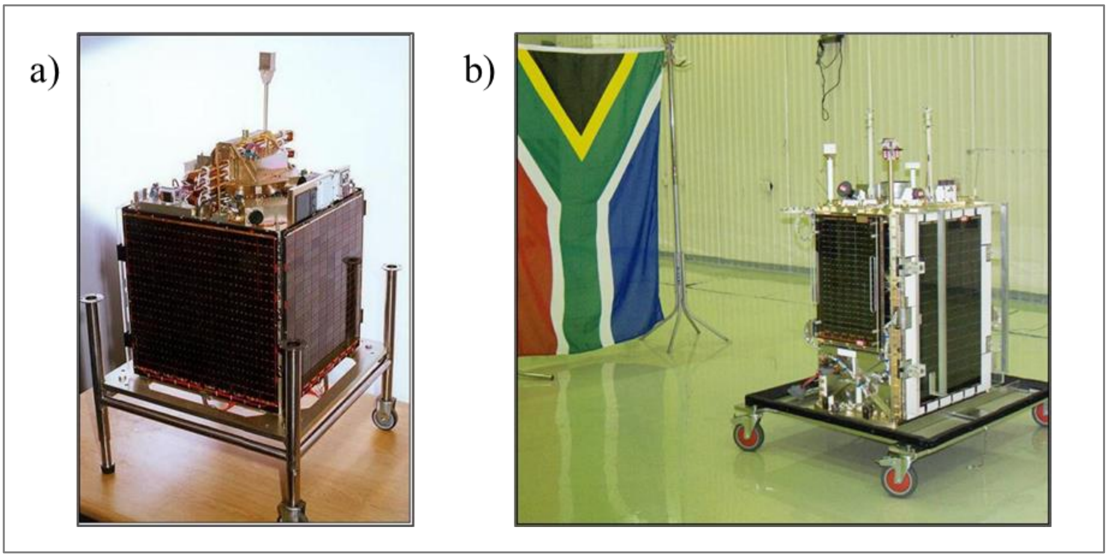

Figure 16: SUNSAT-1, Africa's first indigenous orbiting satellite, and SumbandilaSat, South Africa's second satellite

A university spin-off company called SunSpace, built South Africa's second satellite which was launched in September 2009 [70]. It was named SumbandilaSat, and produced more than 1200 useful images before a power switch failure in 2011 resulted in the satellite losing the pointing stability required by the high resolution imager, ultimately rendering the satellite useless. SumbandilaSat can be seen in Figure 16b.

South Africa's first nano-satellite, a CubeSat named ZACUBE-1, was developed by the Cape Peninsula University of Technology (CPUT), the South African National Space Agency (SANSA), and Stellenbosch University (SU), with the mission of characterizing the Super Dual Auroral Radar Network (SuperDARN) radar array at the South African Antarctic station SANAE-IV [72]. ZACUBE-1 is a 1U CubeSat with a mass of 1.2kg and a total power output of 3W. The main payload of the satellite is a high frequency (HF) radio beacon with an innovative antenna deployment mechanism for the 10m antenna to efficiently transmit the signal at 14.099MHz [72]. ZACUBE-1 can be seen in Figure 5a below, with the specialized antenna deployment mechanism depicted in Figure 5b.

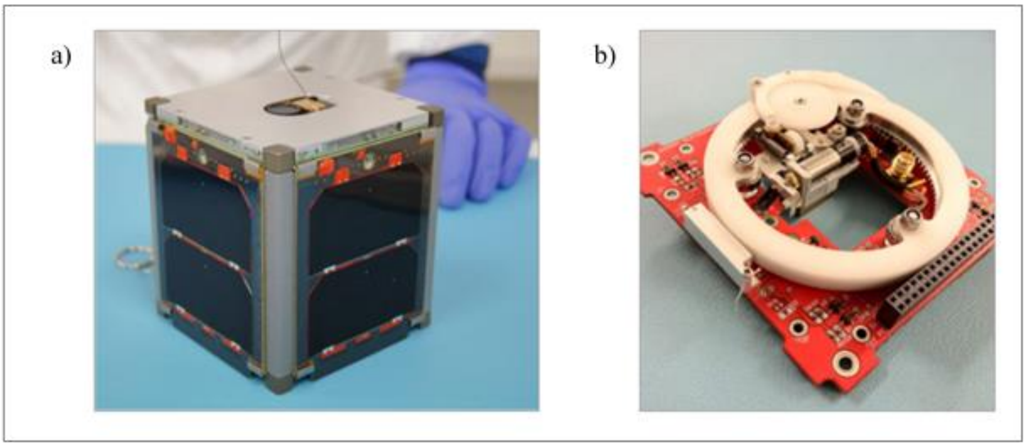

Figure 17: ZACUBE-1 and its specialized antenna deployment mechanism (Adapted from [72])

2.5.2 Market Allocation

SpaceWorks is an aerospace engineering company that specializes in designing and assessing advanced concepts for space, has actively monitored the global small satellite activities since 2008 [73]. Table 3 below describes the different classes of small satellites and their comparative mass ranges. According to this data, a CubeSat is defined as a Nano-satellite as the maximum allowable weight of the 1U design must not exceed 1.33kg.

Table 3: Different satellite classes and their respective mass ranges (Adapted from [73])

Satellite Class	Mass Range
Femto-satellite	10 – 100 g
Pico-Satellite	< 1 kg
Nano-Satellite	1 – 10 kg
Micro-Satellite	10 – 100 kg
Small Satellite	100 – 500 kg

Figure 18 shows the launch data for satellites under 50 kg from the year 2000 to 2016. The number of satellites per year is split into two segments, 1 – 10 kg and 11 – 50 kg. for the purpose of this study, emphasis will be placed on the 1 – 10 kg segment, as this contains the weight range for a 1 U CubeSat. Small satellite use saw a steady increase throughout the early 2000s. This steady growth can be attributed to universities and academic institutions adopting the CubeSat platform to provide an educational experience for students. As component technologies were further miniaturised, the capabilities of these small, lightweight satellites with their comparatively low costs, became a suitable platform for various mission concepts, including technology demonstration, scientific investigation, remote sensing and deep space exploration [74].

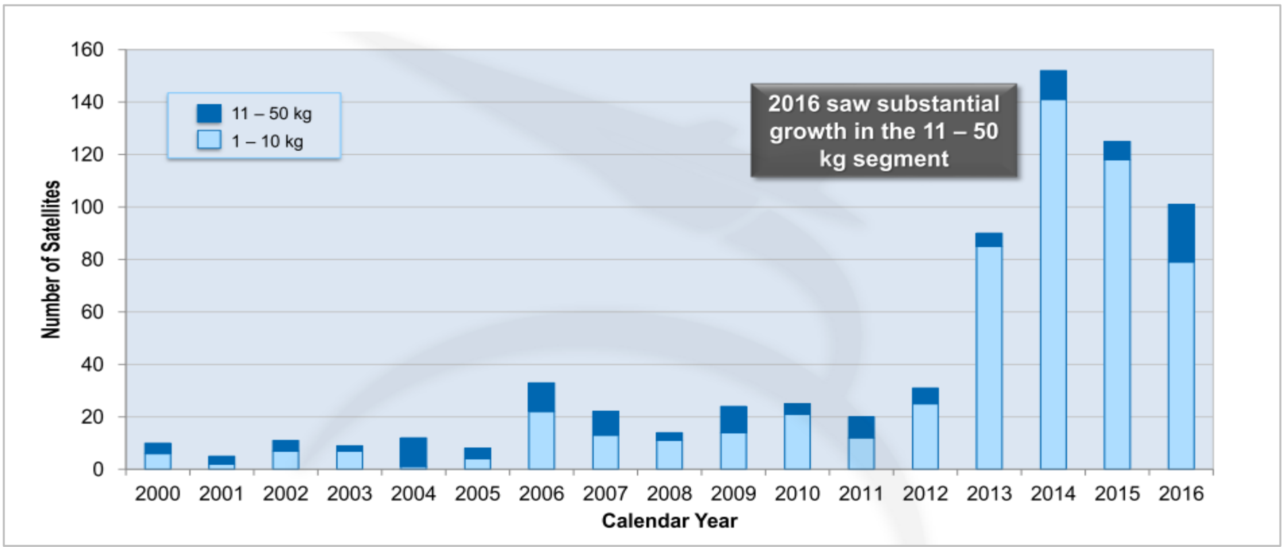

Figure 18: Historical small satellite launch data illustrating the market growth of the industry (Adapted from [74])

The reason for the drastic increase in the number of satellites in 2013 is directly proportionate to the availability of launch opportunities small satellites. Since 2008, NASA has strived to provide launch opportunities for small satellite payloads through their CubeSat Launch Initiative (CSLI) [75]. The first successful initiative launched in 2010 and caught the attention of the small satellite community. With an average development lifecycle for a CubeSat being +- 2 years, and if testing is included, it would take approximately 3 years for a CubeSat to be launch-ready, thus the high spike in the number of satellites in 2013, three years after the first successful CSLI launch. This assumption is backed up by NASA's 2012 plan to launch three more scheduled missions by the end of 2013, with each of these missions carrying anywhere from three to six P-POD's into orbit [75]. This translates to anywhere from 27 to 54 1U CubeSats being flown by NASA's CubeSat Launch Initiative alone in 2013.

In 2014, the number of satellites almost doubled when compared to that of the previous year, thanks to Planet Lab's Flock 1 constellation. Planet Labs Incorporated is a San Francisco base company, founded in 2011 with the specific mission of providing medium-to-high resolution imaging of the entire planet on a daily, recurring basis [76]. Flock 1 consisted of 28 satellites that were deployed over 3 weeks in February from the International Space Station (ISS), via the NanoRacks deployment system [76]. The NanoRacks CubeSat Deployer (NRCSD) is a self-contained CubeSat deployment system that isolates the CubeSats, mechanically and electrically, from the ISS, cargo resupply vehicles and the crew of the ISS [77]. The Flock 1 Constellation can be seen in Figure 19a. Figure 19b is the Planet Dove nanosatellite in full operational configuration with deployed solar panels and the communications antenna flap opened.

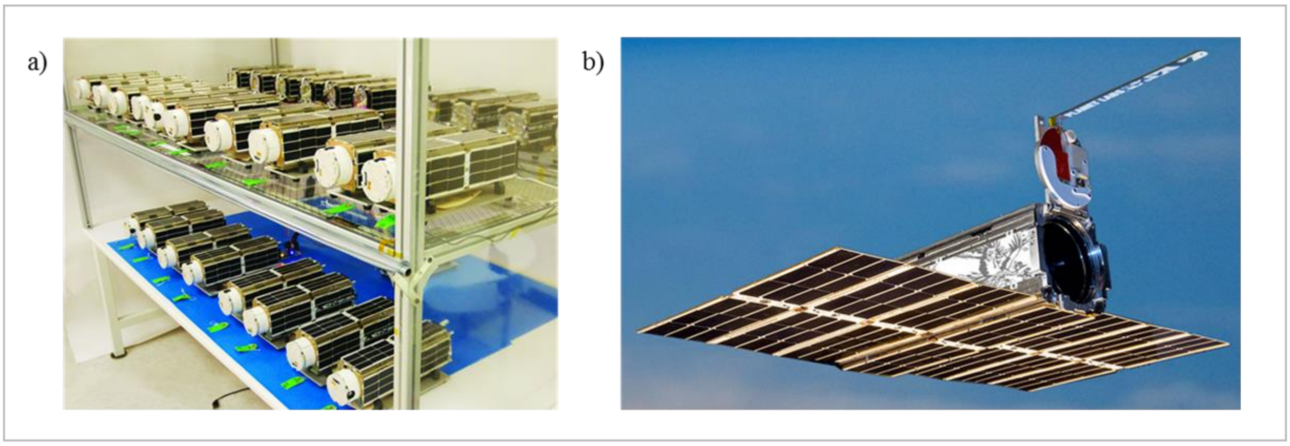

Figure 19a) Flock 1 Constellation and b) Planet Dove nanosatellite in full operational configuration (Adapted from [84])

2.5.3 Manufacturers of CubeSat Spaceframes

This section will look at some of the companies that manufacture CubeSat spaceframes. The cost and weight of each structure will be determined and then compared to the final KletsKOUS prototype. The design efficiency will also be calculated for further, in depth comparison.

2.5.3.1 Innovative Solutions In Space (ISIS)

Innovative Solutions In Space (ISIS) was founded in 2006 as a spin-off from Delft University of Technology's Delfi-C3 nanosatellite project [78]. The company sells space solutions to customers and combines research and development, testing, launch services and small space system operation to provide the right solution to each customer. The 1U CubeSat structure of ISIS can be seen in Figure 20. According to their website, this design offers [79]:

- A highly modular platform
- Detachable side panels
- Supports multiple Printed Circuit Board (PCB) sizes
- Dual kill-switch mechanism
- Scalable design

Figure 20: ISIS 1U CubeSat design

The results of the design analysis are listed in Table 4 below:

Table 4: 1U ISIS CubeSat components list and structure weight

Part	Description	Primary Component	Material	Quantity	Weight (grams)
1	Side Frame	Y	-	2	-
2	Ribs	Y	-	2	-
3	Kill Switch Mechanisms	Y	-	2	-
4	Fasteners	Y	-	16	-
5	Aluminium Shear Panels	N	-	6	-
6	M3 Threaded Rods	N	-	4	-
7	M3 Helix Nuts	N	-	8	-
8	M3 Bus Spacers	N	-	20	-
9	M3 Washers	N	-	48	-
			Total	**108**	**200**

It should be noted that the ISIS spaceframe has a large number of parts, most of which are secondary components, thus rendering a sub-optimal design. A total structure weight of only 200 grams implies that a payload of up to 1.1kg can be carried into space. The calculations for the design efficiency of the 1U ISIS structure are as follows:

$$DE = \frac{Number\ of\ Primary\ Components}{Total\ Number\ of\ Components} \times 100$$

$$DE = \frac{22}{86} \times 100$$

$$DE = 25.58\%$$

The DE value of 25.58% reflects the fact that the structure has a lot of components that are not needed for primary assembly. This result could be interpreted to mean that the spaceframe is harder to assemble due to the high variety of components needed for assembly.

2.5.3.2 EnduroSat

EnduroSat was founded in 2015 with the purpose of enabling the next generation of space mission through the creation of remarkable spacecraft [80]. The company designs, builds and space-qualifies CubeSat platforms for missions ranging from Low Earth Orbit to solar system exploration. Their main focus is on swarm satellite applications and inter-satellite connectivity. The 1U CubeSat structure of EnduroSat can be seen in Figure 21. This design offers the following features:

- An option between one or two kill-switches
- Two separation springs
- Customizable design

Figure 21: EnduroSat 1U CubeSat structure

Even though EnduroSat is a young company when it comes to CubeSat spaceframe manufacturing, they offer a competitive product that is very lightweight when compared to other industry leaders. The results of the design analysis for the 1U EnduroSat Structure are listed in Table 5 below:

Table 5: 1U EnduroSat components list and structure weight

Part	**Description**	**Primary Component**	**Material**	**Quantity**	**Weight (grams)**
1	Top Element	Y		1	-
2	Bottom Element	Y		1	-
3	Leg Unit	Y		4	-
4	Fasteners	Y		16	-
5	Kill Switch	N		2	-
6	Separation Springs	N		4	-
7	Custom Stack Rods	N		8	-
8	Custom Nuts	N		8	-
			Total	**44**	**98**

One observation that could be interpreted as a possible negative factor during the integration phase is the high number of fasteners needed to assemble the structure. The calculations for the design efficiency of the 1U EnduroSat structure are as follows:

$$DE = \frac{Number\ of\ Primary\ Components}{Total\ Number\ of\ Components} \times 100$$

$$DE = \frac{22}{44} \times 100$$

$$DE = 50\%$$

Even though the EnduroSat structure has some standardised components, the low DE score can be attributed to the high amount of secondary components.

2.5.3.3 *Pumpkin Space Systems*

Pumpkin Space Systems, a business unit of Pumpkin Inc., focusses on nanosatellite buses and operating software, with CubeSat solutions ranging from sub-1U through to 3U [81]. Figure 22 illustrates the 1U CubeSat design from Pumpkin Space Systems.

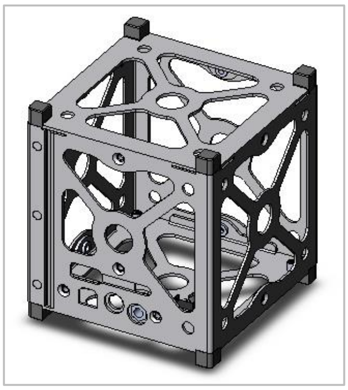

Figure 22: Pumpkin Space System's 1U CubeSat structure

This CubeSat structure is one of the most commonly used products up to date, and the company provides a wide range of solutions to support the customer with. It is evident that this is a market leader in its field, and the results of the design analysis for the 1U Pumpkin Structure are listed in Table 6 below:

Table 6: 1U Pumpkin CubeSat components list and structure weight

Part	Description	Primary Component	Material	Quantity	Weight (grams)
1	Chassis Walls	Y		1	71
2	Base Plate Assembly	Y		1	52
3	Cover Plate Assembly	Y		1	37
4	Fasteners	Y		8	9
5	RBF Bracket Kit	N		2	10
6	Mid-Plane Standoffs	N		2	20
7	Rod-and-Spacer Kit	N		1	-
			Total	**16**	**199**

The calculations for the design efficiency of the 1U Pumpkin structure are as follows:

$$DE = \frac{Number\ of\ Primary\ Components}{Total\ Number\ of\ Components} \times 100$$

$$DE = \frac{11}{16} \times 100$$

$$DE = 68.75\%$$

Seeing as Pumpkin Space started manufacturing CubeSat structures since 2000, it is not surprising to see that the DE value has increased substantially over the previous two spaceframes. The structure weight of 199 grams places the Pumpkin CubeSat on par with the ISIS structure, but with an increased DE value of 68.75%.

2.5.3.4 Clyde Space

Clyde Space is a privately owned company founded in 2005. They design innovative products and tailor make solutions to meet the project requirements of the customer. Clyde Space's 1U CubeSat design is seen in Figure 23. This design offers the following features:

- Full compatibility with CubeSat standard
- Adaptability to a wide range of mission requirements

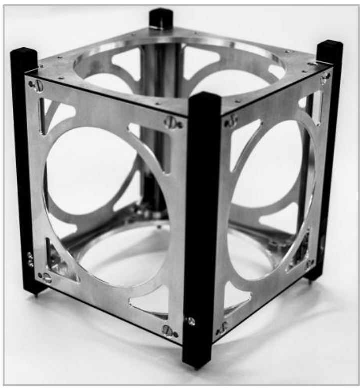

Figure 23: Clyde Space's 1U CubeSat structure

Clyde Space is one of the market leaders when it comes to spaceframe design. They offer a highly adaptable CubeSat structure that weighs in at well below the industry mean. The results of the design analysis for the 1U Clyde Space Structure are listed in Table 7 below:

Table 7: 1U Clyde Space CubeSat components list and structure weight

Part	Description	Primary Component	Material	Quantity	Weight (grams)
1	Rail Unit	Y		4	-
2	Z-Axis Panel	Y		2	-
3	Side Panel	Y		4	-
4	Fasteners	Y		24	-
5	Separation Switches	N		2	-
6	Separation Springs	N		2	-
			Total	**38**	**155**

The total weight of the Clyde Space structure amounts to 155 grams, and it offers the highest DE value out of all the spaceframes used for the benchmark study. This can be attributed to the standardization of parts used to assemble the structure. The calculations for the design efficiency of the 1U Clyde Space structure are as follows:

$$DE = \frac{Number\ of\ Primary\ Components}{Total\ Number\ of\ Components} \times 100$$

$$DE = \frac{34}{38} \times 100$$

$$DE = 89.47\%$$

Even though this CubeSat spaceframe uses more fasteners than the other benchmarked products, it still manages to achieve an efficient design with a DE value of 89.47%. This is well above the standard and seems to be a good structure to use in the benchmark study.

2.5.4 Design Specifications

Cal Poly, the developer of the Poly-Picosatellite Orbital Deployer (P-POD), has the primary responsibility of ensuring the safety of the CubeSat and protecting the launch vehicle (LV), primary payload and other CubeSats. Therefore it is necessary that all the participants of the CubeSat Program meet the design and minimum testing requirements outlined in the CDS [7].

2.5.4.1 General Specifications

Cal Poly's CubeSat Design Specifications lists various requirements that a CubeSat must adhere too to be allowed to enter space [7]. If, for any reason, a CubeSat incorporates a deviation from the CDS, a Deviation Waiver Approval Request (DAR) must be submitted. All parts must remain attached to the satellite during launch as to not create any additional space debris. The use of pyrotechnics is not permitted and any propulsion system on board the CubeSat must be designed, integrated and tested in accordance with the Air Force Space Command Manual 91-710 Volume 3 (AFSPCMAN 91-710, Vol. 3) [7], and must have at least three inhibits to activation. The maximum allowed stored chemical energy capacity is 100 Watt-Hours. Although the use of higher storage capacities is permitted (via a DAR), it could potentially limit the launch opportunities. All hazardous materials present on the

CubeSat must conform to the AFSPCMAN 91-710, Vol. 3, which defines the Hazardous Materials Selection Criteria to be the requirements for preventing or minimizing the consequences of catastrophic releases of toxic, reactive, flammable, or explosive materials that may result in toxic, fire, or explosion hazards [82]. All of the CubeSat materials must satisfy the NASA approved low out-gassing criteria to prevent the contamination of other spacecraft during integration, testing and launch. All CubeSats must have a Total Mass Loss (TML) of less than 1%, and a Collected Volatile Condensable Material of less than 0.1%.

2.5.4.2 Mechanical Requirements

For the CubeSat to be allowed onto the launch pod, it must adhere to the various mechanical requirements specified in the CubeSat Design Specifications [7]. This includes the coordinate system of the satellite, which must match that of the P-POD. All deployables must be constrained by the CubeSat and not the P-POD. At least 75% of the rails must be in contact with the P-POD rails, while the remaining 25% of the rails may be recessed. No part of the rail is allowed to exceed this specification. The maximum allowable weights of the various CubeSat units are displayed in Table 8. All larger masses may be evaluated on a mission to mission basis.

Table 8: Maximum allowable weight for each CubeSat unit ranging from 1U up to 3U

CubeSat Unit	**Maximum allowable weight (*kg*)**
1U	1.33
1,5U	2.00
2U	2.66
3U	4.00

The centre of gravity of the CubeSat must be located within 2 cm from its geometric centre in the X- and Y-direction for all CubeSat units. Table 9 provides the required position of the centre of gravity in the Z-direction for all CubeSat units.

Table 9: Position of the centre of gravity of the CubeSat in the Z-direction for all CubeSat units ranging from 1U up to 3U

CubeSat Unit	**Centre of gravity position in the Z-direction (cm)**
1U	2.00
1,5U	3.00
2U	4.50
3U	7.00

To prevent any cold welding within the P-POD, the CubeSat rails and standoff, which come into contact with the P-POD rails and adjacent CubeSat standoffs, must be manufactured out of hard, anodized aluminium. In order to ensure adequate separation between the units in the P-POD, it is required that the 1U, 1.5U, and 2U CubeSats use separation springs illustrated in Figure 24 to achieve this.

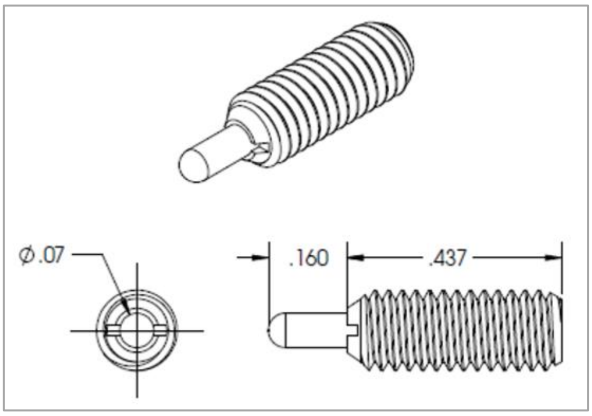

Figure 24: CubeSat separation spring dimensions in inches for use in the 1U, 1.5U and 2U CubeSats

The recommended separation spring characteristics is shown in Table 10.

Table 10: Recommended separation spring characteristics to insure that adequate separation occurs between the CubeSat units inside the P-POD

Characteristic	**Value**
Plunger Material	Stainless Steel
Initial End Force	0.41 lbs
Final End Force	0.9 lbs
Throw Length	0.16 inch. Min above the standoff surface
Thread Pitch	8-36 UNF-2B

The 3U CubeSat does not require the use of a separation spring, as it will be the only satellite inside the P-POD. The separation springs must be at or below the level of the standoff when compressed situated on the end of the standoff on the CubeSat's Z-face, as seen in Figure 25.

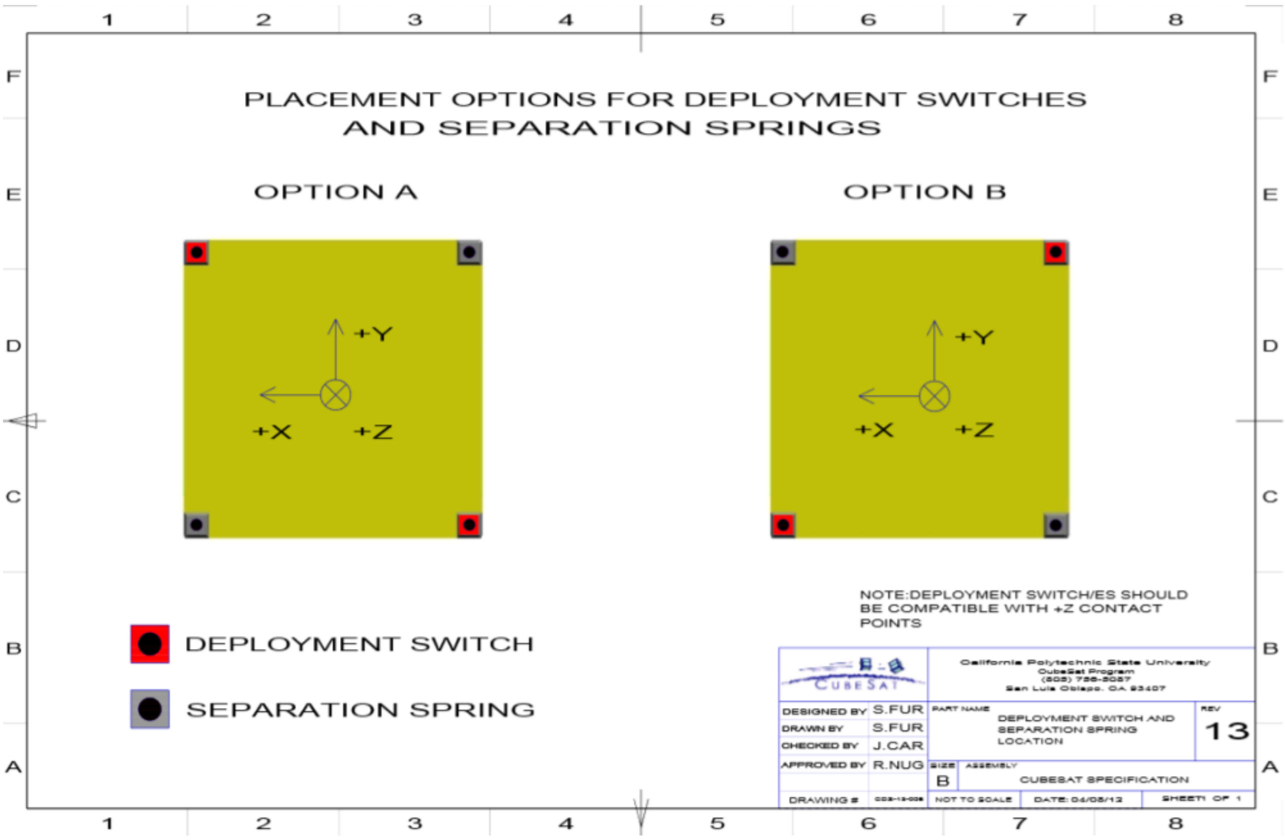

Figure 25: Placement options for deployment switches and separation springs for 1U, 1.5U and 2U CubeSat units

2.5.4.3 Electrical Requirements

To prevent the CubeSat from activating any powered functions while integrated in the P-POD, the power system must be in an off state, from the time of delivery to the launch vehicle, through to on-orbit deployment. There must be at least one deployment switch on a rail standoff as seen in Figure 5 above. The function of the deployment switch is to electrically disconnect the power system from the powered functions while the CubeSat resides in the actuated state and must remain so at all times during integration in the P-POD, with the deployment switch being at or below the level of the standoff. Toggling the deployment switch between the actuated and normal state must reset the transmission and deployable timers to zero. All CubeSats must contain a remove before flight (RBF) pin that is not allowed to protrude more than 6.5 mm from the rails when it is fully inserted. The function of the RBF pin is to cut all power to the satellite once it's inserted after which it will be removed as soon as the CubeSat is integrated with the P-POD. All CubeSat umbilical connectors, as well as the RFB pin must be situated within the designated Access Port locations, the green shaded areas of the CubeSat Design Specification Drawings. These drawings can be seen in Appendix A. To avoid unbalanced cell conditions, the CubeSat must incorporate a battery circuit protection for charging or discharging.

2.5.4.4 Operational Requirements

All CubeSats must comply with their respective countries' radio licence agreements and restrictions and for the use of radio frequencies, documentation of proper licenses must be obtained and provided by the operators. In order to limit the orbital debris, the CubeSat's mission design and hardware must be in accordance with NASA's Procedural Requirements, NPR 8715.6. A minimum waiting time of 30 minutes is required after the CubeSat is ejected from the P-POD before any of the deployables such as booms, antennas and/or solar panels are allowed to deploy and a waiting time of 45 minutes is required after on-orbit deployment before the CubeSat can generate or transmit any signal.

Chapter 3 Research Methodology

The research methodology that was used to complete this study is depicted in Figure 26. It consists of four phases, designed specifically to reach all of the research objectives. The grey diamond shape in the background of the figure not only represents the knowledge gained as the phases progressed, but also the effort required during each of the phases.

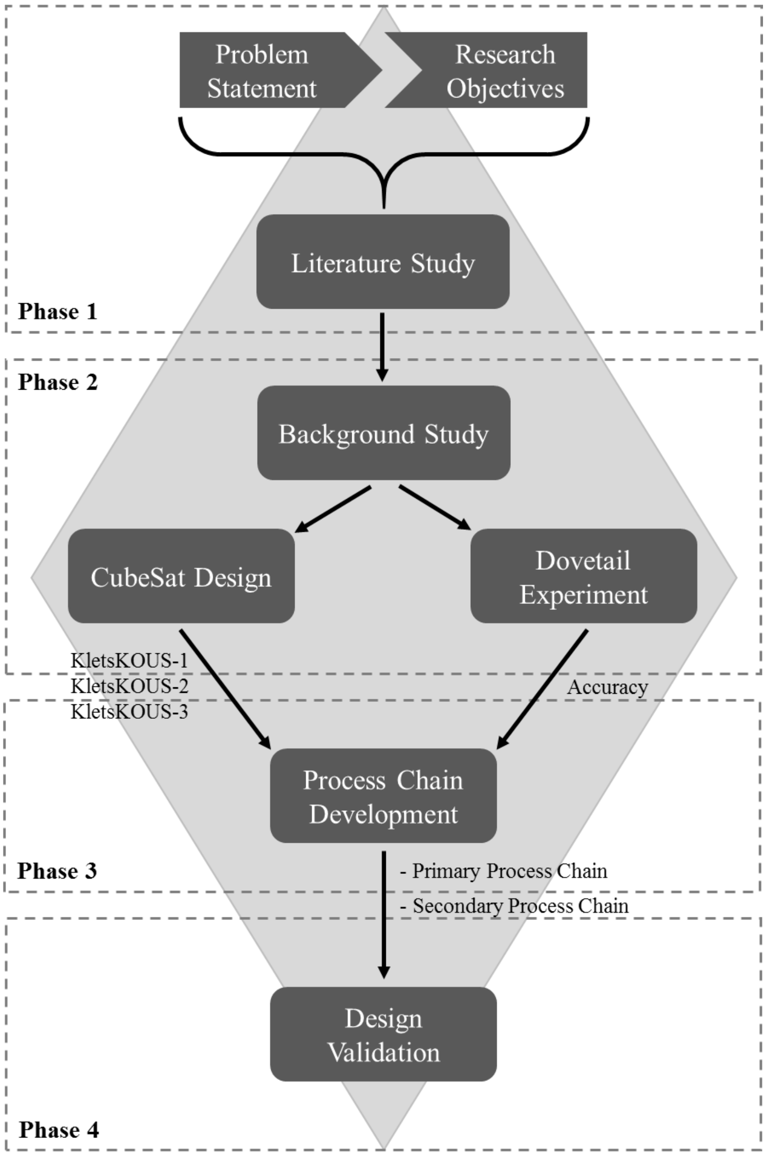

Figure 26: Schematic of the research methodology that was followed to complete all of the research objectives

Phase one was aimed at bridging the knowledge gap that existed at the start of the study. Focus was placed on resource efficient manufacturing practises, material properties and applications, and CubeSat market allocations and design specifications. Four competitors in the field of CubeSat spaceframe manufacturing were identified and an investigation was done to determine the cost and weight of each competing structure. These results would later be used to validate the final CubeSat spaceframe prototype. The background study in Phase two consisted of previous work done with regards to material selection of a CubeSat spaceframe. With this information, the optimal spaceframe design was developed and a dovetail experiment was done to determine the accuracy of which the rail components could be manufactured. Phase three incorporated the experimental results to form the resource efficient process chain, and Phase four validated the design by comparing it to the spaceframes of other companies.

3.1 Background Study

In 2015, SA AMSAT enlisted the help of Stellenbosch University to design a spaceframe with a higher strength-to-weight ratio than that of their current prototype. The student developed a Material Selection Procedure as a stepping stone towards the optimum design. The rationale behind this process was that if the optimal materials were selected for certain components, the overall structure of the satellite will be more efficient. This section will describe the work that was previously done and provide some insight into the project and to set the context on which this thesis is based.

3.1.1 Material Selection Procedure

A process for concurrently selecting the optimal design, material and manufacturing procedure was developed as part of a final year thesis in 2015. Figure 27 illustrates this procedure and the interaction between each process with the outcome being a full product specification that meets the needs of the customer and fulfils the product specifications.

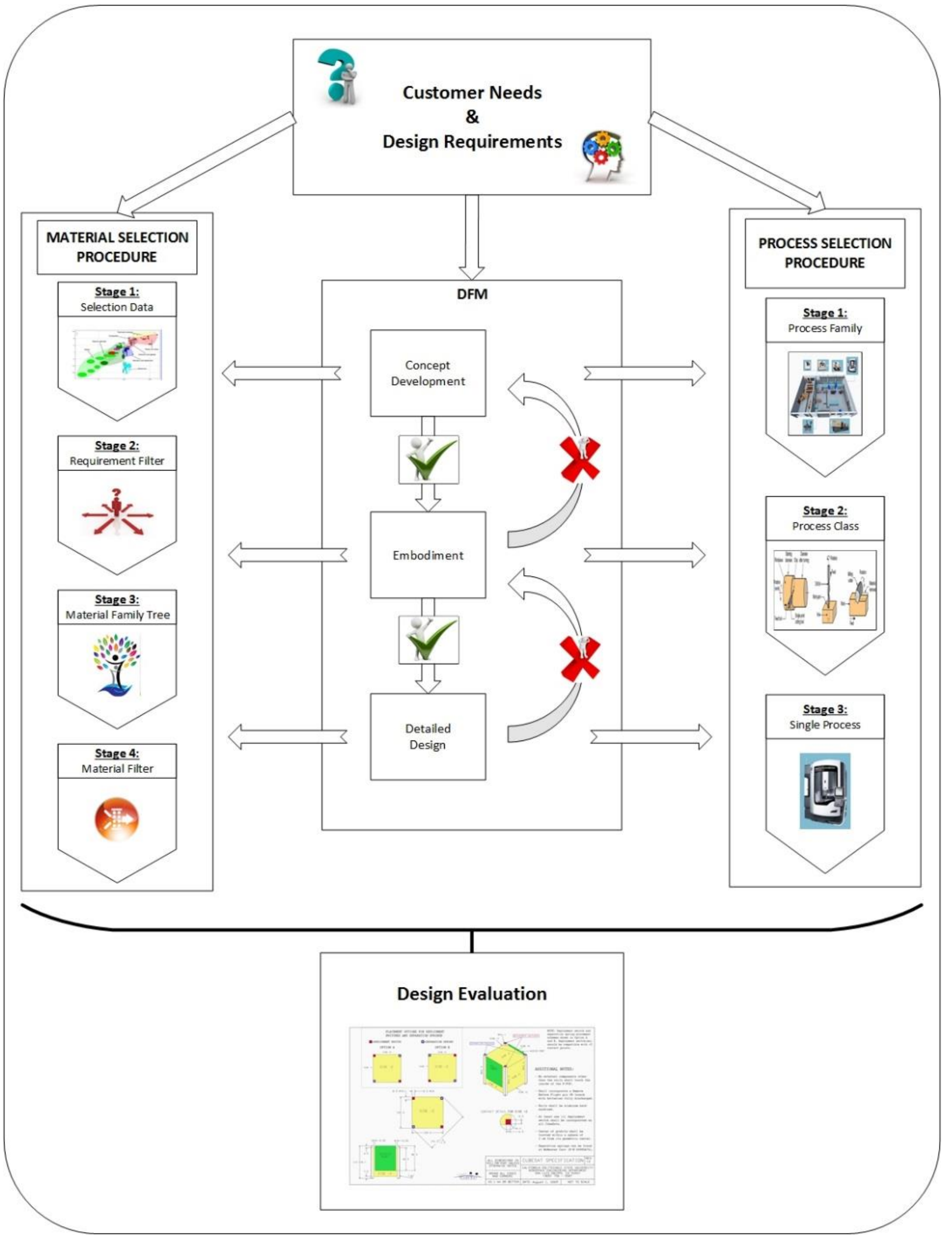

Figure 27: Process for concurrently selecting the optimal design, process and material to meet specific customer needs and design requirements

The first step in the design process is to fully understand the customer's needs and the design requirements. This is done by formulating a needs statement to specify all the tasks and requirements of the design. Once the customer needs and design requirements have been established, it is possible to undertake the Material Selection Procedure to determine the best material to use for the design. By taking account the customer needs, design requirements and the results of the material selection, it is possible to select the optimal manufacturing process. The Design for Manufacture (DFM) phase of the design process involves three stages, each with a screening process to ensure that the design is kept in line with the material properties, process capabilities and overall objectives. By evaluating the final design we can ensure that the given solution is optimal and falls within the design specification while meeting all of the customer needs.

This thesis will only use the results of the Material Selection Procedure as material and financial constraints in 2015 prohibited the use of the resulting material, which in the end influenced the final result.

3.1.1.1 Customer Needs and Design Requirements

By analysing the CubeSat Design Specification document, through correspondence with the KletsKOUS team and carefully researching available spaceframes and their shortcomings, the following customer needs and design requirements were established:

Customer needs:

- The new design must yield a lighter spaceframe
- The spaceframe must allow for the use of a specialised antenna deployment system to minimise the effect that the resulting force will have on the orientation of the spaceframe
- The spaceframe must allow for the use of deployable solar panels to increase the power capacity of the satellite

Design requirements:

- The CubeSat must have a total mass loss (TML) of less than 1%
- All deployable elements of the CubeSat must be constrained by the spaceframe and not the P-POD
- At least 75% of the CubeSat's rails must be in contact with the P-POD's rails at all times
- The CubeSat's rails and standoffs must be manufactured out of anodized aluminium
- The CubeSat's centre of gravity must be located within 2cm of the geometric centre of gravity in the X-, Y-, and Z-directions
- The maximum allowable weight of the CubeSat is 1.33kg
- The assembly process of the spaceframe should not require the use of screws

3.1.1.2 Material Selection Procedure

The vast amount of materials that is available at the moment can cause the material selection procedure to become a tedious and time-consuming task. Selecting the material during the early stages of development allows the designers to determine the material's limitations in terms of manufacturing. This allows the design to be made with these manufacturing constraints in mind, which in turn lowers the overall production costs and produces a product that is easier to manufacture and assemble.

The four stages of the Material Selection Procedure ensures that the most suitable material will be selected for use. Figure 28 shows the Material Selection Procedure with the four stages namely: Selection Data, Requirement Filter, Material Family Tree, and Material Filter. The CES EduPack 2015 software provides a comprehensive database of materials and process information, powerful materials software tools and a range of supporting literature. This software was used to acquire the necessary data that was needed during the material selection procedure.

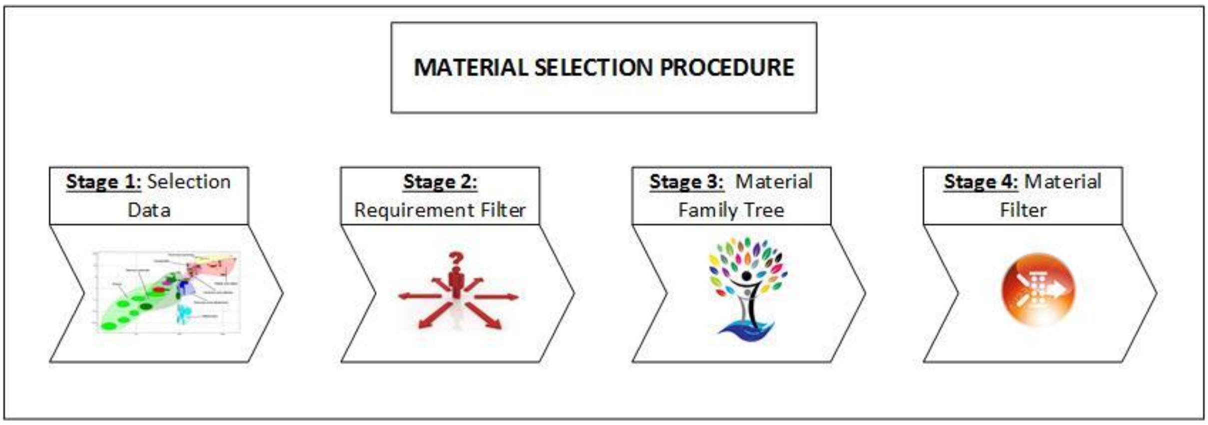

Figure 28: Material Selection Procedure used to determine the optimal material to use for the rail and side panel components of the CubeSat prototype

By analysing the generic CubeSat structure in the CubeSat Design Specifications document in Appendix A, two components stand out as important: The rails (corners of cube) and the side panels. The material selection was done for each of the components and the results are as follows:

3.1.1.2.1 CubeSat Rails

The rails of the CubeSat can be compared to a square rod with a specified length of L that is required to carry a tensile force F without failure while weighing as little as possible. Maximising the performance of the side strut translates into minimizing the mass of the component while still carrying the load safely. The equation describing the quantity to be minimized, referred to as the objective function, is:

$$m = AL\rho \qquad (1)$$

Where m is the mass, A is the cross-sectional area of the side strut and ρ is the density of the material. It is possible to reduce the mass by reducing the cross-section, but the area, A, needs to be sufficient enough to carry the load, F. This requires that

$$\frac{F}{A} \leq \sigma_f \qquad (2)$$

Where σf is the failure strength. Eliminating the area, A, between these equations gives

$$m \geq FL\left(\frac{\rho}{\sigma_f}\right) \qquad (3)$$

The brackets in this equation contain the material properties. By inverting the material properties, the material index, M, is defined as

$$\boldsymbol{M = \frac{\sigma_f}{\rho}} \tag{4}$$

The next step is to identify, from the subset of materials that meet the constraints of stages 1 – 3, those that maximise the performance of the component. It is necessary to rewrite the equation above into a form that is compatible with the logarithmic scale of the bubble charts. Consider

$$M = \frac{\sigma_f}{\rho} = constant, C$$

For a specific value of σf we have, using logs,

$$\boldsymbol{\log \sigma_f = \log \rho + \log C} \tag{5}$$

If we substitute

$$y = \log \sigma_f$$

$$x = \log \rho$$

And

$$\boldsymbol{c = \log C} \tag{6-8}$$

The material index equation becomes a straight line with a gradient of one, and can now be plotted on the logarithmic graph. The results are displayed in Appendix B1.

3.1.1.2.2 CubeSat Side Panel

In the equation

$$\boldsymbol{M_p = \frac{E^{\frac{1}{3}}}{\rho}} \tag{9}$$

E is Young's Modulus, ρ is the material density and Mp is the material index for a light, stiff panel [83]. By converting the material index equation above to the linear logarithmic equation

$$\log M_p = 3 \log \rho + 3 \log C$$

If we substitute

$$y = \log M_p$$

$$x = \log \rho$$

And

$$c = 3 \log C$$

The logarithmic equation becomes a linear equation with a slope of three, and can now be plotted on the logarithmic graph. The results are displayed in Appendix B2.

3.2 Design Analysis of a CubeSat Spaceframe

The analysis of the CubeSat design makes it possible to determine the feasibility of the prototype before moving into the manufacturing stage. This will not only allow for the increase of the quality of the product by ensuring that design flaws are recognised early on, it will shorten the cycle time as the parts will be designed with manufacturing in mind, and it will reduce the overall cost of the product by eliminating the iteration cycle of design-manufacture-redesign-remanufacture.

The design analysis consists of three steps. First, the number of parts needed to complete the spaceframe is determined along with the weight of each part. The parts are then grouped into primary and secondary components. A component is classifies as a primary component when it is needed for assembly of the spaceframe, and a secondary component when it is combined with a primary component to form part of the final product. Finally, the design efficiency (DE) of the CubeSat spaceframe is calculated with the use of Equation 10 below.

$$DE = \frac{Number\ of\ Primary\ Components}{Total\ Number\ of\ Components} \times 100 \tag{10}$$

Chapter 4: Experimental Setup and Design

4.1 CubeSat Design

The customer needs and design requirements that formed part of the needs statement in Chapter 3.1, along with the results of the Material Selection Procedure, was used as a baseline for the development of the CubeSat spaceframe. For any design to be deemed sufficient, it had to conform to needs and requirements used during the material selection procedure. The spaceframe, which is to be manufactured, should not only serve as a platform for the KletsKOUS CubeSat of SA AMSAT, but also provide the opportunity for any customer to design and develop their own satellite based on this CubeSat platform.

4.1.1 KletsKOUS-1

This design of the KletsKOUS-1 prototype utilizes a sliding fit principle, similar to dovetails but with a different shape, to lock the body of the spaceframe in place. KletsKOUS-1 and the dovetail-like sliding mechanism can be seen in Figure 29. The top and bottom panel is fastened in place using screws on each corner of the frame. Connector pins located on the top and bottom panels serves as the hinges for the deployable solar panels. The top panel was designed to house the antenna deployment system. This system makes use of a circular component that houses the antenna, and by rotating the antenna housing, the antenna is retracted into the spaceframe and held in place with a locator pin. Upon deployment, the housing is released and the antenna is deployed, utilizing magnets to slow the deployment down to an acceptable rate.

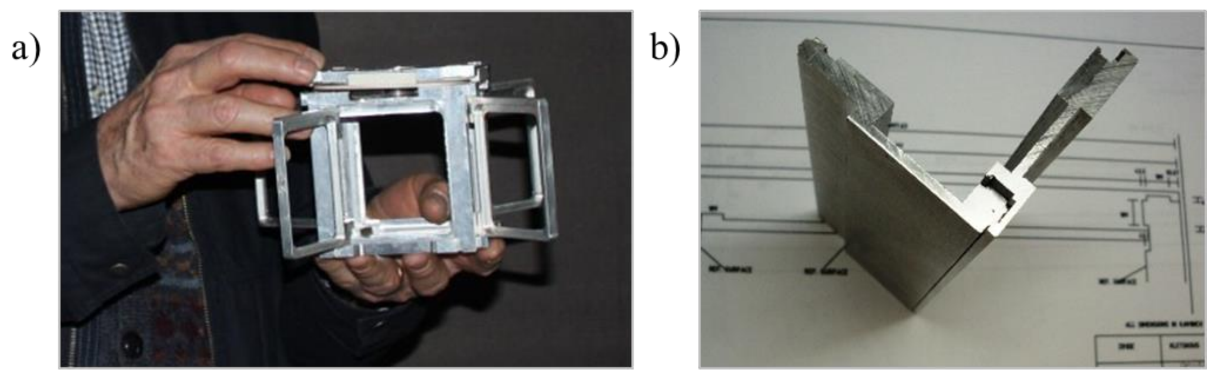

Figure 29: KletsKOUS-1 CubeSat prototype and innovative dovetail-like sliding fit mechanism

All of the components of KletsKOUS-1 was manufactured using a manual milling machine. The operator designed his own clamping tools and employed a trial and error approach to manufacture the structure. Due to this method, the components of the spaceframe is not interchangeable and can only be assembled in a specific sequence. Table 11 below lists the results of the analysis procedure.

Table 11: KletsKOUS-1 CubeSat components list, material selection and structure weight

Part	Description	Primary Component	Material	Quantity	Weight (grams)
1	Bottom Panel	Y	Al 7075 T6	1	48,9
2	Side Panel Male	Y	Al 7075 T6	2	49,7
3	Side Panel Female	Y	Al 7075 T6	2	30,1
4	Antenna Housing	Y	Al 7075 T6	1	99,8
5	Antenna Axis	N	Al 7075 T6	1	-
6	Top Panel	N	Al 7075 T6	1	51,3
7	Solar Panel Housing	N	Al 7075 T6	4	17,2
8	Large Axis	N	300WA Steel	4	5,2
9	Small Axis	N	Stainless Steel	4	3
10	Antenna Axis Screws	N	Brass	3	-
11	Fastening Screws	Y	300WA Steel	8	1,4
			Total	**31**	**472,4**

The KletsKOUS-1 prototype requires many parts to complete the assembly, as seen in the table above. Several limitations of the manual milling machine had severe implications on the material removal process, as there was no standardization to ensure accurate repeatability of the manufacturing process. This prototype was intended as a baseline on which improvements should be made. Focus was not placed on a resource efficient design and manufacturing process to produce a refined CubeSat structure, but rather on producing a prototype spaceframe on which the various other CubeSat components can be tested.

4.1.2 KletsKOUS-2

The KletsKOUS-2 prototype is the result of previous work done on the project. Even though the proposed design conformed to the necessary customer specifications and CubeSat design requirements, material restrictions lead to a sub-optimal result. A 3D model for the proposed KletsKOUS-2 design can be seen in Figure 30 below, and the detailed design drawings is found in Appendix C1.

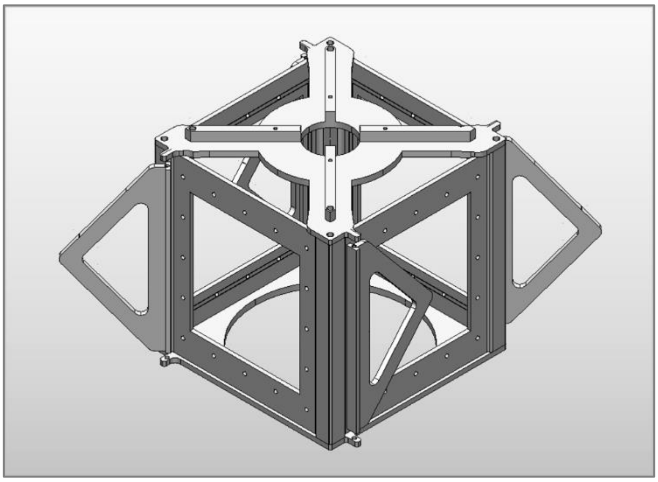

Figure 30: 3D CAD rendering of the KletsKOUS-2 CubeSat prototype

The prototype consisted of four identical side panels that locked into place with a sliding fit, to form the body of the spaceframe. The bottom panel utilizes a small groove to keep it from slipping and four corner-screws locks it into place. The antenna deployment system was re-envisioned as a mechanism that uses the natural spring characteristics of the antenna to deploy itself at the appropriate time. This allowed for the redesign of the previous deployment system with the subsequent result of having a great impact on weight reduction. The antenna deployment panel is fastened using screws on each of the four corners. Finally, the eight CubeSat standoffs were attached to the corners using the same fastening screws as stated before. The proposed manufacturing method for the KletsKOUS_2 spaceframe prototype was milling. A copy of the quotation can be seen in Appendix D1. This prototype was not manufactured, but served as a stepping stone towards the final design. Several lessons were learned and will be further explained in Chapter 4.1.3. Because this prototype was not manufactured, the weight of each component was calculated using the part volume and material density. Table 12 shows the results of the design analysis for KletsKOUS-2.

Table 12: KletsKOUS-2 CubeSat components list, material selection and structure weight

Part	**Description**	**Primary Component**	**Material**	**Quantity**	**Volume (cm^3)**	**Weight (grams)**
1	Bottom Cover	Y	Al 7075 T6	1	12,22	33,00
2	Side Panel	Y	Al 7075 T6	4	14,03	37,87
3	Antenna Deployment	Y	Al 7075 T6	1	18,6	50.22
4	Solar Panel Flap	N	Al 7075 T6	4	4,83	13,05
5	Standoff	N	Al 7075 T6	8	0.567	1.53
6	Fastening Screws	Y	300WA Steel	8	-	1,4
			Total	**26**	**-**	**310.34**

The standardization of many of the components on the KletsKOUS-2 prototype, not only reduced the number of components needed for assembly, but also added to the repeatability of the final manufacturing process. Increased repeatability increases the accuracy of the final part and is easier to manufacture. The weight of each component was also reduced, as CAD/CAM software drastically increases the capabilities of a milling machine.

4.1.3 KletsKOUS-3

The design principles used while developing the KletsKOUS-2 prototype were carried over, refined and implemented to reach the optimal design for the CubeSat spaceframe. To achieve the competitive edge over existing products in the market, the spaceframe had to be modular, fully scalable and easy to assemble. The aim of a modular design is to provide the customer with as much freedom as possible to add or remove features, as they require. This allows the customer to choose from a wider variety of CubeSat components, as the spaceframe is not company specific, but rather customer specific. Modularity also encourages the customer to develop his or her own components because it can be seamlessly integrated with the spaceframe. Standardising the parts of the spaceframe contributed to the ease of manufacture, lowered production costs and made the structure easy to assemble. The scalability of the spaceframe design allows any size CubeSat, from 1U up to 3U to be assembled without the use of any extra components. This will lower the manufacturing costs significantly, as there are no other machine setup or part programming necessary, other than which already exists in the process chain. The ease of assembly allows the customer to quickly assemble and de-assemble the spaceframe during the integration process. A decision was made to develop a spaceframe that uses interference fits to assemble the structure, rather than making use of small screws, that has traditionally been used for assembly. Not only does this save the time that would normally be spent during the assembly process, but it also save the customer the frustration of having to work with multiple tiny screws. This unique fastening method, in conjunction with the deployment method of the P-POD ensured that the structure will don disassemble during the flight to space. The solution proved to be a unique spaceframe that can be easily manufactured, easily assembled and seamlessly integrated with existing or newly developed CubeSat components.

The detailed design of the KletsKOUS-3 spaceframe can be found in Appendix C2. The rails are manufactured using a WEDM machining process with the machining parameters acquired from the dovetail experiment results in Chapter 5.3. Tiny grooves in the rails allow the side panels to be fixed in place, completing the core structure of the satellite. The side panels are manufactured from Ti-6Al-4V grade 5 titanium plate. The top and bottom panel are manufactured from 1200 Aluminium plate by virtue of a laser beam cutting process. A key component of the spaceframe is the CubeSat standoffs. The unique design fixes the top and bottom plates into position, adding the needed rigidity to the structure whilst preserving the *'no screw'*-policy for ease of assembly. The results of the design analysis for the KletsKOUS-3 prototype is seen in Table 13 below.

Table 13: KletsKOUS-3 CubeSat components list, material selection and structure weight

Part	Description	Primary Component	Material	Quantity	Weight (grams)
1	Rail	Y	Al 7075 T6	4	-
2	Side Panel	Y	Ti-6Al-4V	4	-
3	Top and Bottom Panel	Y	Al 1200	2	-
4	Standoff	Y	Al 7075 T6	8	-
			Total	**18**	**134**

The reduction in the number of parts necessary for assembly is attributed to the part standardization process. A lot of effort was expended to find a solution where parts can be re-used to complete the assembly, in a Lego-like fashion, rather than having to manufacture multiple components for the same purpose. The Lego-like design means that each component has an effect on the next, when it comes to assembly, as the interference fits between the components keeps the structure together.

4.2 WEDM Dovetail Experiment

The design of the spaceframe relies on interference fits to keep all the components together. This indirectly implies that the accuracy of the parts is extremely important to ensure that all these tolerances are adhered to. An experiment was designed to test the accuracy of a WEDM machine when cutting dovetail joints. Three different dovetail sizes (small, medium and large) were compared to three different surface roughness values (Ra=0.5, Ra=1, Ra=5) to see what interaction occurred in terms of accuracy. The results of this experiment will be used to determine the optimal combination of part size and machine parameter to use to achieve the most accurate cut. Figure 31a below indicates the dovetail cut with the dimensions in the table next to it. A plate size of 110mm x 8mm was used and the dovetails were cut along the entire length of the plate. The cutting path of the wire can be seen in Figure 31b.

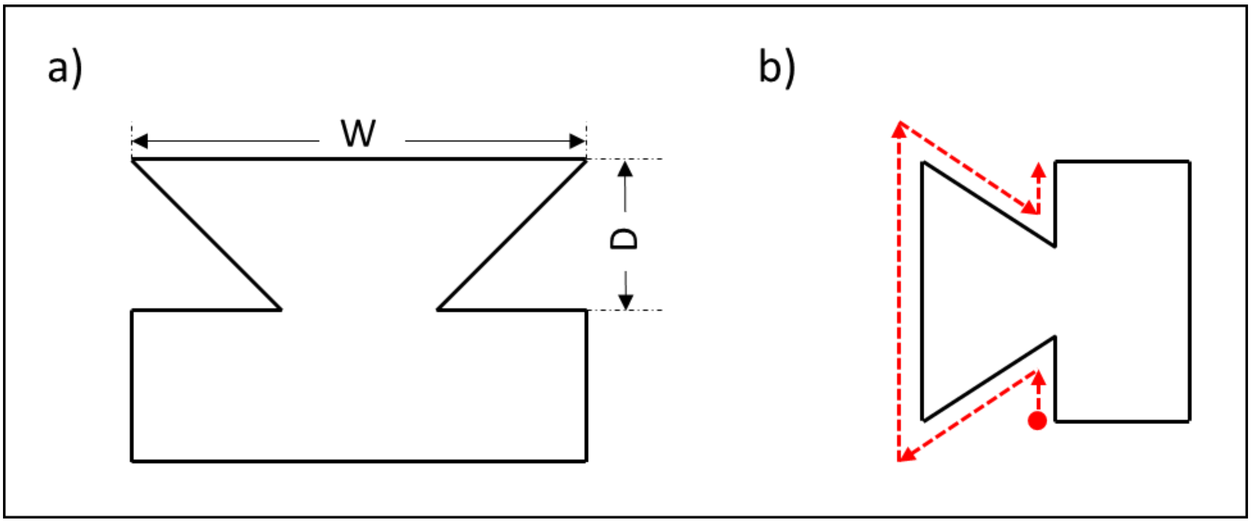

Figure 31a) Dovetail profile with variable dimensions and b) Cutting path for the wire

The CAD design for each of the dovetail sizes were completed and exported to the WEDM machine. The different sizes can be seen in Table 10. Because the dovetail is cut through the length of the plate, it was important to ensure that the part setup was done correctly. It was of high importance to secure the plate perfectly perpendicular to the wire as to ensure a straight cut throughout the entire length of the plate. Once the plate was setup in the cutting bed, the CAD designs were imported into the WEDM machine and the cutting path was programmed, as seen in Figure 17b, and the manufacturing process was initiated.

Each of the three sizes were cut with each of the different surface roughness (Ra) values to ensure that the optimal data was acquired for the factorial design. Table 14 below illustrates how the different factors were combined during the WEDM experiment.

Table 14: Illustration of how the different factors of size and Ra were combined during the experiment

			Ra Value		
			Low	Medium	High
			0	1	2
Size	Small	0	00	01	02
	Medium	1	10	11	12
	Large	2	20	21	22

After the completion of the cutting process, the parts were transferred to the reverse engineering laboratory to measure how closely the actual part measurements resembled that of the theoretical values. It was decided to use the CMM machine to plot a profile around the dovetail at three places, as to accurately resemble the full profile of the entire part and not just at one point. These coordinate plots were then measured to determine the average tail width and the average tail depth respectively. The coordinate measuring machine that was used to gather the data is a Mitutoyo Bright Apex 710 with an accuracy of ±5µm. The machine is fitted with a Renishaw PH10M swivel head and a TP2 touch trigger system. The probe consisted of a 10mm staff connected to a 0.5mm diameter tip. The CMM machine was programmed to set a coordinate system for each part when it was measured. This ensured repeatability of the measuring method that was used and minimized the human error on the output without having to use a jig to keep the parts in place. The program used a plane and line system to locate the part and determine its orientation, before the measurement process was initiated. Each part has a length of 110mm and the three measurements were taken in the middle and 20mm from each end point, as indicated in Figure 32a. Figure 32b is a representation of one of the coordinate plots obtained by the CMM machine.

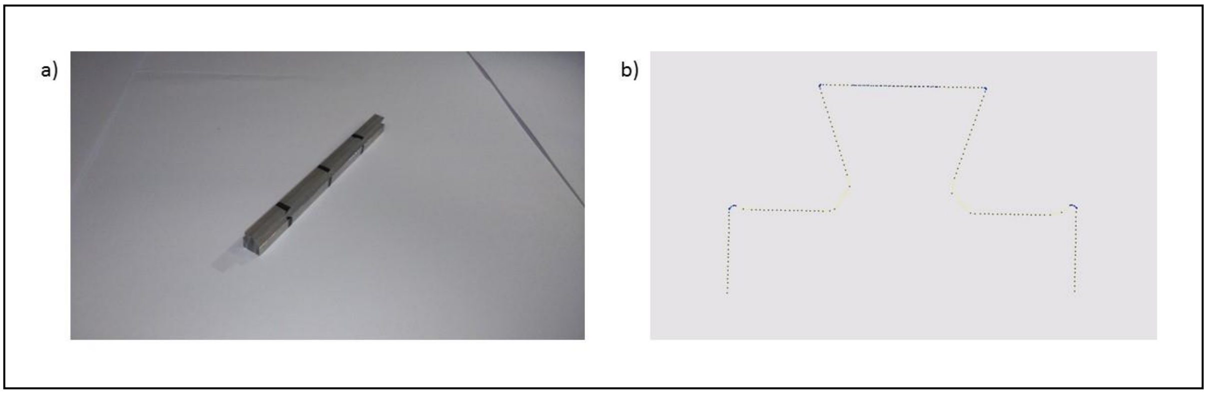

Figure 32: a) Positions at which the dovetails were measured by the CMM; b) Coordinate plots obtained by the CMM at one of the measurement points.

Once the measurements were completed, the accuracy of each part was calculated as a fraction of the total deviation from the theoretical size, as seen in Equation 11, where π is the theoretical size and α is the actual measurements.

$$\boldsymbol{A = 1 - \frac{\pi - \alpha}{\pi}} \quad (11)$$

A 2–factorial interaction model was developed to test the validity of the data with the use of Design Expert 10.0.03 software. The proposed relationship between the interaction of the surface roughness and the part size is described in Equation 12, where y is the response variable, x_1 is the change in part size, x_2 is the change in surface roughness, ε is the experimental errors and β_0, β_1, β_2, and β_3 are the model parameters to be estimated.

$$\boldsymbol{y = \beta_0 + \beta_1 x_1 + \beta_2 x_2 + \beta_3 x_1 x_2 + \varepsilon} \quad (12)$$

4.3 Resource Efficient Process Chain Design

This section describes the rationale behind the process chains that were developed to manufacture the final CubeSat spaceframe. The aim of these process chains are to facilitate in the development of a finished product from a raw material in a resource efficient manner. Figure 33 is the manufacturing process chain that was developed for the KletsKOUS-3 prototype. Each manufacturing process followed similar steps, and this process chain grouped these steps together to form a standardized process chain used by each of the manufacturing processes.

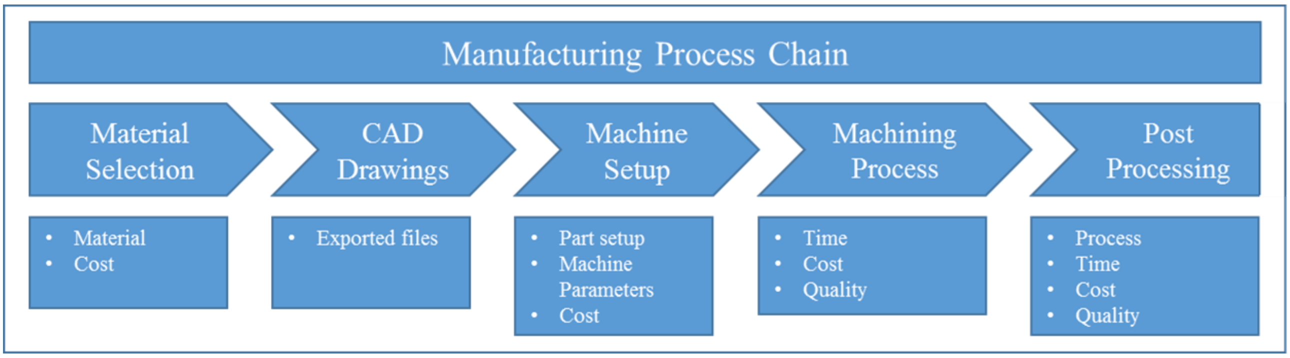

Figure 33: Resource efficient process chain for the KletsKOUS-3 prototype

The initial conversion of raw materials into a semi-final product is described by the material selection, machine setup and manufacturing process. The output of the primary manufacturing processes is then subjected to a secondary process during post processing to obtain the final part geometry. The final part inspection ensures that the finished part falls in-between the necessary tolerances to achieve the correct fit when assembling the spaceframe.

Chapter 5: Experimental Results and Discussion

5.1 CubeSat Design

This section will evaluate each of the KletsKOUS CubeSat spaceframes according to design efficiency and cost. The results of the evaluation process is used to compare the KletsKOUS platform to that of ISIS Space, EnduroSat, Pumpkin Space Systems and Clyde Space as a validation. The results of the validation process can be seen in Chapter 5.2.

5.1.1 KletsKOUS-1

The components for the KletsKOUS-1 prototype that forms basis of the design efficiency calculations is described in detail in Table XX of Chapter XX. The calculations for the design efficiency of the KletsKOUS_1 prototype are as follows:

$$DE = \frac{Number\ of\ Primary\ Components}{Total\ Number\ of\ Components} \times 100$$

$$DE\ = \frac{14}{31} \times 100$$

$$DE = 45.16\%$$

This result is a reflection of the manual manufacturing process, as part repeatability was not possible. The high number of components needed for assembly, along with the complex antenna deployment that formed part of the main body assembly led to a suboptimal result. Lots of lessons were learnt during the development process of the KletsKOUS-1 prototype, such as the importance of part repeatability and machining accuracy. The sliding fit concept originated from this prototype and will be carried over to the final spaceframe.

The overall quality of the spaceframe was found lacking, as there was limited access to an accurate clamping system, no CAD/CAM software to help with the design and the milling machine that was used was not calibrated in a very long time. Each component only fit in at a certain position, and the corners of the structure was marked to help determine which part goes where during the assembly process.

Because the KletsKOUS-1 prototype is a home built prototype based on a trial-and-error process, analysing the costs in an accurate manner was a challenging endeavour. The accuracy of the times for each step are only an approximation, and the hourly rate for a manual machinist was taken to be R200. It is assumed that this hourly rate takes into account the tooling and energy costs, as well as any overtime. The results were extensively studied in previous work and can be seen in Table 15 below.

Table 15: Manufacturing time and cost breakdown for the KletsKOUS-1 Prototype

Task	Time (Hours)	Cost
Cutting the aluminium plate into the required sizes	6	R 1 200.00
Cutting the grooves for the assembly of the sides	10	R 2 000.00
Reducing the sides to a frame structure	8	R 1 600.00
Cutting the locking grooves in the top plate	5	R 1 000.00
Reducing the thickness of the centre section of the top plate	4	R 800.00
Cutting the centre rotation section of the top plate	7	R 1 400.00
Cutting the locking grooves in the bottom plate	5	R 1 000.00
Reducing the thickness of the centre section of the bottom plate	4	R 800.00
Cutting the locking grooves in the top plate of the antenna release mechanism	5	R 1 000.00
Cutting of the antenna housing cavity	4	R 800.00
Cutting weight reducing pattern in top plate of antenna housing	3	R 600.00
Cutting and drilling of the hinge section of the solar panel frames	8	R 1 600.00
Removing centre section of solar panel frames	8	R 1 600.00
Machining hinge pins	4	R 800.00
Cutting the plastic antenna spool and housing	4	R 800.00
Cut out for antenna retarding mechanism	2	R 400.00
Magnetic retarding mechanism	6	R 1 200.00
Drilling and tapping of various fastening screw holes	8	R 1 600.00
Total	**101**	**R 20 200.00**

The total manufacturing time to complete the entire CubeSat spaceframe is estimated to be 101 hours. It must be noted that during the entire manufacturing process, problems were solved as they arose. This means that there is room to streamline this process, but it serves as a good baseline for further improvement. The total manufacturing cost of the structure added up to be R20200.00. This is excluding the material costs, which is estimated to be R192.36, excluding VAT, shipping costs and additional expenditures.

5.1.2 KletsKOUS-2

Table XX in Chapter XX lists all the components and their respective weights for the KletsKOUS-2 prototype. Emphasis was placed on the material selection procedure and the design process of this spaceframe, as it was not manufactured. Material restrictions at the time severely limited the outcome for KletsKOUS-2, as is evident in the DE result. The calculations for the design efficiency of the KletsKOUS_2 prototype design are as follows:

$$DE = \frac{Number\ of\ Primary\ Components}{Total\ Number\ of\ Components} \times 100$$

$$DE = \frac{14}{26} \times 100$$

$$DE = 53.85\%$$

Material selection, part standardisation and the availability of CAD software streamlined the manufacturing process which led to the DE value of just over 50%.

The cost for the KletsKOUS-2 prototype is based on a quotation received from Stellenbosch University's Institute for Advanced Tooling in 2015. This data formed part of previous work done on the project and the detailed quotation can be seen in Appendix D1. The total cost for manufacturing the prototype added up to R10317.00 and the total material cost is estimated to be R164.88. VAT, shipping costs and additional expenditures are excluded in the cost of material.

5.1.3 KletsKOUS-3

The design KletsKOUS-3 prototype is based on the resource efficient manufacturing principles of part reduction and part standardization. The DE value of KletsKOUS-2 is mainly attributed to the standardizing of the side panel components. This lesson had a big influence on the design of KletsKOUS-3. By standardizing the components, the manufacturing process was severely simplified and made it possible for the components to be manufactured by more than one entity, and still fit together when assembled. The weight restriction of the CubeSat platform had the biggest influence, and the aim was to produce a spaceframe that weighed less than 200 grams. The result of the design efficiency calculations are as follows:

$$DE = \frac{Number\ of\ Primary\ Components}{Total\ Number\ of\ Components} \times 100$$

$$DE = \frac{18}{18} \times 100$$

$$DE = 100\%$$

The unique interference fit that is utilized during the assembly of the spaceframe, has the resultant effect that every component is needed to keep the structure in place. Thus it is possible to have a DE value of 100%. It should be noted that this structure was designed to be as efficient as possible and it is not surprising that the results are so high.

A time-cost breakdown for the KletsKOUS-3 prototype can be seen in Table 16. The Total manufacturing time for the CubeSat spaceframe is 1020 minutes, and the total cost can be rounded to

R3600. This cost does not include VAT, shipping costs or any additional expenditures that might have been incurred. The lengthy manufacturing time is the trade-off that is made for the accuracy that was achieved during manufacturing. By improving the resource efficiency of the process chains, the manufacturing cost severely reduced when compared to that of KletsKOUS-1, and is about a third of the cost of KletsKOUS-2, even though KletsKOUS-3 is the lightest structure with the highest DE value.

Table 16: Time-cost breakdown for the KletsKOUS-3 prototype

		Time (min)			Cost (Rand)					
Component	**Number**	**Setup**	**Machine**	***Total***	**Setup**	**Machine**	**Material**	***Total***	**Weight (grams)**	**Quality**
Standoff	8.00	15.00	45.00	*480.00*	150.00	300.00	46.23	*2 596.23*	-	0.05
Rail	4.00	30.00	120.00	*510.00*	200.00	100.00	92.49	*692.49*	-	0.0013
Top panel	2.00	5.00	10.00	*15.00*	0.00	29.69	0.00	*59.38*	-	0.2
Side panel	4.00	5.00	10.00	*15.00*	0.00	19.77	171.40	*250.48*	-	0.2
Total	**18.00**	**55.00**	**185.00**	***1 020.00***	**350.00**	**449.46**	**310.12**	***3 598.58***	**134**	**0.4513**

The quotation for buying the Al 7075-T6 plate needed for the construction of the rails can be seen in Appendix D2, with the total cost of acquiring five 10mm aluminium plates adding up to R790.59. From this, a simple calculation was done to determine the price per volume of the material so that the material needed for the rails and the standoffs could be calculated accurately. The Quotation from the Institute for Advanced Tooling for wire cutting the rails amounted to R684.00, as seen in Appendix D3, and the total cost for manufacturing the top, bottom, and side panels added up to R576.54, as shown in Appendix D4. Detailed quotations for all of the purchase orders can be seen in Appendix D.

5.2 CubeSat Design Validation

The validation of the KletsKOUS-3 design was done in three parts. First, the design efficiency of the CubeSat was compared to the benchmarked components, to determine if the structure would be easy to manufacture, and easy to assemble. Secondly, the weight comparison between the different spaceframes would show how competitive the structure would be in the market place. Lastly, the cost analysis would determine whether KletsKOUS-3 would have a competitive edge to gain entry to the market. The results of the design comparison between the CubeSat structures is seen in Figure 34.

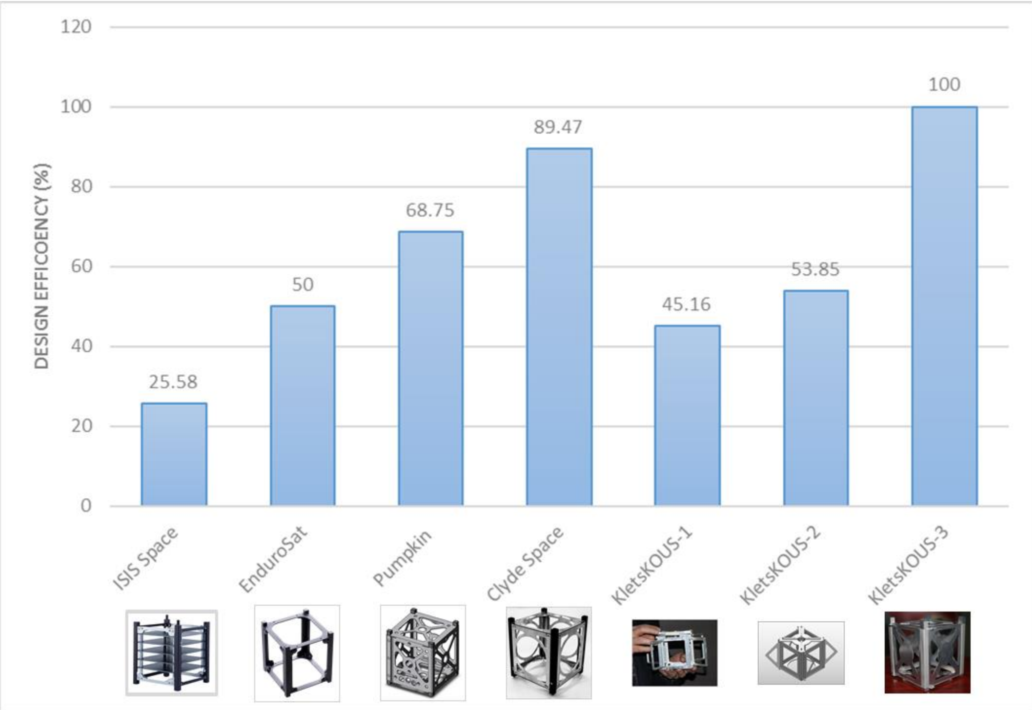

Figure 34: Design efficiency comparison between all the applicable CubeSat entities

The manufacturing principles of part reduction and standardization, in conjunction with the unique design of the structure, resulted in the high DE value. The assumption could be made that the KletsKOUS-3 prototype is easier to manufacture, and easier to assemble, due to the interference fits of the assembled structure. It should be noted that CubeSat structures that require a lot of components for assembly scored poorly in this category.

There is a big difference between the costs of the CubeSat structures, especially when the KletsKOUS prototypes are compared to the international products. The focus of part- and process-standardization during the design phase had a defining impact in the overall cost of the spaceframe. The repeatability of components meant that the setup times could be reduced, while the manufacturing process could be completed in a shorter time as a result of the 'manufacturing-centred' mind-set when designing the structure. Shorter setup and manufacturing time equals lower production costs, and this in turn, reduces the cost of the final product. The cost comparison between the different CubeSat structures can be seen in Figure 35.

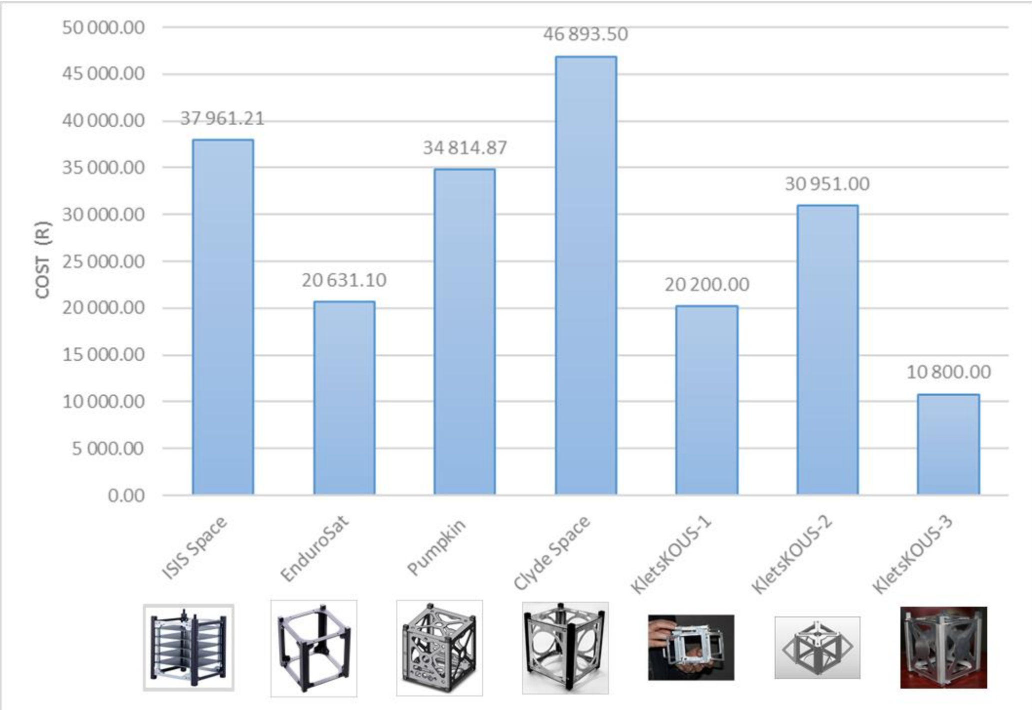

Figure 35: Cost comparison between the different CubeSat spaceframes

It should be taken into account that at the time of the study, the Rand was very weak, which could have led to this cost difference. Even so, the KletsKOUS-3 prototype is by far the most affordable structure to purchase, especially if you are in South Africa. Because the available cost of the benchmarked CubeSat spaceframes is the sales price, the manufacturing cost of KletsKOUS-3 was multiplied by a factor of three to simulate the sales price for a more accurate comparison.

With an innovative design, and through creative manufacturing processes, the KletsKOUS-3 prototype placed second in terms of weight. The results of the comparison between the structure weights of each of the CubeSats can be seen in Figure 36 below.

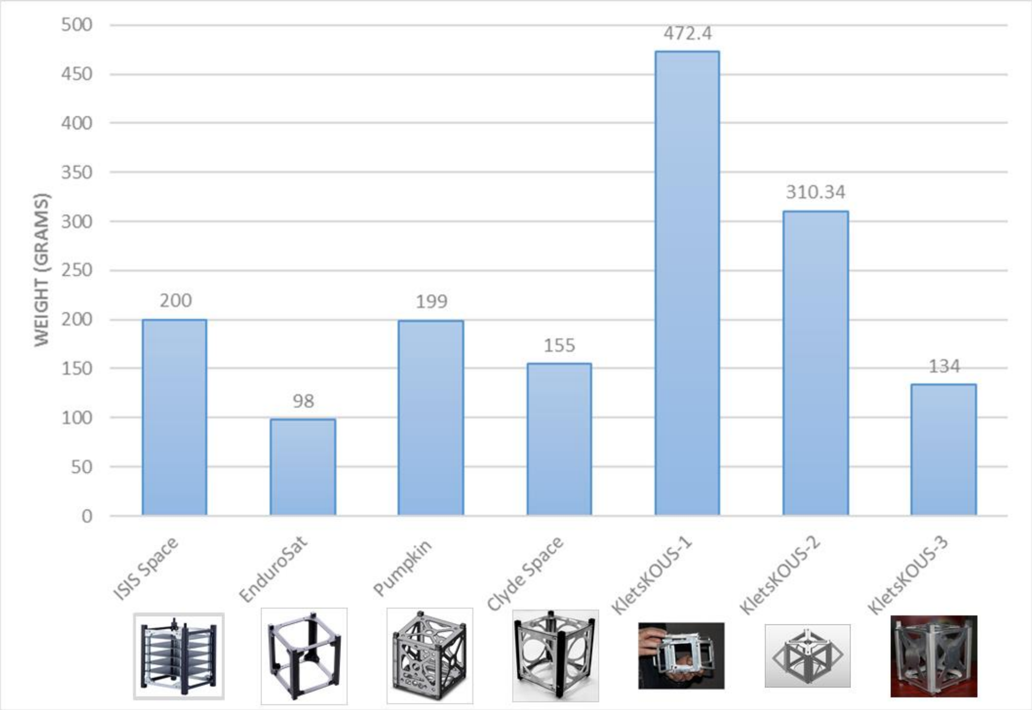

Figure 36: Weight Comparison between all the CubeSat spaceframes

One of the most influencing factors of a CubeSat is the overall weight restriction. It stands to reason that the less the structure weighs, the heavier the payload can be. Finding the perfect balance between weight and strength is essential during the development of the spaceframe. Even though the goal is to have the structure as light as possible, it must still be able to protect the payload during launch.

5.3 WEDM Dovetail Experiment

The postulated model for accuracy based on the measurements of the 9 parts is:

$$\boldsymbol{y = 0.99036 + 7.17 \times 10^{-4} x_1 - 4.5 \times 10^{-3} x_2 + 7.57 \times 10^{-4} x_1 x_2}$$

The ANOVA analysis of the model is displayed in Table 17. Here the model F-value of 13.07 implies that the model is significant with only a 0.84% chance that an F-value of this size could occur due to noise. All values of “Prob > F” that are less than 1.05 indicates that the model terms are significant. In this case, the part size A, the surface roughness B, and the interaction between the two AB are significant.

Table 17: ANOVA table for response surface 2-FI model

Source	Sum of Squares	df	Mean Square	F-Value	p-Value Prob > F	
Model	0.000274114	3	9.13712E-05	13.0697426	0.008401261	***significant***
A-Size	*0.000169939*	*1*	*0.000169939*	*24.30806743*	*0.00435839*	
B-Ra	*8.61811E-05*	*1*	*8.61811E-05*	*12.32735054*	*0.017081815*	
AB	*5.73591E-05*	*1*	*5.73591E-05*	*8.204654019*	*0.035225558*	
Residual	3.49552E-05	5	6.99105E-06			
Corr Total	0.000309069	8				

The normal probability plot of the studentized residuals can be seen in Figure 37a, and it clearly indicates the normality of the residuals as the data points tend to follow a linear equation. Figure 37b displays the results of the model in a 3D plot. Here it is seen that the surface roughness has little effect on the accuracy if the part size is large compared to the significant effect is has when the part size is small.

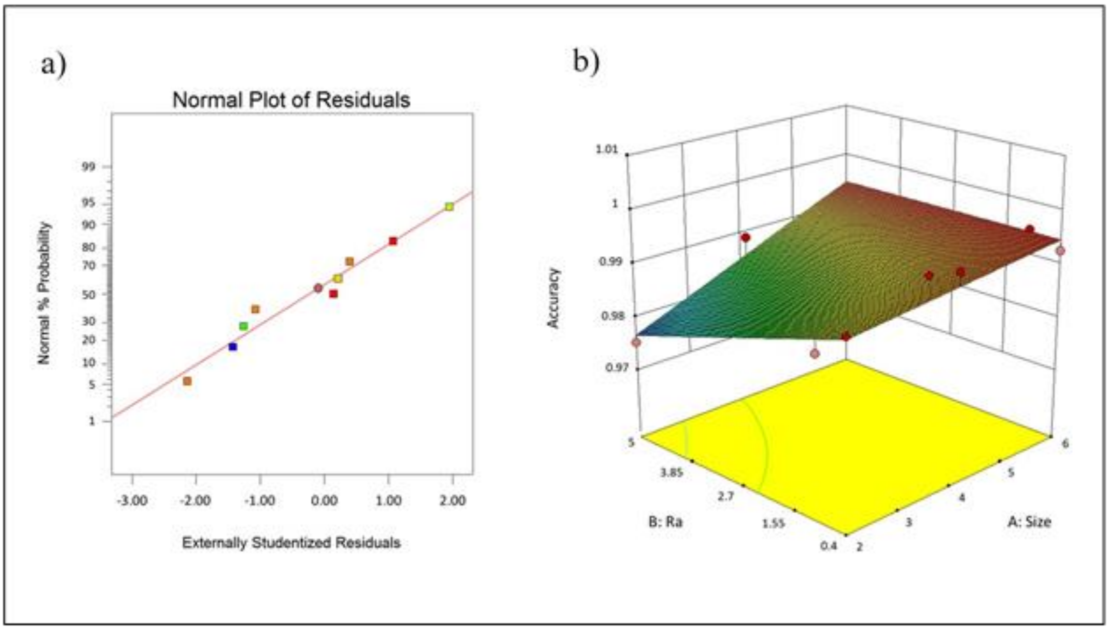

Figure 37a) Normal probability plot of studentized residuals; b) 3D plot of the results of the model.

To achieve the highest part accuracy when manufacturing dovetails using a WEDM process, it can be observed that the best results were achieved with larger part sizes and smaller surface roughness value. The interaction plot between the surface roughness and the part size can be seen in Figure 37b. It is important to note that all of the experimental results falls within the 95% CI confidence band. This is an indication that the model can accurately predict what the accuracy would be, should any of the parameters change.

5.4 Resource Efficient Process Chain Design

The entire production process for manufacturing the CubeSat spaceframe was mapped out in Figure 38 as an adaptation of the Value Stream Design described in Chapter XX. This ensured that the improvements of the individual production processes did not get lost in the bigger picture.

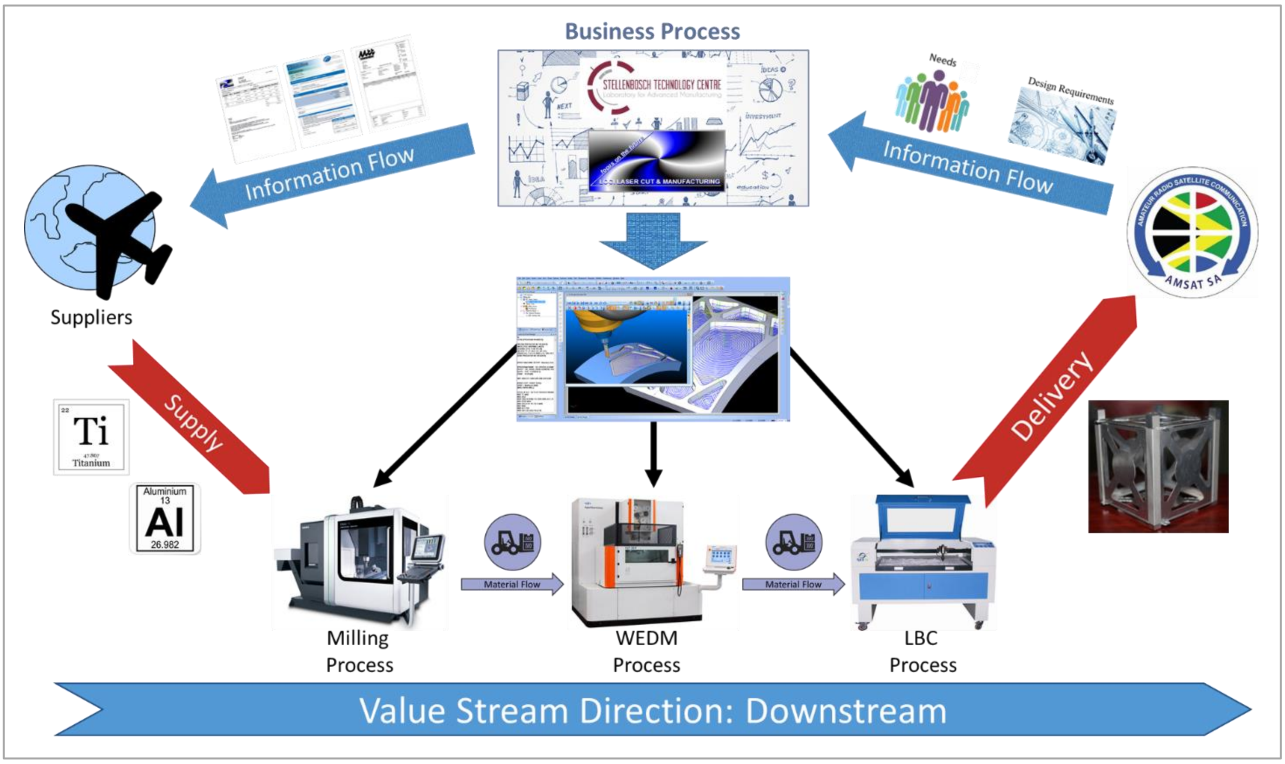

Figure 38: Value Stream Design for the KletsKOUS-3 spaceframe illustrating the information flow and value addition between the various stakeholders

The customer information that feeds the business process include the needs statement and design requirements. This information is then filtered into material selection, product design and process selection, which then moves on to the respective entities. Information flow to the suppliers include the necessary material specifications, while the design and manufacturing data is processed by various CAD/CAM programs to produce the optimal manufacturing solution. The resource efficient process chains developed for each of the manufacturing processes ensured that all of the information culminated into the maximum value added to the customer.

5.4.1 WEDM Manufacturing Process Chain

The WEDM process involves cutting the rails of the CubeSat spaceframe from a 7075-T6 aluminium plate. Figure 39 below depicts the primary process chain for the rails. The material was sourced from Metal and Tool Trade (PTY) LTD. A copy of the purchase order can be found in Appendix D2. The aluminium plate is clamped in the machine bed with a tolerance of ±0.005mm to ensure that the resulting part falls within the required part dimensions. Setting up the machine involves importing the 2D wireframe of the profile to be cut. The starting position of the wire is offset 1mm from the edge of the plate. The reason for this starting position is that the WEDM machine needs a flat surface on the part to start the cut. To achieve the required surface roughness, multiple passes needs to be made, thus the machine time per part is 120 min. The inspection process involves making sure that the grooves in the rails which will house the side panels falls within the required tolerances to achieve a sliding fit with interference. Certified gauge blocks are used to check for a go/no-go tolerance. The post processing of the rails ensure that the length of the rails correlates to the design specifications and is micro-milled to within ±0.05mm, which is well within the required tolerance range.

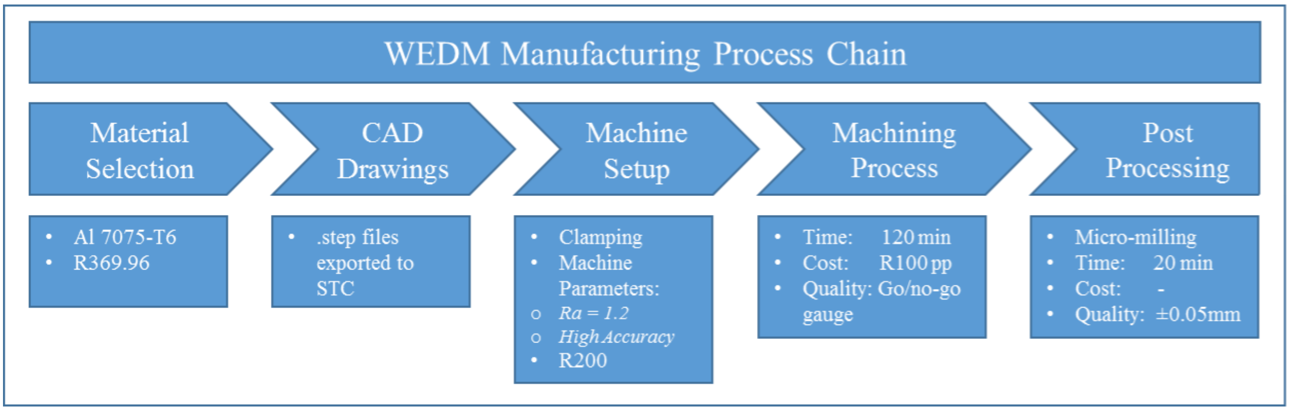

Figure 39: Resource efficient WEDM process chain to manufacture the CubeSat rails

The WEDM Dovetail Experiment provided great insight into the accuracy of the machine at different cutting parameters, and provided the necessary information needed to select the machining parameters.

5.4.2 LBC Manufacturing Process Chain

The laser cutting process was outsourced to a local manufacturing company called Loci Laser. They also supplied the material that was used to cut the top and bottom panel for the CubeSat and the material price is included in the manufacturing price. The process chain for the Laser Beam Cutting process can be seen in Figure 40 below. Because the laser cutting process is a two dimensional process, Loci Laser required a wireframe format of the top view of the part to be cut. The correct CAD file was exported as a .STEP file and the production engineer at Loci Laser uploaded the file to the machine. The correct material was loaded onto the cutting bed after which the manufacturing process was initiated. The exact time of manufacture could not be measured as the CubeSat components formed part of a batch operation in which multiple components for various customers are manufactured in one job. The complete quotation to manufacture these components can be seen in Appendix D4.

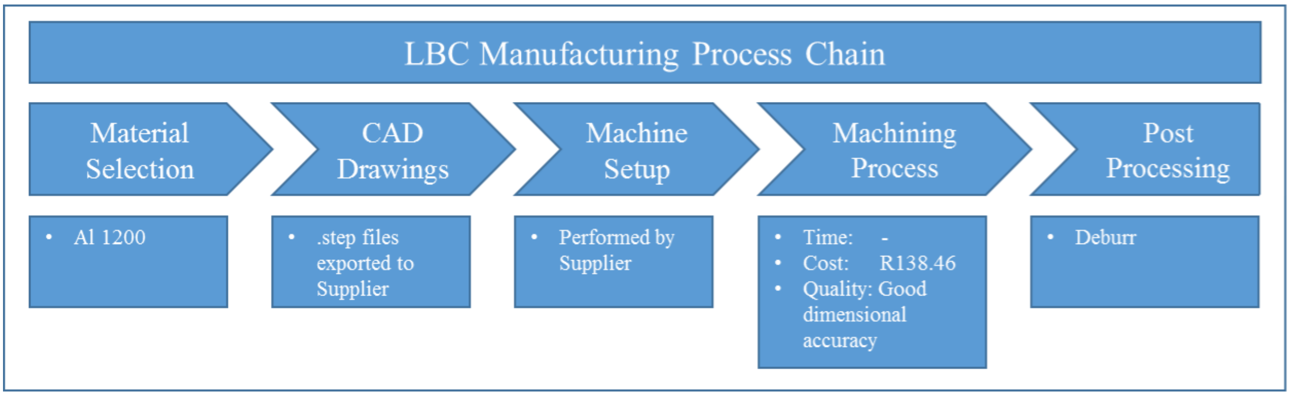

Figure 40: Resource efficient LBC process chain to manufacture the CubeSat top, bottom and side panels

The deburring process is necessary to remove all of the rough edges from the panels after laser cutting. All the edges of the part in question is manually smoothed out using a deburring tool and each panel is visually inspected to ensure that all of the edges are smoothed out. The dimensions are then verified using a Vernier to ensure that they conform to the technical specifications. This will insure that there are no unwanted interferences during the assembly process and that the component fits perfectly when assembled.

5.4.3 Milling Manufacturing Process Chain

Figure 41 illustrates the resource efficient process chain that was used to manufacture the CubeSat standoffs. The CubeSat standoffs are milled from a 9mm x 9mm x 15mm block of 7075-T6 Aluminium. Each CubeSat spaceframe has eight standoffs, four on top, and four on the bottom. The purpose of the standoffs are to ensure separation between the CubeSats in the P-POD by minimising the surface contact between each satellite. The specialized clamping method that held the workpiece to the machine bed ensured repeatability of the process while greatly decreasing the setup time. Once the zero point was established, the chamfer of the standoff was cut, after which the workpiece is turned upside down to mill the top profile, which is needed for assembly. The top profile is a key feature of the standoff that integrates precisely with the rails to hold the spaceframe together. The quality control of the standoffs were done with a Vernier to ensures that each part falls within the specific design requirements. This strict QC process is in place because the standoffs not only protects the payload of the KletsKOUS CubeSat, but also ensures the safety of all of the CubeSats in the P-POD by providing adequate separation and minimal surface contact.

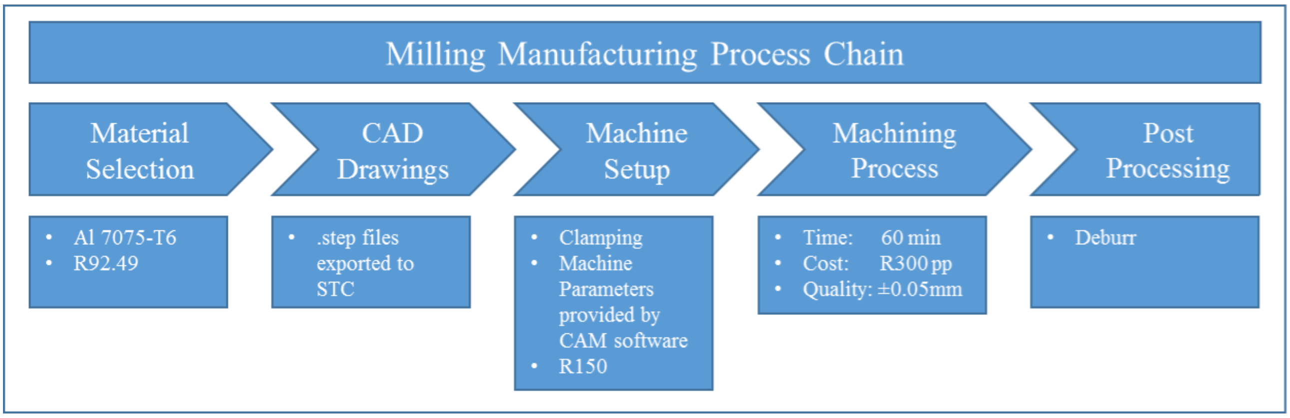

Figure 41: Resource efficient Milling process chain to manufacture the CubeSat standoffs

Chapter 6: Conclusion and Future Work

Future technological advancements will ensure that the miniaturization of components continues to satisfy all of the market trends regarding small satellites. The reduced weight of these satellites inevitably lowers the launch cost, while at the same time surpassing the capabilities of satellites that once weighed upwards of 1000kg. With the developments of launch opportunities, especially for small satellites, the market segment is expected to maintain a steady growth deep into the future.

The KletsKOUS-3 CubeSat prototype provides a competitive edge through its modular design. Not only does this provide the users with a *blank canvas* when it comes to satellite design, but it also makes the manufacturing of the components very easy. This is supported by the fact that the CubeSat spaceframe scored the highest out of all the competitors with regards to design efficiency. The low weight of the structure also allows for a heavier payload to be carried into space. This can vary from a larger battery pack for increased function on the dark side of earth, or a more powerful camera for higher resolution earth observations. This versatile CubeSat structure can provide the user with more opportunities to expand small satellite development, rather than limit his/her capabilities through a non-flexible spaceframe.

The resource efficient process chains of the KletsKOUS-3 CubeSat utilises both traditional and non-traditional machining methods to manufacture the components. This allows for increased flexibility in the manufacturing system while at the same time producing high quality, extremely accurate components. The value stream design follows each process that adds value to the customer, and in doing so, prevents tunnel vision by never losing sight of the bigger picture. Figure 42 shows the cost; weight and DE value of the KletsKOUS-3 prototype and it is evident that it can provide future customers with a superior CubeSat spaceframe.

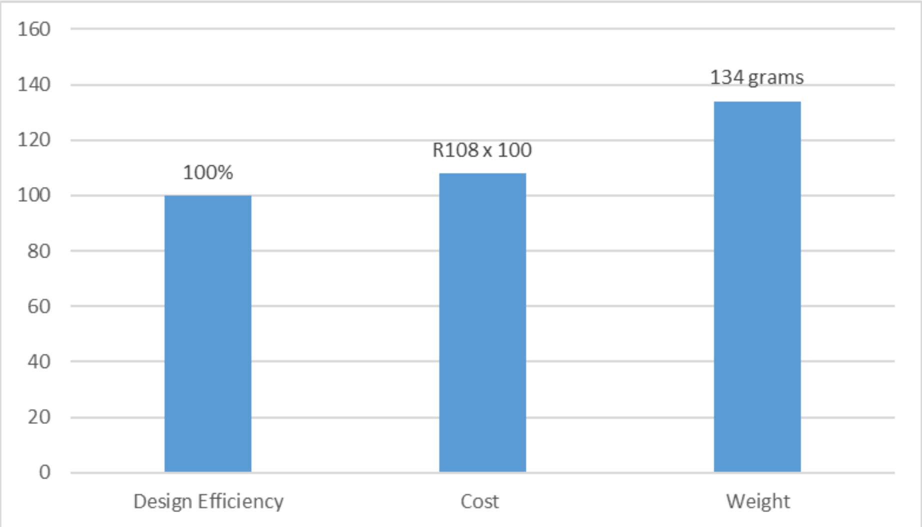

Figure 42: Design Efficiency, Cost and Weight of the KletsKOUS-3 CubeSat spaceframe prototype

Costing only R10800, KletsKOUS-3 is nearly half the price as that of the closest competitor, and with a structure weight of only 134 grams, it is well below the industry standard of 200 grams. The unique interference fit mechanism makes assembling and disassembling the structure much easier, which simplifies the integration process with the rest of the satellite components.

Future work on the project should include a FEA analysis to determine the structural limits of the spaceframe. This will highlight any further weaknesses in the structure and efforts can be made to help better the design even further. A KletsKOUS spaceframe should be used as a platform for the development of a CubeSat to test how compatible the structure is with small satellite components, even though the design does allow for a highly customized structure.

When compared to other designs, it is clear that KletsKOUS is a worthy option, when compared to the other CubeSat structure providers. With the low cost, high design efficiency and acceptable structure weight, the opportunity exists for KletsKOUS to be fully commercialised and become a market leader in the field of CubeSat spaceframe manufacturing.

Bibliography

[1] H. Heidt, P. J. Puig-suari, P. A. S. Moore, P. S. Nakasuka, and P. R. J. Twiggs, "SSC00-V-5 Experimentation."

[2] J. Cutler and G. Hutchins, "OPAL : Smaller , Simpler , and Just Plain Luckier," *14th Annu. Conf. Small Satell.*, p. 4, 2000.

[3] A. Toorian, K. Diaz, and S. Lee, "The CubeSat approach to space access," *IEEE Aerosp. Conf. Proc.*, vol. 1, no. 1, 2008.

[4] NRO, "National Reconnaissance Office 2013 Innovation Campaign: The CubeSat Program," 2013.

[5] E. Blundell, "Aiaa-rs3 2005-3001," pp. 1–9, 2005.

[6] A. Chin, R. Coelho, R. Nugent, R. Munakata, and J. Puig-Suari, "CubeSat: The Pico-Satellite Standard for Research and Education," *AIAA Sp. 2008 Conf. Expo.*, no. September, pp. 1–11, 2008.

[7] CalPoly, "Cubesat design specification rev. 13," *CubeSat Program, Calif. Polytech. State …*, vol. 8651, p. 22, 2009.

[8] W. B. Banerdt *et al.*, "INSIGHT: A DISCOVERY MISSION TO EXPLORE THE INTERIOR OF MARS."

[9] G. Williams, "project report . An annual Update."

[10] P. Hines and N. Rich, "Mapping Tools," *Int. J. Oper. Prod. Manag.*, vol. 17, no. 1, pp. 46–64, 1997.

[11] K. Erlach, *Value Stream Design. The Way Towards a Lean Factory*, vol. 53. 2013.

[12] St. Edward's University, *Perspectives in Business*, vol. 3. 2006.

[13] M. Pienkowski, "Waste Measurement Techniques for Lean Manufacturing Companies," *Int. J. Lean Six Sigma*, vol. 5, no. 1, pp. 1–16, 2014.

[14] K. K. Lim, P. K. Ahmed, and M. Zairi, "Techniques Managing waste and looking beyond : the IMI approach," *TQM Mag.*, vol. 11, no. 5, pp. 304–310, 1999.

[15] B. J. Hicks, "Lean information management: Understanding and eliminating waste," *Int. J. Inf. Manage.*, vol. 27, no. 4, pp. 233–249, 2007.

[16] T. Kitajima, H. Sawanishi, M. Taguchi, K. Torihara, O. Honma, and N. Mishima, "A proposal on a resource efficiency index for EEE," *Procedia CIRP*, vol. 26, no. 1, pp. 607–611, 2015.

[17] Y. Koren, *Globalization and Manufacturing Paradigms*, no. April. 2010.

[18] C. I. Ras, G. A. Oosthuizen, J. F. W. Durr, P. D. E. Wet, and J. F. Oberholzer, "Social manufacturing bamboo bikes for africa," *Int. Assoc. Manag. Technol.*, pp. 066–077, 2016.

[19] I. S. Jawahir, "Sustainable Manufacturing: The Driving Force for Innovative Products, Processesand Systems for Next Generation Manufacturing," *Symp. Sustain. Prod. Dev. IIT*, no. 859, 2008.

[20] I. S. Jawahir and R. Bradley, "Technological Elements of Circular Economy and the Principles of 6R-Based Closed-loop Material Flow in Sustainable Manufacturing," *Procedia CIRP*, vol.

40, pp. 103–108, 2016.

[21] H. Q. Wu, Y. Shi, Q. Xia, and W. D. Zhu, “Effectiveness of the policy of circular economy in China: A DEA-based analysis for the period of 11th five-year-plan,” *Resour. Conserv. Recycl.*, vol. 83, pp. 163–175, 2014.

[22] M. Kutz, *Environmentally conscious mechanical design*. John Wiley & Sons, 2007.

[23] F. Edition and M. P. Groover, *Fundamentals of Modern Manufacturing*. JOHN WILEY & SONS, INC, 2010.

[24] E. P. (Ernest P. DeGarmo, J. T. Black, and R. A. Kohser, *Degarmo’s materials and processes in manufacturing*. .

[25] F. Klocke, *Manufacturing processes 1: Cutting*. 2010.

[26] B. Aksu, C. Çelebi, and E. Budak, “An experimental investigation of oblique cutting mechanics,” *Mach. Sci. Technol.*, vol. 20, no. 3, pp. 495–521, Jul. 2016.

[27] T. Özel, X. Liu, and A. Dhanorker, “Modelling and simulation of micro-milling process,” *4th Int. Conf. Exhib. Des. Prod. Mach. Dies/Molds*, no. December 2009, pp. 21–23, 2007.

[28] C. Kim, “cl!!! Experimental Analysis of Chip Formation in Micro-Milling author(s),” no. JANUARY 2002, 2015.

[29] F. Klocke, *Manufacturing Processes 2: Grinding, Honing, Laping*. .

[30] “On the mechanics of the grinding process – Part I. Stochastic nature of the grinding process,” *Int. J. Mach. Tools Manuf.*, vol. 43, no. 15, pp. 1579–1593, Dec. 2003.

[31] M. Kunieda, B. Lauwers, K. P. Rajurkar, and B. M. Schumacher, “Advancing EDM through Fundamental Insight into the Process,” *CIRP Ann. - Manuf. Technol.*, vol. 54, no. 2, pp. 64–87, 2005.

[32] N. Mohd Abbas, D. G. Solomon, and M. Fuad Bahari, “A review on current research trends in electrical discharge machining (EDM),” *Int. J. Mach. Tools Manuf.*, vol. 47, no. 7–8, pp. 1214–1228, 2007.

[33] K. H. Ho, S. T. Newman, S. Rahimifard, and R. D. Allen, “State of the art in wire electrical discharge machining (WEDM),” *Int. J. Mach. Tools Manuf.*, vol. 44, no. 12–13, pp. 1247–1259, 2004.

[34] A. B. Puri and B. Bhattacharyya, “An analysis and optimisation of the geometrical inaccuracy due to wire lag phenomenon in WEDM,” *Int. J. Mach. Tools Manuf.*, vol. 43, no. 2, pp. 151–159, 2003.

[35] W. M. Steen and J. Mazumder, *Laser Material Processing*. 2010.

[36] A. Kumar Dubey and V. Yadava, “Multi-objective optimisation of laser beam cutting process,” *Opt. & Laser Technol.*, vol. 40, no. 3, pp. 562–570, 2008.

[37] C. Leyens and M. Peters, *Titanium an Titanium Alloys*. 2003.

[38] G. Welsch, R. Boyer, and E. W. Collings, *Materials Properties Handbook: Titanium Alloys*. ASM International, 1993.

[39] P. Fonda, Z. Wang, K. Yamazaki, and Y. Akutsu, “A fundamental study on Ti-6Al-4V’s thermal and electrical properties and their relation to EDM productivity,” *J. Mater. Process. Technol.*, vol. 202, no. 1–3, pp. 583–589, 2008.

[40] Cambridge University Engineering Department, “Materials data book,” *Mater. Courses*, pp. 1–41, 2003.

[41] T. R. Bieler, M. G. Glavicic, and S. L. Semiatin, “Using OIM to investigate the microstructural evolution of Ti-6Ai-4V,” *Jom*, vol. 54, no. 1, pp. 31–36, 2002.

[42] ABKOWITZ and S., “The Emergence of the Titanium Industry and the Development of the Ti-6Al-4V Alloy,” *JOM Monogr. Ser.*, vol. 1, 1999.

[43] G. C. Marshall, “machining of titanium and its alloys Nasa,” vol. 204, no. 6, pp. 53–60, 1965.

[44] E. O. Ezugwu and Z. M. Wang, “Titanium alloys and their machinability,” *J. Mater. Process. Technol.*, vol. 68, no. 3, pp. 262–274, 1997.

[45] X. Yang and C. Richard Liu, *Machining Titanium and Its Alloys*, vol. 3, no. 1. 1999.

[46] E. O. Ezugwu, J. Bonney, and Y. Yamane, “An overview of the machinability of aeroengine alloys,” *J. Mater. Process. Technol.*, vol. 134, no. 2, pp. 233–253, 2003.

[47] L. N. L??pez De Lacalle, J. P??rez, J. I. Llorente, and J. A. S??nchez, “Advanced cutting conditions for the milling of aeronautical alloys,” *J. Mater. Process. Technol.*, vol. 100, no. 1, pp. 1–11, 2000.

[48] C. Cui, B. Hu, L. Zhao, and S. Liu, “Titanium alloy production technology, market prospects and industry development,” *Mater. Des.*, vol. 32, no. 3, pp. 1684–1691, 2011.

[49] M. Yamada, “An overview on the development of titanium alloys for non-aerospace application in Japan,” *Mater. Sci. Eng. A*, vol. 213, no. 1–2, pp. 8–15, 1996.

[50] R. R. Boyer, “An overview on the use of titanium in the aerospace industry,” *Mater. Sci. Eng. A*, vol. 213, no. 1–2, pp. 103–114, 1996.

[51] M. Peters, J. Kumpfert, C. H. Ward, and C. Leyens, “Titanium alloys for aerospace applications,” *Adv. Eng. Mater.*, vol. 5, no. 6, pp. 419–427, 2003.

[52] R. R. Boyer and R. D. Briggs, “The use of ?? titanium alloys in the aerospace industry,” *J. Mater. Eng. Perform.*, vol. 22, no. 10, pp. 2916–2920, 2013.

[53] R. R. Boyer, “Titanium for aerospace: Rationale and applications,” *Adv. Perform. Mater.*, vol. 2, no. 4, pp. 349–368, Oct. 1995.

[54] R. . Schutz and H. . Watkins, “Recent developments in titanium alloy application in the energy industry,” *Mater. Sci. Eng. A*, vol. 243, no. 1–2, pp. 305–315, 1998.

[55] F. H. Froes, H. Friedrich, J. Kiese, and D. Bergoint, “Titanium in the family automobile: The cost challenge,” *Jom*, vol. 56, no. 2, pp. 40–44, 2004.

[56] E. B. Taddei, V. A. R. Henriques, C. R. M. Silva, and C. A. A. Cairo, “Production of new titanium alloy for orthopedic implants,” *Mater. Sci. Eng. C*, vol. 24, no. 5, pp. 683–687, 2004.

[57] K. Wang, “The use of titanium for medical applications in the USA,” *Mater. Sci. Eng. A*, vol. 213, no. 1–2, pp. 134–137, 1996.

[58] D. S. Mackenzie, *Handbook of Aluminum*. 2003.

[59] R. Den Hond, I. Hiralal, and A. Rijkeboer, “Alumina Yield in the Bayer Process Past, Present and Prospects,” in *Essential Readings in Light Metals*, Cham: Springer International Publishing, 2016, pp. 528–533.

[60] “CORROSION RESISTANCE OF ALUMINIUM AND PROTECTIVE MEASURES

WHERE APPROPRIATE CONTENTS.”

[61] J. Davis, “Corrosion of Aluminum and Aluminum Alloys.”

[62] R. Society and R. Society, “ON THE MANUFACTURE , PROPERTIES AND APPLICATIONS OF ALUMINIUM AND ITS ALLOYS Author (s): Colin J . Smithells Source : Journal of the Royal Society of Arts , Vol . 98 , No . 4828 (25th AUGUST , 1950), pp . Published by : Royal Society for the Encourage,” vol. 98, no. 4828, pp. 822–863, 2017.

[63] P. G. Sheasby and R. Pinner, “Introduction : Aluminium , Its Properties , Alloys and Finishes,” *Met. Finish.*, pp. 435–450, 2001.

[64] J. R. Davis, “Aluminum and Aluminum Alloys,” *Light Met. Alloy.*, p. 66, 2001.

[65] A. Heinz, A. Haszler, C. Keidel, S. Moldenhauer, R. Benedictus, and W. S. Miller, “Recent development in aluminium alloys for aerospace applications,” *Mater. Sci. Eng. A*, vol. 280, no. 1, pp. 102–107, 2000.

[66] T. Conductivity, H. Reflectivity, S. To, W. Ratio, and C. Resistance, “Aluminium Alloy : Introduction to Aluminium Alloy : Introduction to,” pp. 1–3.

[67] T. K. and R. Bidulský, *ALUMINIUM ALLOYS , Edited by Tibor Kva č kaj and Róbert Bidulský*. 2011.

[68] M. M. Tash, K. A. Abuhasel, and S. A. Alkahtani, “Correlation between Alloying Elements and Aging Parameters and Hardness and Machinability of Aluminum-Silicon Alloys Using Minitab Software,” *Adv. Mater. Res.*, vol. 1101, pp. 217–224, Apr. 2015.

[69] 3 & Wisley F. Sales3 & Mário C. Santos Jr1 & Alisson R. Machado2 and Marcos A. S. Barrozo4 & Emmanuel O. Ezugwu, “Machining of aluminum alloys: a review,” *Int J Adv Manuf Technol*, 2016.

[70] W. H. Steyn, R. Van Zyl, M. Inggs, and P. J. Cilliers, “Current and future small satellite projects in South Africa,” *Int. Geosci. Remote Sens. Symp.*, pp. 1294–1297, 2013.

[71] G. W. Milne *et al.*, “SUNSAT - Launch and First Six Month â€™ s Orbital Performance .”

[72] R. R. Van Zyl, D. F. Visser, P. J. Cilliers, and B. D. L. Opperman, “ZACUBE-1 space weather mission: Characterize the superDARN HF radar antenna array at SANAE-IV,” *Sp. Weather*, vol. 11, no. 2, pp. 52–54, 2013.

[73] E. Buchen, “Small Satellite Market Observations,” *29th Annu. AIAA/USU Conf. Small Satell.*, pp. 1–5, 2015.

[74] J. Straub and J. Straub, “CubeSats : A Low-Cost , Very High-Return Space Technology,” 2012.

[75] S. L. Obispo, “SSC12-V-5 ELaNa – Educational Launch of Nanosatellite Providing Routine RideShare Opportunities Garrett Lee Skrobot Roland Coelho ELaNa - Education Launch of Nanosatellite Providing Routine RideShare Opportunities Skrobot Conference on Small Satellites Sk,” pp. 1–6, 2012.

[76] C. R. Boshuizen, J. Mason, P. Klupar, and S. Spanhake, “Results from the Planet Labs Flock Constellation,” *28th Annu. AIAA/USU Conf. Small Satell.*, p. SSC14-I-1, 2014.

[77] NanoRacks LLC, “NV NanoRacks CubeSat Deployer (NRCSD) Interface Control Document,” vol. 77058, no. 815, pp. 1–15, 2013.

[78] “History - ISIS - Innovative Solutions in Space.” [Online]. Available: https://www.isispace.nl/about-us/history/. [Accessed: 05-Nov-2017].

[79] "1-Unit CubeSat structure - ISIS - Innovative Solutions in Space." [Online]. Available: https://www.isispace.nl/product/1-unit-cubesat-structure/. [Accessed: 05-Nov-2017].

[80] "About | CubeSat by EnduroSat." [Online]. Available: https://www.endurosat.com/about/. [Accessed: 05-Nov-2017].

[81] "About Us - Pumpkin, Inc." [Online]. Available: http://www.pumpkinspace.com/about-us.html. [Accessed: 05-Nov-2017].

[82] "RANGE SAFETY USER REQUIREMENTS MANUAL VOLUME 3 LAUNCH VEHICLES, PAYLOADS, AND GROUND SUPPORT SYSTEMS REQUIREMENTS," *AIR FORCE Sp. Command Man. 91-710 Vol. 3*, vol. 3, no. July 2004, 2015.

[83] P. Fortescue, G. Swinerd, and J. Stark, *Spacecraft Systems Engineering*. Wiley, 2011.

[84] C. Boshuizen, "Results from Flock 1 (Presentation)," *28th Annu. AIAA/USU Conf. Small Satell.*, 2014.

Appendix A: Technical Specifications Drawing for the 1U CubeSat Design

This appendix includes the technical specification drawing of the 1U CubeSat design suggested by the California Polytechnic State University. Within this design, two major components notably stands out, the side strut, and the support panel. This drawing also includes the position of the access point and the coordinate system to which the CubeSat must conform.

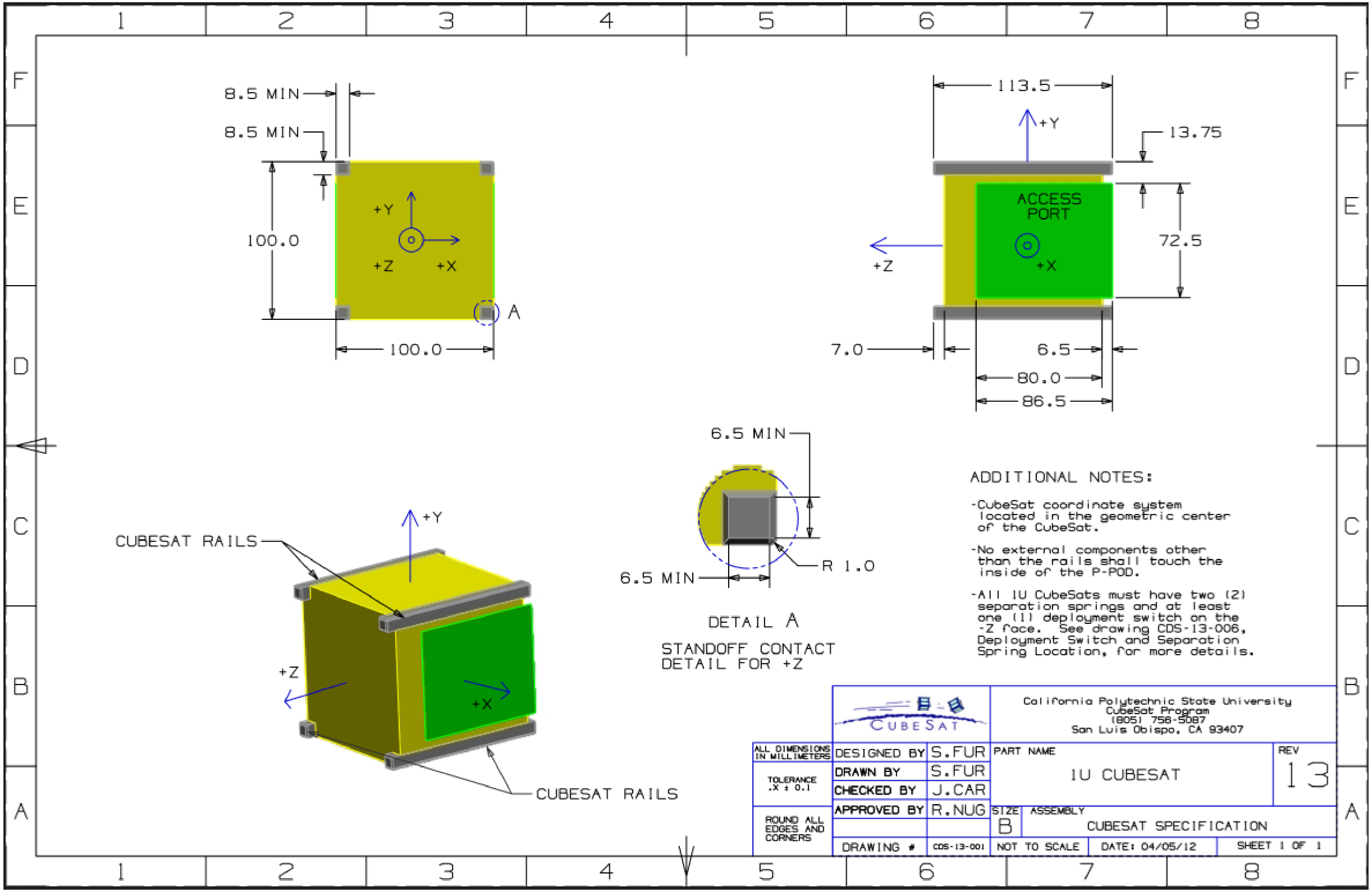
8.5 MIN
8.5 MIN
100.0
+Y
+Z
+X
A
100.0
113.5
+Y
13.75
ACCESS PORT
72.5
+Z
+X
7.0
6.5
80.0
86.5
6.5 MIN
6.5 MIN
R 1.0
DETAIL A
STANDOFF CONTACT DETAIL FOR +Z
CUBESAT RAILS
+Y
+Z
+X
CUBESAT RAILS
ADDITIONAL NOTES:
-CubeSat coordinate system located in the geometric center of the CubeSat.
-No external components other than the rails shall touch the inside of the P-POD.
-All 1U CubeSats must have two (2) separation springs and at least one (1) deployment switch on the -Z face. See drawing CDS-13-006, Deployment Switch and Separation Spring Location, for more details.
CUBESAT
California Polytechnic State University
CubeSat Program
(805) 756-5087
San Luis Obispo, CA 93407
ALL DIMENSIONS IN MILLIMETERS
TOLERANCE .X ± 0.1
ROUND ALL EDGES AND CORNERS
DESIGNED BY S.FUR
DRAWN BY S.FUR
CHECKED BY J.CAR
APPROVED BY R.NUG
DRAWING # CDS-13-001
PART NAME
1U CUBESAT
REV
13
SIZE B
ASSEMBLY
CUBESAT SPECIFICATION
NOT TO SCALE
DATE: 04/05/12
SHEET 1 OF 1

Appendix B: Material Selection Procedure Results

B2: Results of the of the Material Selection Procedure for the CubeSat Rails

This appendix contains the results of the Material Selection Procedure for the rails of the CubeSat spaceframe. The results were obtained by entering the required data into the CES EduPack software. The viable candidates are displayed in colour, while the discarded materials are displayed in grey. Even though it seems that the Stainless Steel Alloy might be the better option to use for the manufacture of the side strut member, the bubble graph indicates that the titanium alloy is able to withstand similar tensile forces while maintaining a lower density.

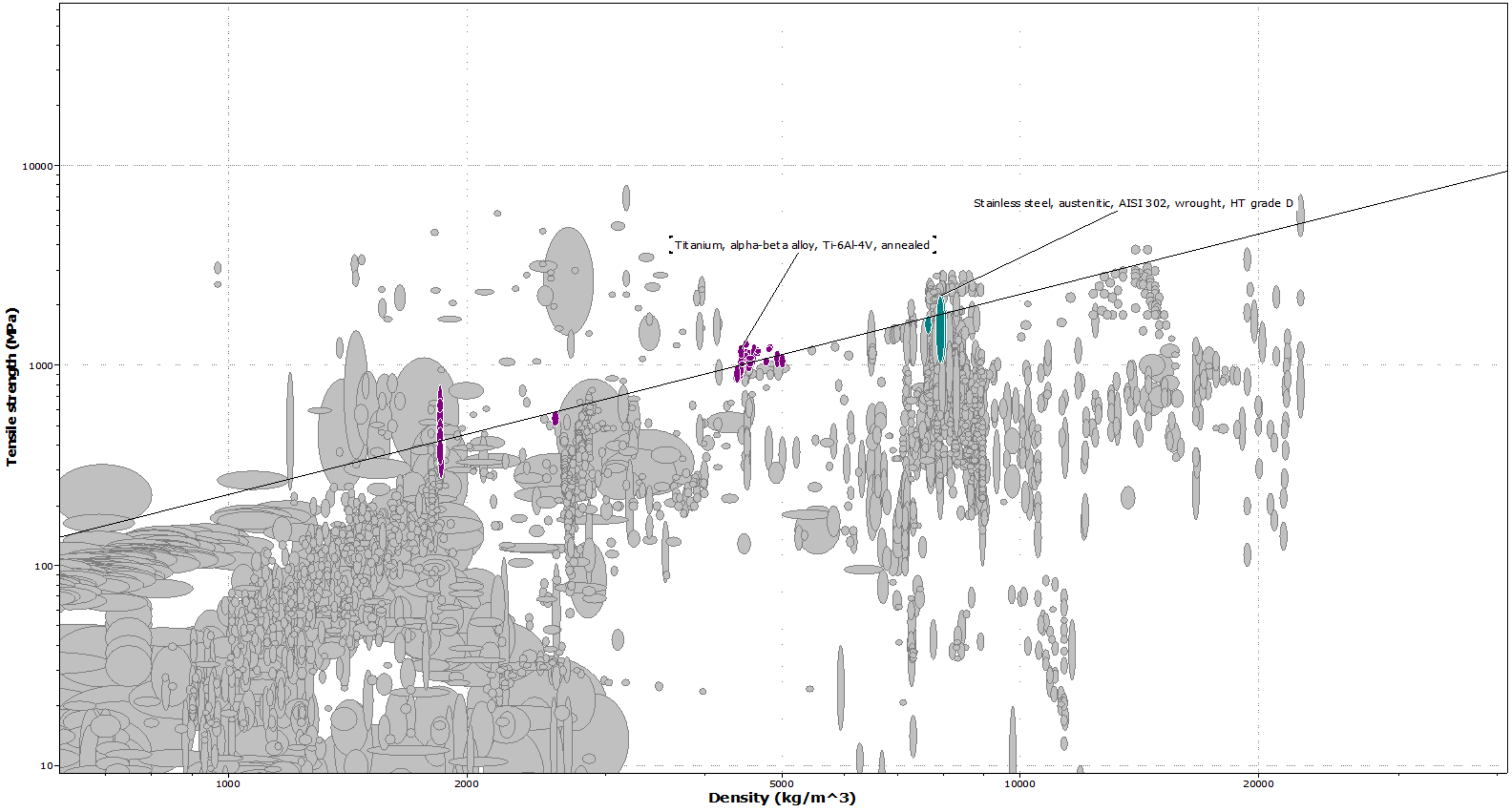

Stainless steel, austenitic, AISI 302, wrought, HT grade D
Titanium, alpha-beta alloy, Ti-6Al-4V, annealed
Tensile strength (MPa)
10000
1000
100
10
1000
2000
5000
10000
20000
Density (kg/m^3)

B2: Results of the Material Selection Procedure for the side panel of the CubeSat spaceframe

This appendix contains the results of the Material Selection Procedure for the side panel of the CubeSat spaceframe. The results were obtained by entering the required data into the CES EduPack software. The viable candidates are displayed in colour, while the discarded materials are displayed in grey. The data displayed on the bubble graph gives a clear result that the 8091 Aluminium alloy is the most viable candidate to use in the manufacture of the support panel.

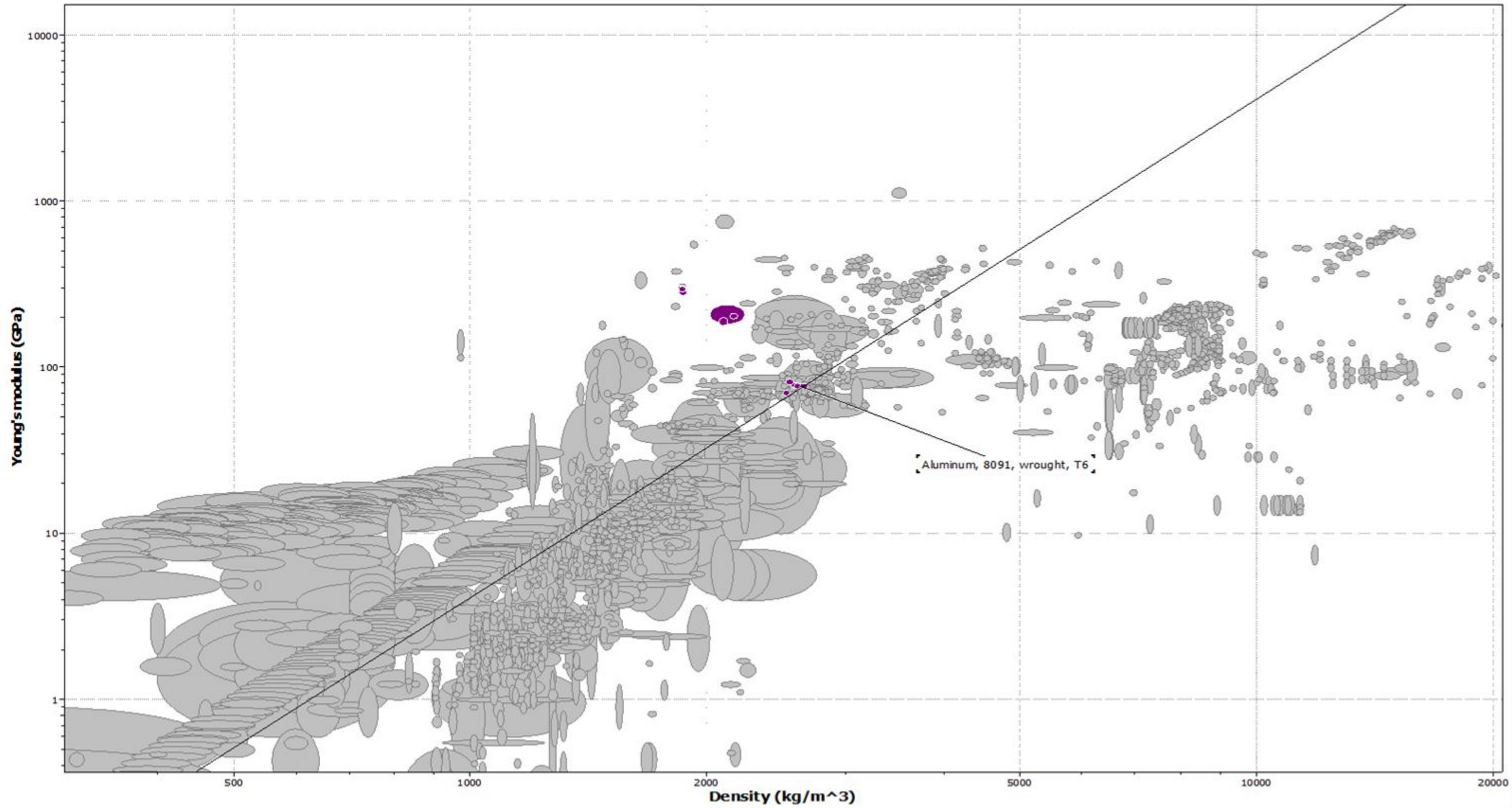
10000
1000
100
10
1
Young's modulus (GPa)
500
1000
2000
5000
10000
20000
Density (kg/m^3)
Aluminum, 8091, wrought, T6

Appendix C: Technical Specification Drawings

C1: Technical Specification Drawings for the KletsKOUS-2 CubeSat Prototype

C1.1: Side Panel Design for the KletsKOUS-2 CubeSat Prototype

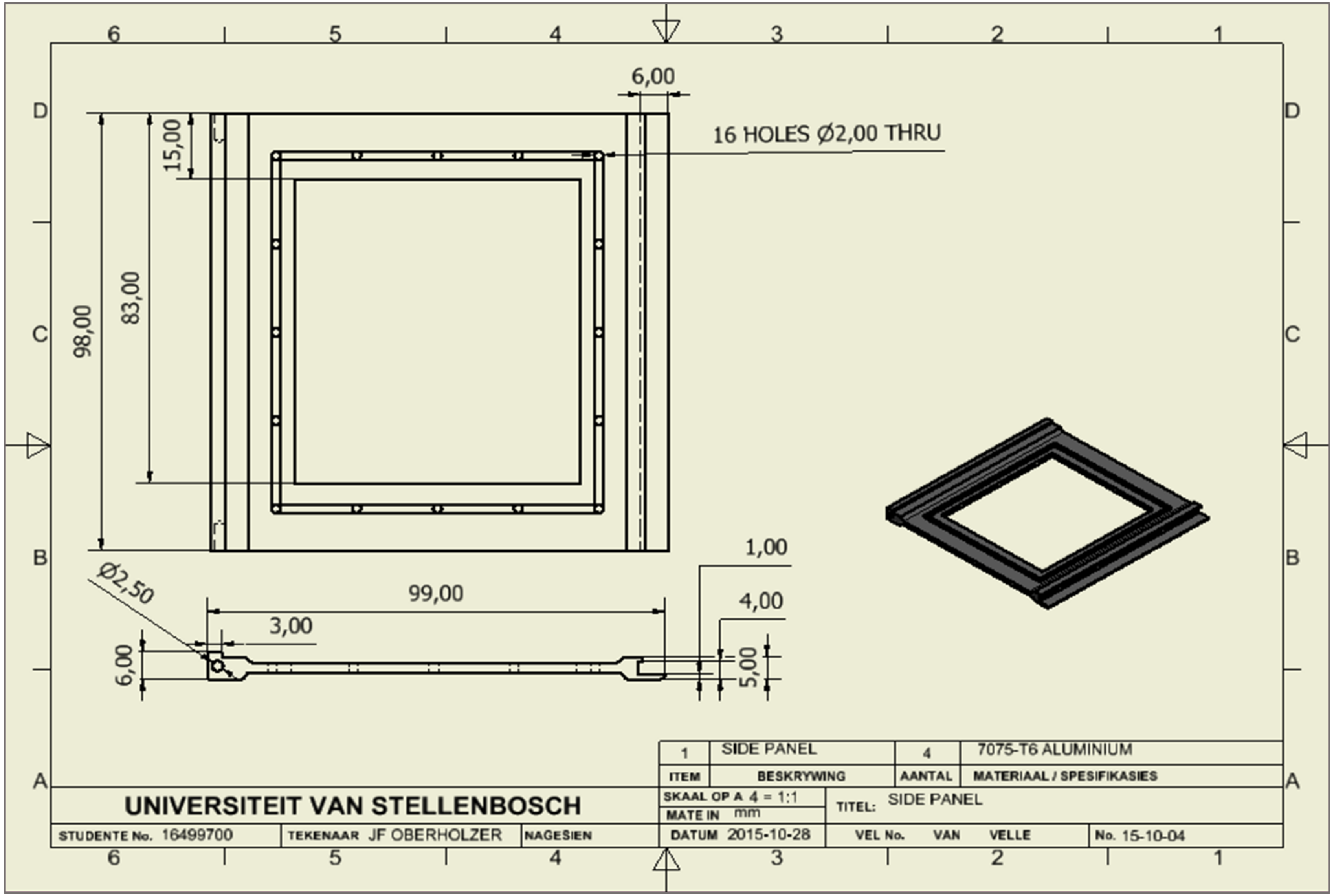
6,00
16 HOLES Ø2,00 THRU
15,00
83,00
98,00
Ø2,50
99,00
3,00
6,00
1,00
4,00
5,00
1 SIDE PANEL 4 7075-T6 ALUMINIUM
ITEM BESKRYWING AANTAL MATERIAAL / SPESIFIKASIES
UNIVERSITEIT VAN STELLENBOSCH
SKAAL OP A 4 = 1:1
MATE IN mm
TITEL: SIDE PANEL
STUDENTE No. 16499700
TEKENAAR JF OBERHOLZER
NAGESIEN
DATUM 2015-10-28
VEL No. VAN VELLE
No. 15-10-04

C1.2: Antenna Deployment Platform Design for the KletsKOUS-2 CubeSat Prototype

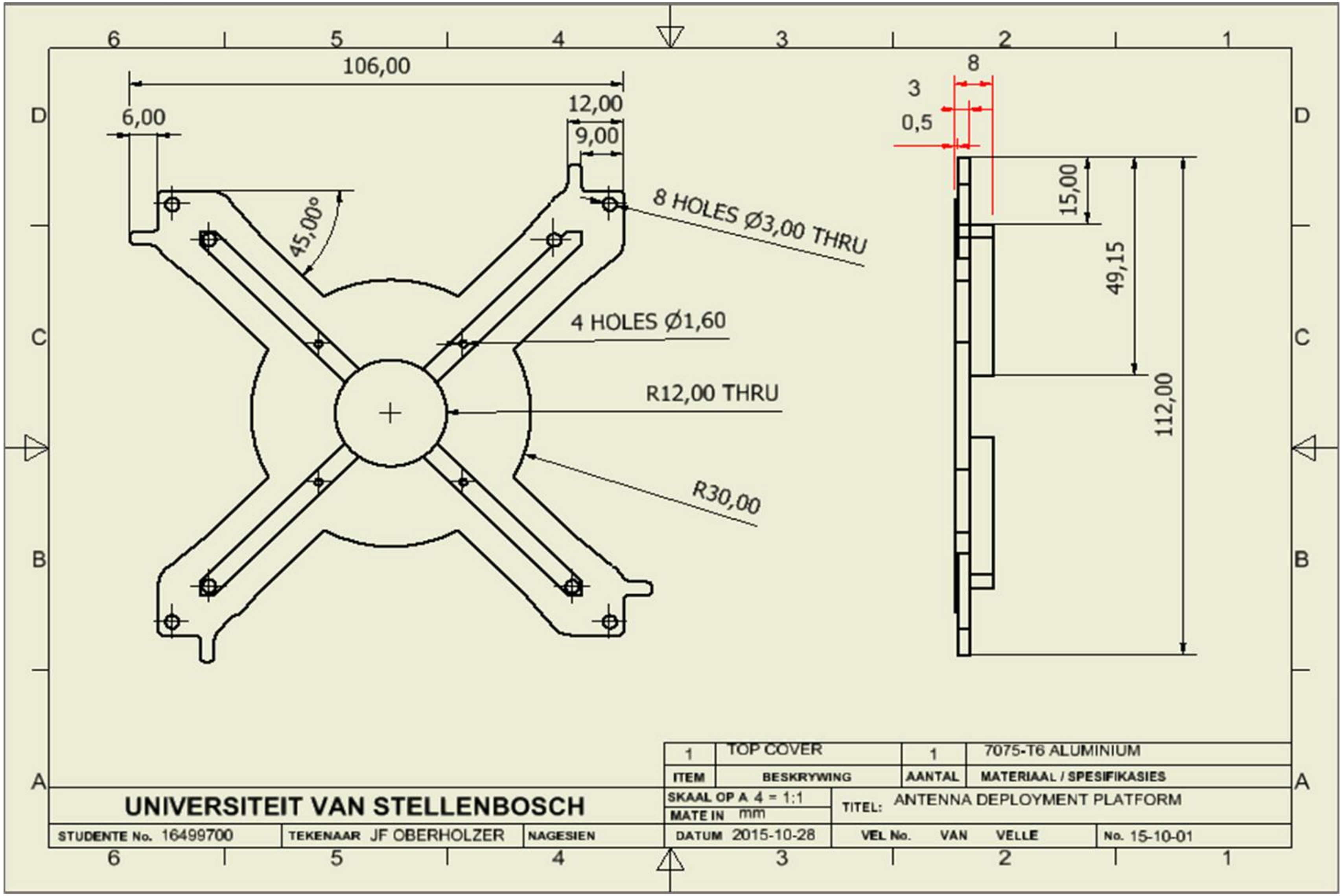
106,00
6,00
12,00
9,00
45,00°
8 HOLES Ø3,00 THRU
4 HOLES Ø1,60
R12,00 THRU
R30,00
8
3
0,5
15,00
49,15
112,00
1 TOP COVER 1 7075-T6 ALUMINIUM
ITEM BESKRYWING AANTAL MATERIAAL / SPESIFIKASIES
UNIVERSITEIT VAN STELLENBOSCH
SKAAL OP A 4 = 1:1
MATE IN mm
TITEL: ANTENNA DEPLOYMENT PLATFORM
STUDENTE No. 16499700
TEKENAAR JF OBERHOLZER
NAGESIEN
DATUM 2015-10-28
VEL No. VAN VELLE
No. 15-10-01

C1.3: Bottom Cover Design for the KletsKOUS-2 CubeSat Prototype

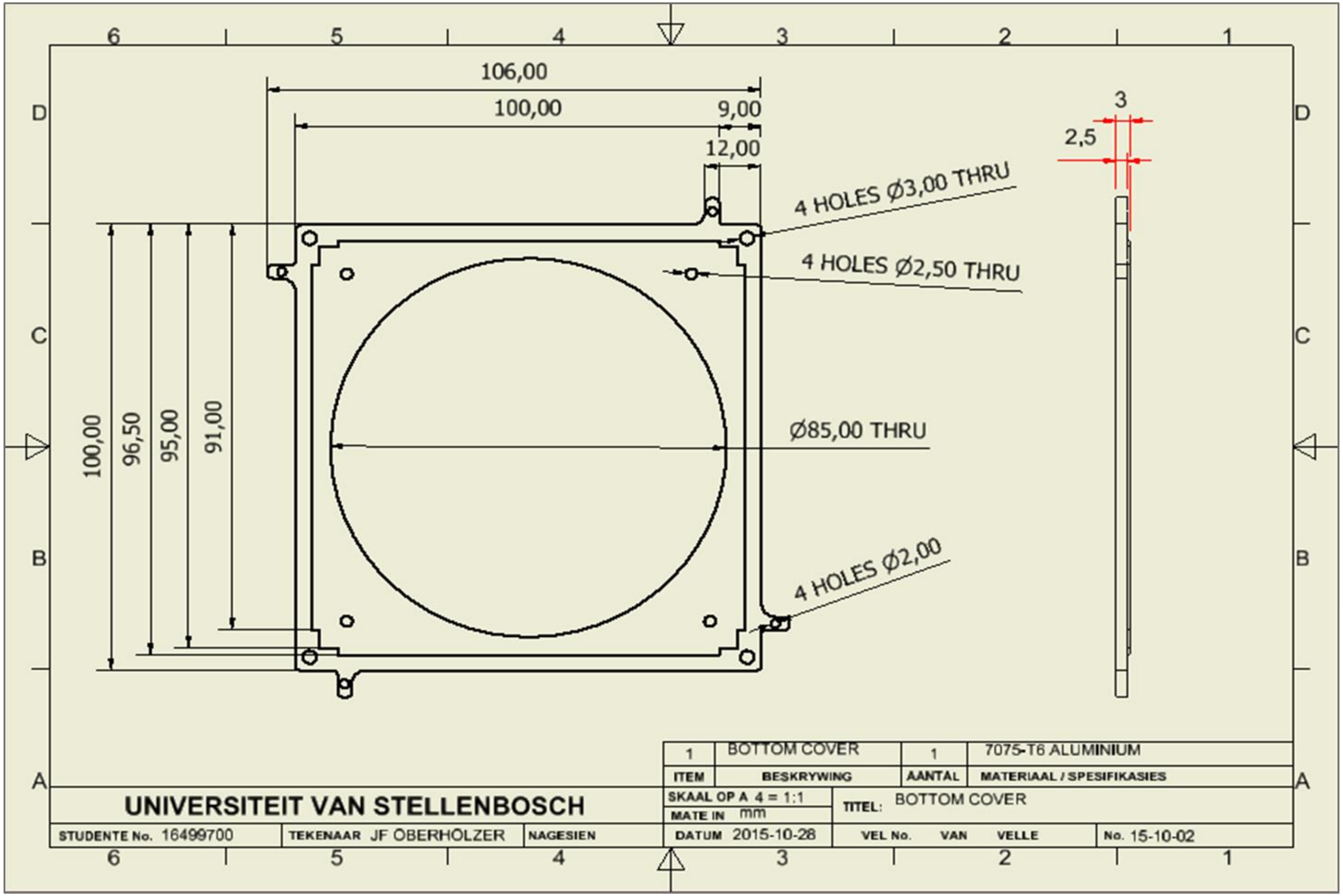
106,00
100,00
9,00
12,00
3
2,5
4 HOLES Ø3,00 THRU
4 HOLES Ø2,50 THRU
Ø85,00 THRU
4 HOLES Ø2,00
100,00
96,50
95,00
91,00
1
BOTTOM COVER
1
7075-T6 ALUMINIUM
ITEM
BESKRYWING
AANTAL
MATERIAAL / SPESIFIKASIES
UNIVERSITEIT VAN STELLENBOSCH
SKAAL OP A 4 = 1:1
MATE IN mm
TITEL: BOTTOM COVER
STUDENTE No. 16499700
TEKENAAR JF OBERHOLZER
NAGESIEN
DATUM 2015-10-28
VEL No.
VAN
VELLE
No. 15-10-02

C1.4: Deployable Solar Panel Flap Design for the KletsKOUS-2 CubeSat Prototype

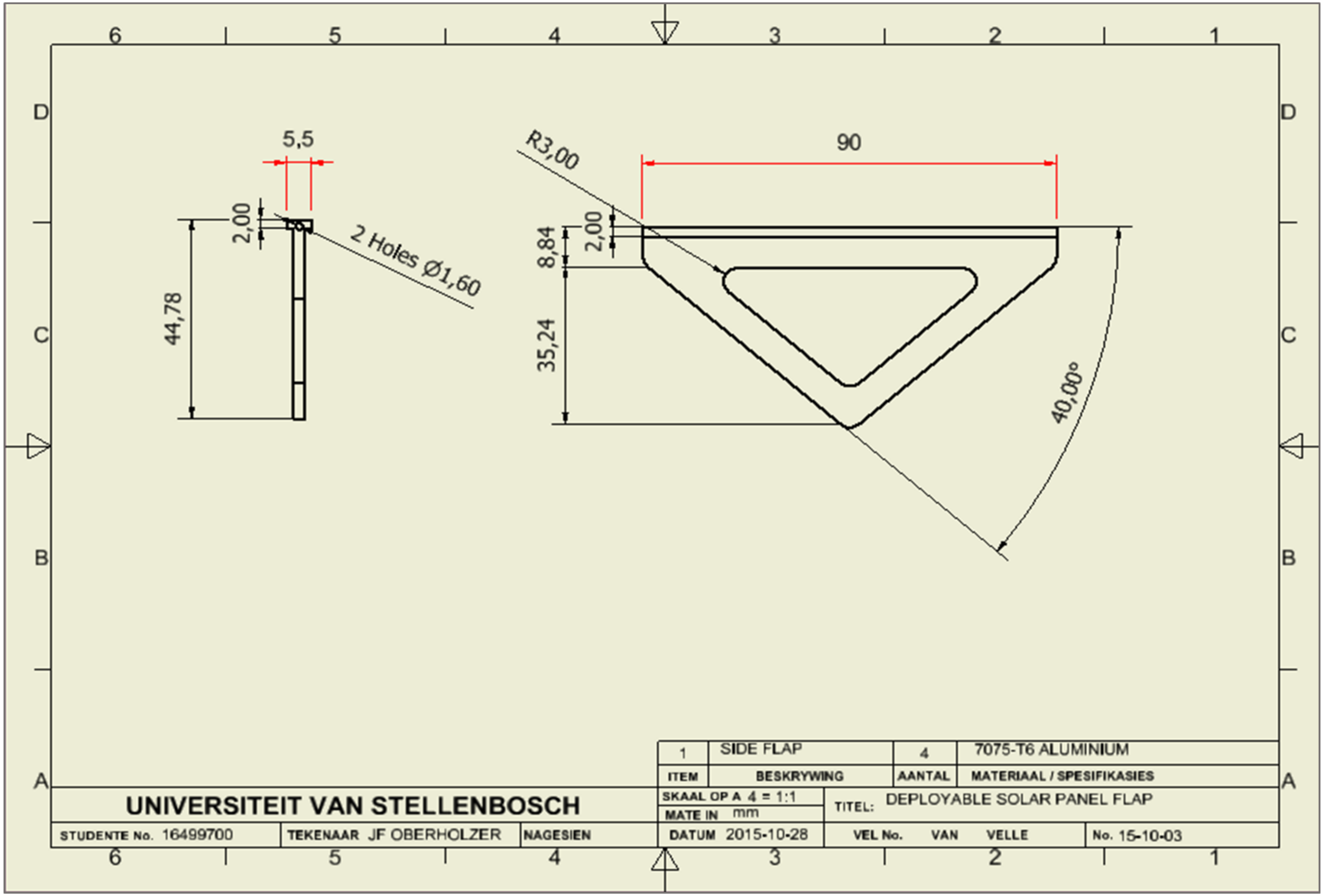
5,5
2,00
44,78
2 Holes Ø1,60
R3,00
90
2,00
8,84
35,24
40,00°
1 SIDE FLAP 4 7075-T6 ALUMINIUM
ITEM BESKRYWING AANTAL MATERIAAL / SPESIFIKASIES
UNIVERSITEIT VAN STELLENBOSCH
SKAAL OP A 4 = 1:1
MATE IN mm
TITEL: DEPLOYABLE SOLAR PANEL FLAP
STUDENTE No. 16499700
TEKENAAR JF OBERHOLZER
NAGESIEN
DATUM 2015-10-28
VEL No. VAN VELLE
No. 15-10-03

C2: Design Drawings for the KletsKOUS-3 CubeSat Prototype

C2.1: Side Panel Design for the KletsKOUS-3 CubeSat Prototype

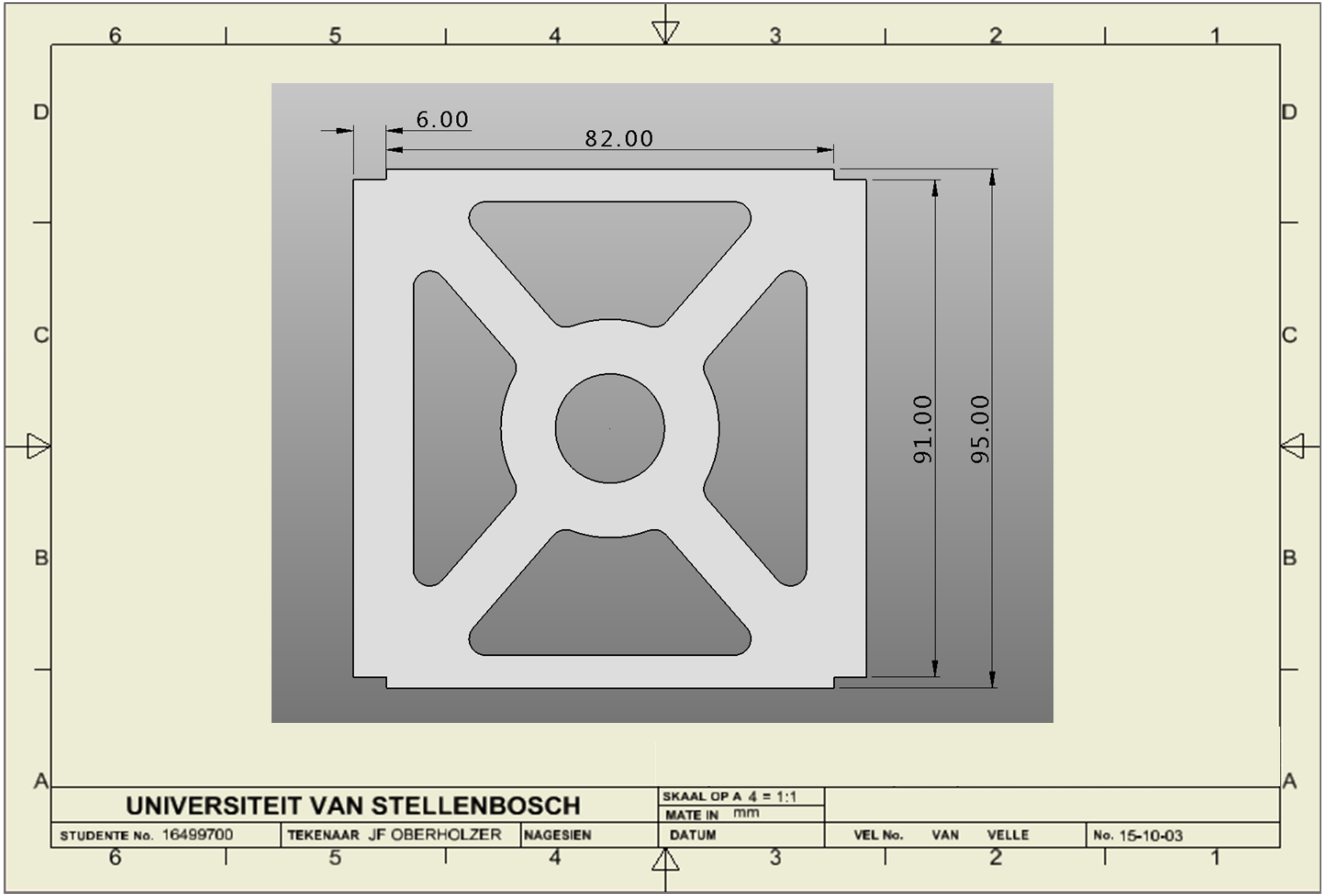
6.00
82.00
91.00
95.00
UNIVERSITEIT VAN STELLENBOSCH
SKAAL OP A 4 = 1:1
MATE IN mm
STUDENTE No. 16499700
TEKENAAR JF OBERHOLZER
NAGESIEN
DATUM
VEL No.
VAN
VELLE
No. 15-10-03

C2.2: Rail Design for the KletsKOUS-3 CubeSat Prototype

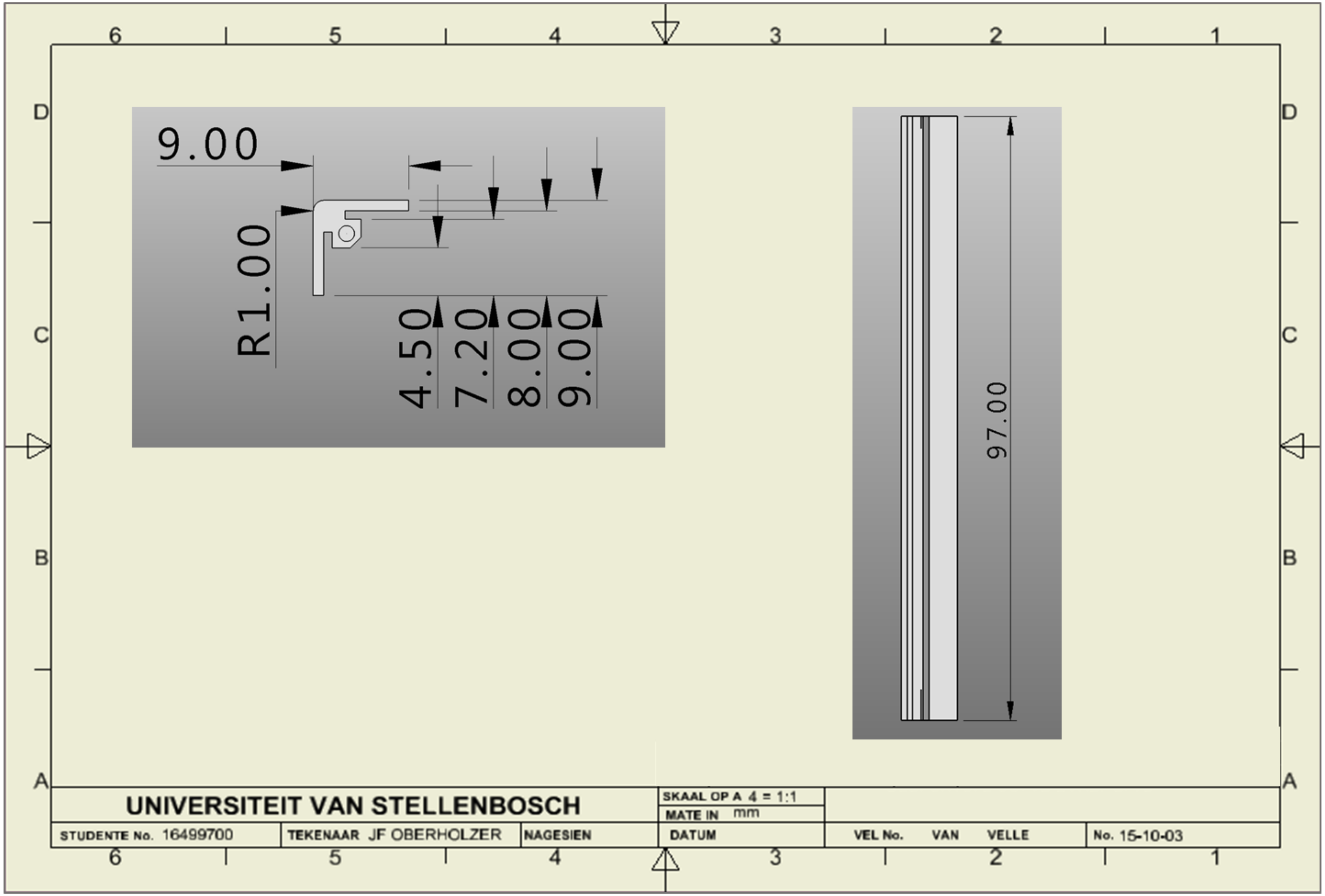

9.00
R1.00
4.50
7.20
8.00
9.00
97.00
UNIVERSITEIT VAN STELLENBOSCH
SKAAL OP A 4 = 1:1
MATE IN mm
STUDENTE No. 16499700
TEKENAAR JF OBERHOLZER
NAGESIEN
DATUM
VEL No.
VAN
VELLE
No. 15-10-03

C2.3: Top and Bottom Panel Design for the KletsKOUS-3 CubeSat Prototype

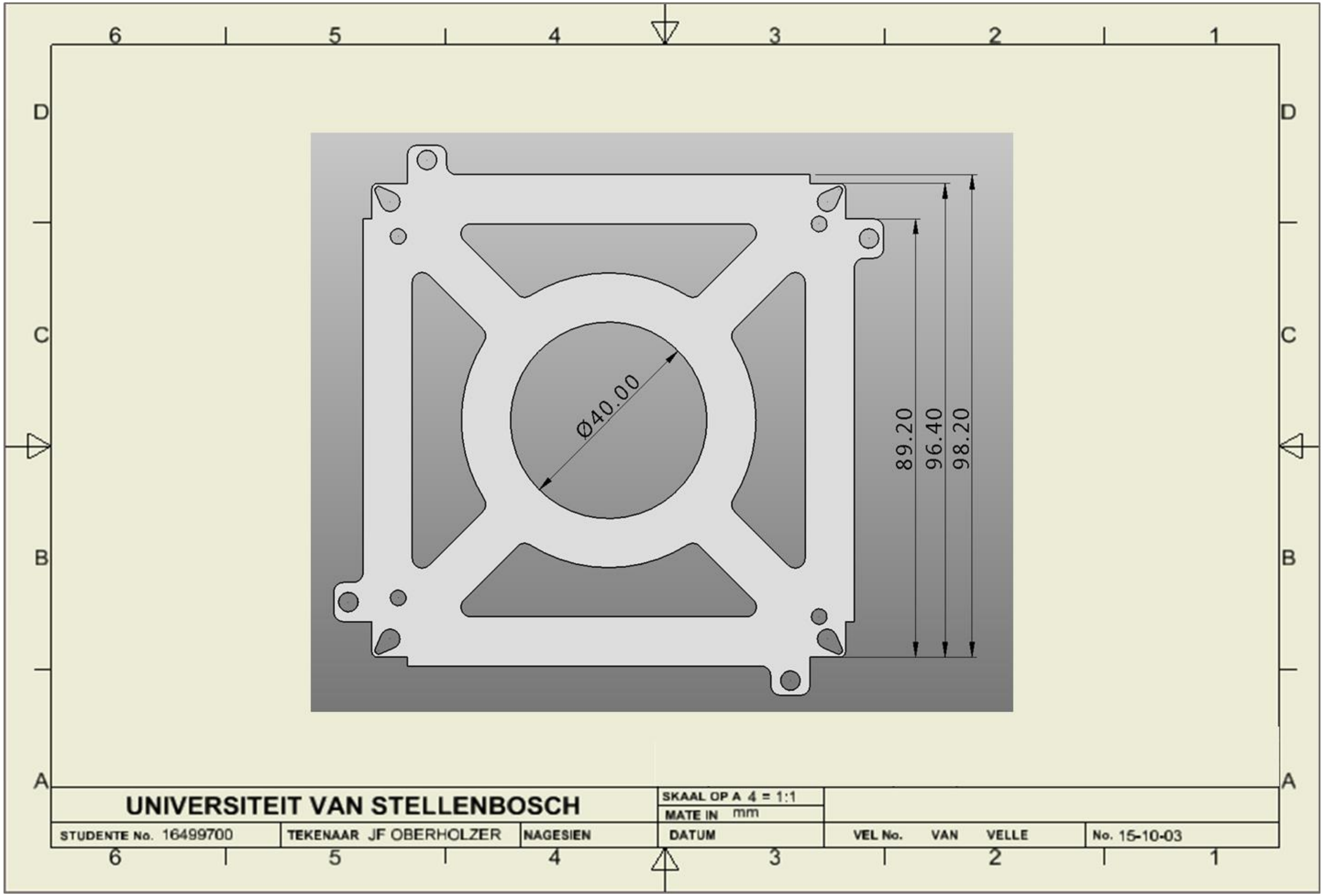
Ø40.00
89.20
96.40
98.20
UNIVERSITEIT VAN STELLENBOSCH
SKAAL OP A 4 = 1:1
MATE IN mm
STUDENTE No. 16499700
TEKENAAR JF OBERHOLZER
NAGESIEN
DATUM
VEL No.
VAN
VELLE
No. 15-10-03

C2.4: Standoff Design for the KletsKOUS-3 CubeSat Prototype

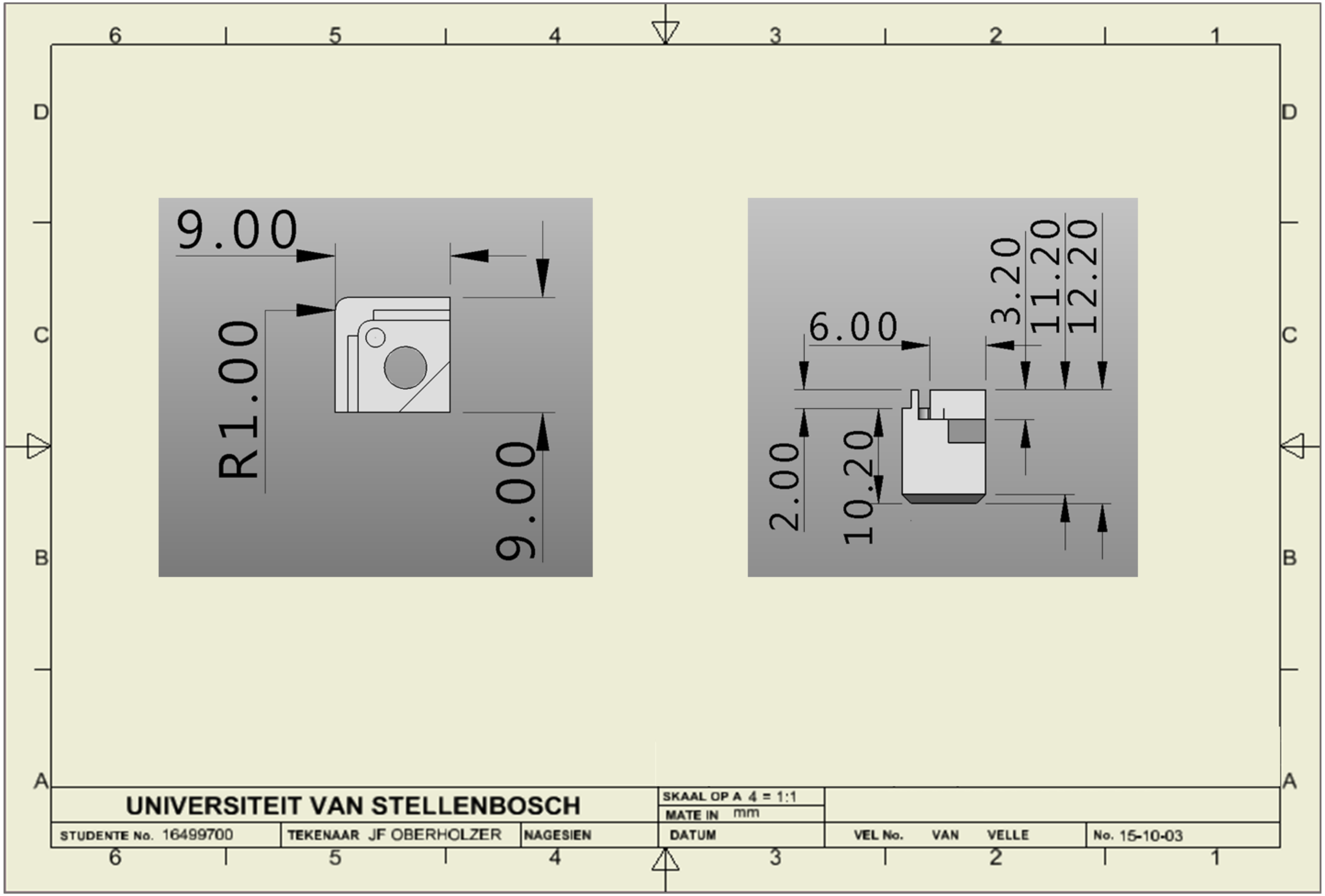
9.00
R1.00
9.00
6.00
3.20
11.20
12.20
2.00
10.20
UNIVERSITEIT VAN STELLENBOSCH
SKAAL OP A 4 = 1:1
MATE IN mm
STUDENTE No. 16499700
TEKENAAR JF OBERHOLZER
NAGESIEN
DATUM
VEL No.
VAN
VELLE
No. 15-10-03

Appendix D: Quotations used to Calculate the Cost of the CubeSat Prototypes

D1: Quotation for manufacturing the KletsKOUS-2 Prototype

Quotation

Prepared for

Company: Dep Ind Eng
Contact: Francois Oberholzer
Telephone:
Email: 16499700@sun.ac.za

Institute for Advanced Tooling
Promoting Sustainable Tooling
University of Stellenbosch, Dept of Industrial Engineering
Cnr of Banhoek and Joubert Street, Matieland, 7602
Tel: +27 21 808 4132 – Fax: +27 21 808 4128

Mike Saxer
Machining Technologist/CNC Specialist
mikesaxer@sun.ac.za

Project Nr.: WC/MS/CNCM/0147
Quotation Date: 12-Oct-15

We thank you for your enquiry and can accordingly quote as follows:

Client input: 3D CAD Models

Deliverables:
4 machined side panels as per 3D
4 machined hinge panels as per 3D
1 machined bottom panel
1 machined antenna panel

Work description:
CAM Programming
CNC Milling

Item Nr	Project Breakdown	Price
1.	CAM Programming	R 4 050.00
2.	CNC Milling	R 5 000.00
	Total Project Value:	R 9 050.00
	Minus 0% Discount:	R 0.00
	Balance:	R 9 050.00
	Add 14% VAT:	R 1 267.00
	Total Price:	**R 10 317.00**

Delivery: The machines are quite booked out- May only be able to start after 15 November earliest but will try to accommodate earlier if possible.

Notes & extra information:
Client to supply material according to sizes specified by us
There will be extra cost related to a fixture to support the parts and provide access to the side grooves

Terms & Conditions

1 This Quotation is valid for 30 days.
2 No results will be delivered before this quote is signed and returned with a valid order number or an official company order has been received by the IAT.
3 Invoices are payed within 14 days.
4 Where applicable, please ensure that all cheques are made out to the University of Stellenbosch.
5 Lead times are applicable only once all terms and conditions have been met by customer.
6 A 50% deposit is required if material is to be purchased including cutting tools

We would be glad to provide you with any additional information. Please feel free to contact us any time.

Best regards

Mike Saxer

Machining Technologist/CNC Specialist

Customer Response Please mark selection & return fax: (021) 808 4128

Considering the above quotation, we wish to

ACCEPT ALL ITEMS with order nr. ____________

Signature Name Date

THANK YOU, BUT DECLINE THIS QUOTATION OFFER

Signature Name Date

D2: Quotation for the Procurement of 7075-T6 Aluminium Plate Needed for the Manufacture of the CubeSat Rails and Standoffs

METAL & TOOL TRADE

P.O. BOX 3131
KEMPTON PARK
1620

Head Office:
102 Plane Road
Spartan
Kempton Park, Gauteng

METAL AND TOOL TRADE (PTY) LTD
Email: mttjhb@mtt.co.za
Website: www.mtt.co.za
VAT No: 4360113619
Reg No: 1985/004404/07

Johannesburg:
Tel: 011-570-1800
Fax: 011-570-1820

Cape Town:
Tel: 021-447-1800
Fax: 021 447 1816

Durban:
Tel: 031 563 4987
Fax: 031 563 4988

SALES QUOTATION 6 683

Postal Address:

UNIVERSITY OF STELLENBOSCH
Private Bag X1

Maitland
7602 South Africa

Physical Address:

UNIVERSITY OF STELLENBOSCH
Joubert Street Entrance Room 106
Stellenbosch
Cape Town
7602 South Africa

Account No:	C00431
Customer VAT No:	4920118959
Customer Order No.:	FRANCOIS
Document Date:	09/11/2016
Document Number:	6 683
Salesperson:	H04
QUOTATION VALID UNTIL:	09/12/2016

Item	Description	Unit Price	No. Pieces:	Thickness /Diameter - mm	Width - mm:	Length - mm:	Row Total
3BL /775010	ALUMINIUM PLATE 10MM 7075	68,70	5	10.0	100	200	343.50

Remarks:

Payment Terms:	30 DAYS NET FROM STATEMEN	Subtotal	ZAR 343.50
Banking Details:		Additional Expense	ZAR 350.00
Name:	METAL AND TOOL TRADE (PTY) LTD	Total Before VAT	ZAR 693.50
Bank:	First National Bank	VAT @ 14%	ZAR 97.09
Account No:	56050024417	Total	ZAR 790.59
Branch:	223626		
Procurement:	mttjhb@mtt.co.za		
Accounts:	valerie@mtt.co.za		

D3: Detailed Quotation for manufacturing the Rails for the KletsKOUS-3 CubeSat prototype

Quotation

Institute for Advanced Tooling
Promoting Sustainable Tooling

University of Stellenbosch, Dept of Industrial Engineering
Cnr of Banhoek and Joubert Street, Matieland, 7602
Tel: +27 21 808 4132 - Fax: +27 21 808 4128

Lazola Ncetani
Junior Tooling Technician
ncetani@sun.ac.za

Prepared for

Company: IND.ENG.STUDENT
Contact: FRANCOIS CONRADIE
Telephone:
Email: 15367894@sun.ac.zaa

Project Nr.: WC/LN/CNCWC/0029
Quotation Date: 01-Dec-16

We thank you for your enquiry and can accordingly quote as follows:

Client input: CLIENT PROVIDED THE STEP FILE OF THE RAIL AND SQUARE BLOCK

Deliverables:
1. FOUR PARTS OF THE RAIL
2. ONE PART OF THE SQUARE BLOCK

Work description: WIRECUTTING OF 4 RAIL AND ONE SQUARE BLOCK

Item Nr	Project Breakdown	Price
1.	WIRECUTTING OF RAIL (4 OFF) AND BLOCK	R 600.00

Total Project Value:	R 600.00
Minus 100% Discount:	R 600.00
Balance:	R 0.00
Add 14% VAT:	R 0.00
Total Price:	**R 0.00**

Delivery:

Notes & extra information:

Terms & Conditions

1 This Quotation is valid for 30 days.
2 No results will be delivered before this quote is signed and returned with a valid order number or an official company order has been received by the IAT.
3 Invoices are payed within 14 days.
4 Where applicable, please ensure that all cheques are made out to the University of Stellenbosch.
5 Lead times are applicable only once all terms and conditions have been met by customer.
6 A 50% deposit is required if material is to be purchased including cutting tools

We would be glad to provide you with any additional information.
Please feel free to contact us any time.

Best regards

Lazola Ncetani

Junior Tooling Technician

Customer Response

Please mark selection & return fax: (021) 808 4126

Considering the above quotation, we wish to

ACCEPT ALL ITEMS with order nr. ______

[signature]	Francois	2016/12/02
Signature	Name	Date

THANK YOU, BUT DECLINE THIS QUOTATION OFFER

Signature	Name	Date

D4: Detailed Quotation for Manufacturing the Top, Bottom and Side Panels for the KletsKOUS-3 CubeSat Prototype

2 Lappan Street
Stellenbosch

TEL : 021 887 1044
FAX : 021 887 0581
E-MAIL : jaco@locilaser.co.za

DATE : 11/9/2016

Quote : LW05089REV1 - PANELS VIR CUBE SAT

Universiteit van Stellenbosch
Francois Oberholzer

From : Lincon
021 887 1044

Preview :	Qty :	Part Name :	Size :	Thickness :	Material :	Unit Price :	Ext. Price :
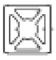	12	Side Panel	97.00 x 94.00	0.90mm	AL1200	R19.77	R237.24
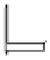	12	Solar Flap	100.00 x 78.00	1.20mm	AL1200	R7.53	R90.36
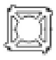	6	Top & Bottom Panel	106.14 x 106.14	1.20mm	AL1200	R29.69	R178.14

Sub Total	R505.74
Tax	R70.80
Shipping	R0.00
Total	**R576.54**

Payment
• 30 Days.

Delivery
• Delivery time can change with out warning due to unforeseen reasons.
• Delivery is subjected to material availability.

• Loci laser does not take any responsibility for wrong drawings. All drawings must be 1:1.
• Loci laser does not take any responsibilities for the designing of parts in terms of sizes and material.
• We will use off cut material for parts where applicable.
• Please provide Loci with a detail drawing or the following drawing files: DXF: DWG.
• We do not take any verbal orders. All orders must be in writing with the specifications specified.
• If in doubt please ask.

Please quote the reference number on your order.
This price is valid for 15 days unless otherwise stated. Price may change if cost of material change in the period.

Banking details
Bank: ABSA
Acc. no: 405 896 9733
Branch Code: 632 656

Thank you